JIMMA UNIVERSITY

SCHOOL OF GRADUATE STUDIES

JIMMA INSTITUTE OF TECHNOLOGY

FACULTY OF CIVIL AND ENVIRONMENTAL ENGINEERING

HYDROLOGY AND HYDRAULIC ENGINEERING CHAIR

MASTER OF SCIENCE IN HYDRAULIC ENGINEERING

FLOOD HAZARD AND RISK ASSESSMENT USING GIS AND REMOTE SENSING: A CASE OF WESTERN WABE SHEBELLE RIVER BASIN, ETHIOPIA

By: Umer Mohammed

A Thesis Submitted to the Chair of Hydrology and Hydraulic Engineering, Jimma Institute of Technology, in Partial Fulfillment of the Requirements for the Degree of Masters of Science in Hydraulic Engineering

December, 2021

Jimma, Ethiopia

JIMMA UNIVERSITY

SCHOOL OF GRADUATE STUDIES

JIMMA INSTITUTE OF TECHNOLOGY

FACULTY OF CIVIL AND ENVIRONMENTAL ENGINEERING

HYDROLOGY AND HYDRAULIC ENGINEERING CHAIR

MASTER OF SCIENCE IN HYDRAULIC ENGINEERING

FLOOD HAZARD AND RISK ASSESSMENT USING GIS AND REMOTE SENSING: A CASE WESTERN WABE SHEBELLE RIVER BASIN, ETHIOPIA

By: Umer Mohammed

A Thesis Submitted to the Chair of Hydrology and Hydraulic Engineering, Jimma Institute of Technology, in Partial Fulfillment of the Requirements for the Degree of Masters of Science in Hydraulic Engineering

Main Advisor: Mr. Fayera Gudu Tufa (Ass. Prof.)

Co-Advisor: Mr. Sanyi Misgana (M. Sc.)

December, 2021

Jimma, Ethiopia

DECLARATION

I hereby declare that this thesis entitled "Flood Hazard and Risk Assessment in Western Wabe Shebelle River Basin, Ethiopia" is my original work which was approved and accepted as a Partial Fulfillment of the Requirements for the Degree of Masters of Science in Hydraulic Engineering at Jimma Institute of Technology and has yet been not submitted as a requirement for the award of any degree in Ethiopian Universities including Jimma University up to now.

By: _____ _____

Name: Umer Mohammed Signature Date

This thesis has been submitted for Examination with our approval as University Main advisor And Co-advisor

Main Advisor: _____ _____

Name: Fayera Gudu (Ass. Prof.) Signature Date

Co-Advisor: _____ _____

Name: Sanyi Misgana (M. Sc.) Signature Date

APPROVAL SHEET

As members of the Examining Board of MSc. of Thesis Approval, we certified and signed that we have read and evaluated the thesis entitled with "**Flood Hazard and Risk Assessment in the Western Wabe Shebelle River Basin, Ethiopia**" was prepared by UMER MOHAMMED. We recommended that the thesis could be accepted as a Partial Fulfillment of the requirements for the Degree of Masters of Science in Hydraulic Engineering.

	Name	Signature	Date
Chairman	Mr. Nasir Gebi (M. Sc.)	_____	_____
Internal Examiner	Mr. Tilahun Hayile (M. Sc.)	_____	_____
External Examiner	Dr. Adane Abebe (Ass. Prof.)	_____	_____

ABSTRACT

Floods are among the most common natural disasters around the world, particularly occurs in the vicinity of rivers. Ethiopia has continuous topographical land arrangement that ranges from high altitude of highlands to plain lands extending to lowlands, experiences high floods during rainy season. Curbing the recurrent flooding through addressing the problem and identifying flood-prone areas; mapping flood hazard, risk and locating the inundated area and stating some recommendable alternative mitigation measures. The main objective of this study was to execute flood hazard and risk assessment using GIS and Remote Sensing in Western Wabe Shebelle River basin. The DEM with high-resolution 30m was used to delineate the basin watershed in the catchment area 5,040.58km^2. Multi Criteria Evaluation procedure was evaluated to meet a specific objective technique to assess flood hazard in the Agarfa catchment using GIS environment for the selected basin and Eigenvector criteria weight was calculated for each factor in IDRISI and Excel software. Flood hazard Weighted Overlay with development factors such as elevation, slope, land cover, rainfall, soil and drainage density. Flood risk were also Weighted Overlay using the elements of population density, land-use and the flood hazard layer within the river basin. The study results showed that the downstream catchment area were more vulnerable to high flood hazard and risk. The best fitted probability distribution was GEV which calculates the maximum peak discharge of 1,215.46m^3/s, 2,595.62m^3/s, 3,179.53m^3/s and 4,978.06m^3/s for a return period of 10, 100, 200 and 1000 years respectively. The inundation map was developed in RAS Mapping tool of HEC-GeoRAS; mapping water surface generation and floodplain along the Western Wabe Shebelle River basin with inundated area of 105.2ha, 143.6ha, 153.9ha, and 178.4ha for 10, 100, 200 and 1000 years of return period, respectively. The flooded area in the return period 1000 years was the highest compared to other return period tested due to the increased stream flow and the flood depth was excessive that ranges from 0.0015m to 92.6m and hence, the consequence of the flood on life and property was very high. The mitigation measures must be taken shall include: taking the application of structural determinations that focuses on reducing the impacts of flooding on communities and taking the non-structural measures like land-use control, sampling signal measures, relocations and early flood warnings.

Key Words: EASY-FIT; Flood Hazard Map; Flood Risk Map; GIS and Remote Sensing; HEC-GeoRAS; HEC-RAS; IDRISI; Inundation Map; Western Wabe Shebelle River Basin

ACKNOWLEDGEMENT

I would like to thank the Almighty GOD (ALLAH) for his giving me strength to successfully achieve this work of thesis whilst the task was critical, bulky and tedious.

Plainly stating, it is my great pleasure to be grateful to my main advisor Mr. Feyera Gudu Fufa and co-advisor Mr. Sanyi Misgana for their scientific guidance, valuable suggestions and advising of me to accomplish this thesis work in finishing in relevant time-frame successfully with great distinction.

Again, I would like to express my deepest thank to the Hydraulics Engineering Department Staffs members who gave me fruitful advices and the post-graduate courses at all.

I also would like to acknowledge the Ethiopian Ministry of Education (MoE) for their covering research funds including the National Metrological Agency (NMA) and Ministry of Water and Energy (MoWE) of Ethiopia for their coordination's too.

Lastly, I would like to manifest my deepest expression of gratitude for the Authors I used in citation to help encourage my work come in range of success.

TABLE OF CONTENTS

LIST OF TABLES

LIST OF FIGURES

ACRONYMS AND ABBREVIATIONS

AHP	Analytical Hierarchy Process
ArcGIS	Arc Geographic Information System
ASTER	Advanced Space-borne Thermal Emission and Reflection Radiometer
CDF	Cumulative Distribution Function
DEM	Digital Elevation Model
DRMFS	Disaster Risk Management and Food Security Sector
EV1	Gumble's Type I
FFA	Flood Frequency Analysis
GEV	Generalized Extreme Value
GIS	Geographic Information System
GOF	Goodness of Fit Test
HEC-GeoRAS	Hydrologic Engineering Center-Geospatial River Analysis System
HEC-RAS	Hydrologic Engineering Center-River Analysis System
IDRISI	A Software Used for Pair Wise Comparisons by Saaty's Scale
IDW	Inverse Distance Weighting
LN2	Two-Parameter Lognormal
LP3	Log-Pearson Type III
MCA	Multi-Criteria Analysis
MCE	Multi-Criteria Evaluation
MIKE	A Software Developed to Help Tackle any Water Challenge
MODIS	Moderate Resolution Imaging Spectro-radiometer
NDRMC	National Disaster Risk Management Council
NMA	National Metrology Agency
OLI	Operational Land Imager
PDF	Probability Distribution Function
Popn	Population
Q-Q	Quantile-Quantile
RAS	River Analysis System
RS	River Section
SNNPRS	Southern Nations, Nationalities And Peoples Regional State
SOBEK	Powerful Modelling Software Suite for Flood Forecasting, etc.
SRTM	Shuttle Radar Topography Mission
TIN	Triangular Irregular Network
TIRS	Thermal Infrared Sensor
UNHCR	United Nations High Commissioner for Refugees
USGS	United State Geological Survey

1 INTRODUCTION

1.1 Background

Floods have caused extreme destruction and affected communities in different ways throughout history in the world (Bhatt, *et al.*, 2014). In recent years, many cities around the world have faced a lot of surface water flooding, as it occurs after a period of heavy rains that overwhelm the drainage system, disrupting services and economic operations, causing property damage and even killing people (Musolino, *et al.*, 2020).

The creation of flood risk maps helps to efficiently present the spatial distribution of flood risk as well as the establishment of an easily comprehensible relationship between the theoretical concepts of flood hazard, exposure, vulnerability and the decision-making procedures are vital tasks in flood risk assessment (Jhong, *et al*., 2020).

Ethiopia is a country with a continuous topographical land arrangement that ranges from high altitude highlands to plain lands and extends to lowland areas and it is drained by 12 river basins, of which 8 are river basins and 1 lake basin with perennial rivers, and 3 intermittent river basins that burst during the rainy season, causing flooding to communities bursting their basins (Luu et al., 2020). Approximately 80% of the rain falls during the rainy season, mainly from June to September and the major perennial rivers including their numerous tributaries make up the country's largest drainage systems (Getahun and Gebre, 2015).

The country, mainly experiences at large the river flooding and flash flooding to some extent. The rivers that breach their banks and inundate downstream plain regions are blamed for many of Ethiopia's flood tragedies. The flood that recently hit Southern Omo Zone and East Shewa (mostly Dugeda Bora Woreda) Zone is a classic example of river flooding. On the other side, the incident that Dire Dawa City experienced was a typical of flash flood (Bishaw, 2012).

This study, mainly concentrated in identifying flood-prone areas and assessing the flood risk due to river flooding in Western Wabe Shebelle River basin that experiences intensive rainfall in the highlands during rainy season as rainfall varies with altitude. Robe River is the main stream flow in the catchment and has the most extensive area coverage but it is considered and known of water scarce due to the low annual runoff.

1.2 Statement of the Problem

Among the natural hazards capable of causing disaster, flood was the most hazardous, frequent and widespread catastrophic event throughout the world. This makes flooding an important

subject of study, particularly in the less developed countries and flood impact tends to be very severe in African cities where urbanization has taken place with improper land use planning and lack of early warning systems (Rieu-clarke, 2008).

In some places of Ethiopia, flood was the most severe, persistent and regular natural hazard. The country, were known of experiencing intensive rainfall from June and September. Particularly, strong and extended rains in Afar, Oromia, Gambella, SNNPR (Southern Nations Nationalities and People's Region), Somalia and Amhara areas have caused flooding and landslides across the country. According to the latest estimation of National Disaster Risk Management Commission (NDRMC), floods have affected about 1,017,854 individuals and displaced 292,863 people across the country during the season (Wondim, 2016).

This study was motivated to be done in the area to deal with the frequent flooding problems at the Agarfa Sub-Catchment. The cause of the problem has been reported in a number of compiled of supported sources such as: in November 2017, the study reports in drivers of hydrological dynamics in the Bale Eco-Region indicated that flood events have occurred regularly in the form of flash floods in the lowland sections of Wabe Shebelle basin causing sheet of soil erosion, affecting 100,000 and causing 154 deaths, particularly forming alluvial plains and in the high-altitude zone, permanent wetlands were an area of producing yearly maximum rainfall; in April 2018, the National Disaster Risk Management Commission (NDRMC) of Ethiopia reported that high flood incidences were in seen hugely in the catchment and in October 2019, Office for the Coordination of Humanitarian Affairs (OCHA) reported that in Agarfa, Gololcha, Gaseara, Goba and Sinana were affected by flooding and as a result several types of crops, houses, properties and livestock were damaged.

Thus, identifying the flood prone-areas in the Western Wabe Shebelle River basin was found very important, essentially for: addressing the problem to its rating scale and identifying flood-prone areas; mapping the flood hazard, risk and inundation area to locate the damaged areas in need of recovery and stating some recommendable alternative mitigation measures that could be good enough for the prevention of the recurrent flooding problems in the study area enhancing the future resilience for the degraded and damaged part of the catchment.

1.3 Objectives

1.3.1 General Objectives

The objective of this study is essentially to execute flood hazard and risk assessment using GIS and Remote Sensing for Western Wabe Shebelle River Basin, Ethiopia.

1.3.2 Specific Objectives

1. To develop best fitting probability distribution function to estimate peak discharges for different return periods
2. To develop map of flood hazard, risk and inundation for the study area
3. To recommend some alternative flood mitigation measures for the basin

1.4 Research Questions

1. Which probability distribution functions best fit the analysis to estimate peak discharges for different return periods?
2. How to develop map of flood hazard, risk and flood inundation for the study area?
3. What alternative mitigation measures are recommended to control flood hazard and risks in the basin?

1.5 Significance of the Study

Flood was a major threat to the study area's resources as it is formed by a range of biophysical and anthropogenic variables, due to the rapid development of urban lands and agricultural lands, particularly because of rapid population growth. Hence, this study mainly dealt with flood hazard and risk assessment to obtain detailed information for future probabilities due to natural flood magnitude, timing and frequency using historical flood characteristics, hydraulic, hydrological and metrological data from the study area.

Hence, preparedness and response by providing knowledge about future floods is essential for the government, the people and any other concerned bodies living along specific flood hazard and inundation areas, would have enough information to prepare for flooding, raise flood hazard awareness and employ alternative flood mitigation measures to lessen the risk of flooding and the harm it causes in the area.

Generally, flood hazard and risk management is an important for communities residing in the area to recognize the consequences that could occur at any time for three reasons: to identify floodplain areas along the river course; to reduce the risk of direct flood damage to people, crops, infrastructures and properties, to create awareness and control flooding problems during critical farming seasons by realizing mitigation measures within the catchment basin.

1.6 Scope of the study

The scope of study was bounded to the title of the research. It was mainly to conduct in concern of addressing issues related to the probability occurrence of flooding that causes flood

hazard and its risk-oriented magnitude that might take place depending on the hydrological response of the selected basin.

1.7 Limitations of the Study

Due to the limitation of sufficient and reliable data on rainfall, river flow and soil data, the flood disaster assessment and mapping of flood-prone areas in the study area might have its own shortcomings. The metrological data of rainfall at reading station and the stream flow at gaging station were more or less not recorded for the consequent months that leads to the filling for missing data using another methods that might be fitting pure or not for analysis.

The recurrent flooding problem in the catchment area was only supported with compiled evidences as of flash and river flooding update in reports, until this study was taken into scouts; addressing the victim zone areas under the risk from the sub-catchment were affected by flooding and as a result several types of crops and livestock were also damaged in the reports.

2 LITERATURE REVIEW

2.1 Introduction

Floods have caused extreme destruction and affected communities in different ways throughout history in the world. Climate change is eminently aggravating flood events, therefore a better understanding of various aspects of flood hazard, particularly for pedestrians, is becoming increasingly important. In recent years, many cities around the world have faced a lot of surface water flooding. It usually happens after a period of heavy rains that overwhelm the drainage system, disrupting services and economic operations, causing property damage and even killing people (Musolino, *et al*., 2020).

This is an evident when one consider, the number of people affected by flooding in recent decades and flooding has accounted too much of the loss events worldwide between 1980 - 2014 more than any other single disaster. Flooding is also the most common disaster agent in the world, according to the total number of disasters reported between 1900 and 2014 (Weldegebriel & Amphune, 2017).

Rapid urbanization and economic growth in developing Asian countries has increased their vulnerability to flooding, particularly in low-lying municipal areas that are currently facing increased threats from heavy precipitation, which has undoubtedly worsened the problem by the impending climate change. The first step in disaster risk management is the identification of hazard area because frequently developing flood hazard maps that can quantify the spatial variance of flooding potential while simultaneously being strong enough to accommodate the change is critical in urban landscape and in precipitation (Jian, *et al.*, 2021).

Flooding has long been acknowledged as one of the major environmental risks in Ethiopia, although receiving less attention than drought. Flooding frequently develops into a disaster, damaging people's lives and livelihoods for many years. However, according to historical flood data, Ethiopia has experienced 47 big floods since 1900, affecting about 2.2 million people.

This is coupled with climate change and variability is likely to increase flooding as one of the major extreme events in the future posing a growing threat to many livelihoods. Flooding is a recurring environmental hazard that is felt most extremely in locations where people are already vulnerable to any unfavorable climatic occurrence due to a lack of resilience. For example, flooding harmed an estimated 210,600 people in just three months (November, 2015 - January, 2016) (Weldegebriel & Amphune, 2017).

2.2 Historical Background of Floods in Ethiopia

In Ethiopia, the beginning flood trends cope with the results of agricultural history of Ethiopia, which starts from 1800 - 1990 by examining the historical setting of the healthy highlands, the ecology of the ox-plow complex and trends in population, farm resources and specialized agriculture. In the estimates of farm-level, food losses of up to 30 percent are common in the community of agricultural specialists in Ethiopia and small body of specialized food-storage literature (McCann, 1995).

The country's geography ranges from the high peak of Ras Dashen 4560 meters above sea level, in the north central section of the country to the lowest desert of Dalol 120 meters below sea level. Ethiopia has 12 river basins, with 8 of them being river basins, 1 being a lake basin with permanent rivers, and the other 3 being dry river basins. From 1960 until the present, the country's flood history and geographical events have been assessed (Mamo, *et al.*, 2019).

Ethiopia's rainfall pattern and magnitude, together with the country's terrain, are primary drivers of surface water flows as flash floods. In analysis, different data source archives, remotely sensed satellite imageries, MODIS, Sentenel-2, data reports such as UNHCR, NDRMC (National Disaster Risk Management Council) including the ArcGIS working environment were utilized. Flood occurrences and extents throughout the previous 6 decades have been marked by regional and temporal variability. From decade to decade, the frequency of floods in the country rose (Mamo, *et al.*, 2019).

The Ethiopian National Meteorological Agency (NMA) released a new weather forecast for the 2018 winter season on May 29, stating that several sections of the northern, northeastern, central, western, southwestern, eastern and bordering rift valleys are predicted to experience above-normal rainfall. Furthermore, rainfall in the southern highlands and southern Ethiopia forecasted to be normal and above normal, while rainfall in reduced areas of northwestern Ethiopia is expected to be average. It is also possible that strong rains will inundate low-lying areas in and around river basins on occasion. Floods in the country are most commonly caused by persistent high rainfall, which causes rivers to overflow and inundate areas along river banks in lowland plains.

Lower Awash River plains; Somalia's Wabe Shebelle, Genale, and Dawa Rivers; Gambella's low-lying districts along the Baro, Gilo, Alwero and Akobo Rivers; SNNPR's lower Omo and Bilate Rivers; the enormous floodplains surrounding Lake Tana and the banks of the Gumera

River are the areas with strong rainfall in neighboring highland areas known of flash floods occurring in lowland areas.

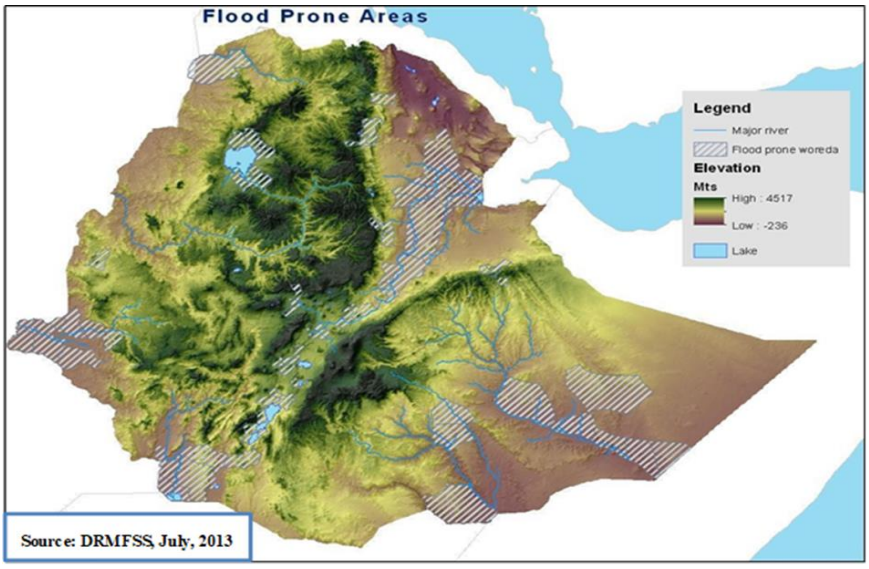

Figure 2.1 Map of flood prone areas in Ethiopia

2.3 Model Software

A geographic information system (GIS) is a computer-based system that handles geo-referenced data input, data management (storage and retrieval), manipulation, analysis and output. It includes a variety of tools for finding flood-affected areas and forecasting locations that are likely to be flooded due to a river's high water level. Information from various maps, aerial photographs, satellite images and digital elevation models (DEM) will be compiled using GIS (Bishaw, 2012).

EASY-FIT is a program that identifies parameters in one-dimensional temporal systems using explicit model functions, steady-state systems, laplace transformations, differential algebraic equations and ordinary differential equations systems (Schittkowski, 2002). Many natural science, engineering and other disciplines rely heavily on data fitting. The main idea is to minimize the gap between some known experimental data and the theoretically expected model function values in a mathematical model that represents a real-life scenario in order to estimate the unknown parameters in mathematical models describing real-life situations (Schittkowski, 2002).

It is a data analysis and simulation program that allows us to fit and simulate statistical distributions using sample data, select the best model and use the analysis results to make

better judgments. This software can function as a stand-alone windows application or as an add-on for Excel spread sheet (Mehrannia & Pakgohar, 2014).

Multi-criteria analysis (MCA) is a decision-making tool that was created to solve complicated multi-criteria problems with qualitative and quantitative features. Ranking and Rating are the two approaches used in multi-criteria analysis. Each decision factor is assigned a ranking that indicates the degree of value it contributes to the decision, whereas rating is similar to ranking but assigns numerical scores to show the level of importance it has in the decision-making process, using layer management techniques such as analytic hierarchy process (AHP), weighted linear combination (WLC) and binary logic to create a specific database of municipal landfills (Chakravarthi, *et al.*, 2017).

The IDRISI and ArcGIS software models are used for the analytic multi-criteria decision-making; a tool developed for solving complex multi-criteria problems that include qualitative and quantitative aspects of the problem. The analytic hierarchy process (AHP) was designed by Saaty's scale. Refraction, comparative judgment and priority synthesis are the three driving principles. The principle of refraction is necessary to arrange decision-making problems into hierarchical patterns (Shahabi, *et al.*, 2014).

HEC-GeoRAS is a geographic river analysis system developed using ArcGIS Desktop, Spatial Analyst and 3D Analyst extensions. The geodatabase design supports analysis of spatial data for hydraulic modeling and floodplain mapping (Meekma and Byard, 2013). Geo-RAS develops spatial data input for HEC-RAS models from digital terrain models and other GIS datasets using ArcGIS Desktop.

After the model results are calculated in HEC-RAS, they can be post-processed in Geo-RAS, then the floodplain depths and extents can be mapped together with other relevant spatial results such as modeled velocity distribution, ice depths, and sediment transport. It can partition enormous terrains into smaller tiles, execute analyses on each tile, and synthesize results from each tile to build maps of HEC-RAS modeling results using the divide-and-conquer strategy to mapping extremely large terrain datasets for the larger area (Merwade, 2016).

As a result, the primary goal of this study is to evaluate the 2D HEC-RAS model's potential and capabilities in rainfall-runoff simulations at the basin scale, by comparing results obtained using a 2D completely with dynamic model constructed by the authors for research objectives

employing both choices with fully dynamic equations and diffusion wave equations (Petaccia, 2020).

2.4 Best Fit Probability Distribution Functions

Probability distribution is a concept related to the statistics, where the outcome of statistical experiments and their probabilities of occurrence are connected with the probability distributions (Soon Kim Tiang, *et al*., 2020). The application of probability distribution model to annual flood flow supposes screening and application of non-parametric tests of randomness, independence, homogeneity and stationarity. It is only when empirical evidence was found to rule out the non-parametric tests, before the available data is considered fit for flood frequency analysis.

For flood frequency analysis using Generalized Extreme Value, Three-Parameter Log-Normal, Generalized Logistic and Pearson Type-III Distributions, through selecting the correct probability distribution and parameter evaluation approach is crucial to compute the yearly maximum steam flow at the site. The performance of these distributions is assessed based on goodness-of-fit tests and accuracy measures (Vrushali Wagh, *et al.,* 2020; Bathrellos, *et al.*, 2016).

It can be difficult to assess the precise information about the shape of a distribution conveyed by its third and higher order moments using the Maximum Likelihood Method (MLM), method of least squares, and probability weighted moments, but to address these shortcomings, Flood Frequency Analysis (FFA) uses an alternative approach called L-Moments (LMO) (Vivekanandan, 2020).

The frequency and magnitude of those events must be determined for flood plain management, hydraulic structure design and civil protection strategies. However, if the length of available records is not enough large to define the risk of peak flood, extreme rainfall, low-flow, drought, etc. in these cases, FFA involves fitting probability distributions to the Annual Peak Flood (APF) data series is considered as an alternative tool to arrive at a design value (Vivekanandan, 2020).

The reliability of a specified for assumed probability distribution function can be analyzed with the Goodness of fit test. The test shows, how much precisely the observed data fit the selected probability distribution model. Root means square error (RMSE) test, Kolmogorov Smirnov (K-S) test, Anderson–Darling (AD) and Chi-square (x^2) test is most frequently used goodness-of-fit tests. In the test, the K-S statistic distribution is independent of the cumulative

distribution function for which it is being tested; the best fitted distribution function and selected as in case for this study. The Chi-square test helps to extract more comprehensive information from the test statistic than any other test (Pal, *et al.*, 2020).

2.5 Flood Hazard Assessment

The assessment of the flood risk must be carried out with the simplest possible classification, which indicates very high, high, moderate, low and very low risk. By combining local knowledge, hydrological, meteorological, and geomorphologic data, inundation or hazard assessment mapping delineates flood hazard zones in the river basin using various methodologies. The final flood hazard component necessitates the addition of extensive local or field knowledge in the model. Assigning a rank to a flood hazard indicator, for example, necessitates local expertise and may vary depending on the circumstances (Getahun and Gebre, 2015).

The net probability of occurrence of flooding in each flood hazard zone is estimated from the total sum of the weight of each contributing factor considered. To obtain this total sum weight, all of the contributing factor maps were overlaid. The sum of all contributing factors determines the total weight for estimating the probability of flooding in a certain flood hazard zone. GIS allows the decision maker to identify a list, meeting a predefined set of criteria with the overlay process. All of these processes, the compilation of contributing factor maps, the overlaying of all maps and the calculation of hazard areas were done by using Raster Calculator in ArcGIS Spatial Analyst tool (Menon & Ajin, 2014).

In India, flood was studied as a major environmental problem as it has devastating effects on life and property. GIS and Remote Sensing was used for identification of flood prone areas which were classified with zone-wise. Flood recurrence maps were developed using Landsat satellite imagery over multiple dates. Flood-affected areas were classified as very low, low, medium, high, very high, and very high according to their vulnerability to potential flood risk. According to their vulnerability to flooding, territories were subdivided into categories of very high, very high, high, medium, low, and very low, respectively (Bhatt, *et al*., 2014).

2.6 Flood Risk Assessment

Natural disasters have claimed the lives of at least 3 million people globally in the last 20 years, as well as affecting about 800 million others. Flood risk can be defined in a variety of ways when it comes to natural disasters, depending on the severity of their effects on people, property, and the economy. Flood risk can be divided into two categories: hazard and

vulnerability. Flood risk mapping is a critical component of flood risk management and is restricted to flood-prone areas (Safaripour, *et al.*, 2012).

Natural disasters have claimed the lives of nearly 1.6 million people worldwide since 1990, with annual economic damages estimated to be between $260 and 310 billion dollars. The scientific and policy communities agree that these dangers must be reduced. As a result, global models for estimating risk from natural catastrophes at the global scale have rapidly developed over the previous decade (Ward, *et al.*, 2020).

In analyzing flood risk, flood exposure and flood vulnerability should be integrated with flood hazard to give a comprehensive resource of reference for flood risk managers. Flood hazard is defined as the risk of harm, loss (or damage) from an occurrence that occurs at a single location. The potential for human risk and property damage during flood occurrences is characterized as exposure to flood hazard (Luu, *et al.*, 2020).

Along the Yom River Basin in northern Thailand, an integrated flood risk and risk assessment surveyed the Phrea floodplain and performed a risk analysis using GIS to integrate the flood risk and vulnerability of the hazard. An exposure-based risk assessment method was applied to assess floodplain risk severity for recurrent 100 year floods. Flood-prone areas were classified as low, medium, high, and high according to the relative magnitude of risk (Tingsanchali, *et al*., 2010).

2.7 Flood Hazard and Risk Mapping

Flood hazard mapping is a critical component for flood-prone land use planning. It generates simply readable, quickly available charts and maps that aid in the identification of risk areas and the prioritization of mitigation effects, and it is not a new attempt in the world's industrialized countries (Forkuo, 2011). Software such as SOBEK, HEC-RAS 2D, and MIKE are some of the most often used 2D flood models for analyzing process (Yin, *et al.*, 2013; Farooq, e*t al*., 2019).

Flood hazard assessment relies heavily on 2D hydraulic flood propagation models, which require an accurate representation of the floodplain in the form of hydro-enforced terrain data and frequently employ a DEM for model parameterizations such as terrain slope, cross sections, and flow pattern. Stream representation in a DEM is critical for the accuracy of 2D flood models, and it can be achieved by hydro-enforcing of the DEM under study (Farooq, *et al.*, 2019).

Floods cause severe damage to people, their health and properties, city infrastructures, ecological systems, agricultural lands and economic activities. Flood events are increasing rapidly around the world as a result of global warming, urbanization along rivers and coasts, and climate change, and it is critical for the public, emergency management professionals, and decision-makers to have access to an accurate estimate of the flood extent (Forest, *et al.*, 2020; Dottori, *et al.*, 2016).

Flood risk prevention measures are planned to reduce the adverse consequences associated with floods on humans, the environment, cultural heritage and economic activity. An economic assessment of the risk provides compensations for the identification of single hazards. As a result, policy-makers gain important information on the sectors and areas at risk, allowing them to conduct an integrated spatial evaluation of the flood risk for people, non-residential, agricultural and environmental sectors (Foudi, *et al.*, 2015).

2.8 Flood Inundation Mapping

Flood inundation mapping is a useful tool for municipal and urban expansion planning, as well as emergency response plans, flood insurance payments, and ecological studies. Forecasting the behavior of the stream in issue for various recurrence interval storm events and being able to interpret the anticipated findings into a plan-view extent of flooding are both required when mapping a floodplain which is used to inform decision-makers about how to best organize resources to prepare for disasters and improve quality of life by analyzing the extent of floods and floodwater inundation (Desalegn & Mulu, 2021).

The River Analysis System (RAS) from the Hydrologic Engineering Center is a software program that can be used to create flood inundation maps for a variety of scenarios, including steady and unsteady flow, as well as sub and supercritical flow regimes (Goodell, *et al*., 2006). Hydrologic modeling to predict the peak flows from storm events, hydraulic modeling to estimate water surface levels, and topography analysis to calculate the inundation area are all part of flood inundation modeling. Understanding the uncertainty associated with the many factors involved in flood inundation mapping is crucial for managing the risk of inundation (Merwade, *et al.*, 2003).

Once the geometry is complete, the hydrology can be entered into the model. HEC-RAS requires flows to be entered at all upstream boundaries. In addition, flow changes can be specified along any of the streams. Flows were provided to the model for the 1 year, 2 year, 10

year, 25 year and 100 year recurrence interval storm events for both present and future conditions (complete build-out of the watershed) (Goodell, *et al*. 2006).

Flood inundation mapping was studied as an important tool for municipal and urban growth planning, emergency action plans, flood insurance rates and ecological studies using HEC-RAS model in Segamat town in Malaysia. Among the probability distribution models, namely Generalized Pareto, Generalized Extreme Value, Log-Pearson 3, Log-Normal (3P) and Weibull (3P) used to test flood frequency analysis to calculate extreme flows with different return periods; the Kolmogorov-Smirnov (K-S) test and the Generalized Pareto was found to be the best fitted distribution for the Segamat River. The peak floods from frequency analysis for selected return periods were set for input into the HEC-RAS model to find the expected corresponding flood levels. Results obtained from HEC-RAS model were used in ArcGIS to prepare floodplain maps for different return periods. For 100 years flood simulation, the inundated area was almost 5 times larger than the simulated 10 years' flood (Romali, *et al.*, 2018).

Along the Awash River basin, the application of GIS and Remote Sensing techniques was used to study the seriously occurring flood problems in the major river basin, Ethiopia. The Flood Hazard and Hazard Map was an effective tool to mitigate flood damage to assess flood risk and risk in the Lower Awash sub-basin. In the GIS environment, factors contributing to flooding have been developed such as slope, elevation, drainage density, soil type and land cover. The computed eigenvectors were also used as factors for each factor map to be merged into weighted overlays in the Arc GIS environment. Flood risk assessments were performed using two risk factors: flood hazard layer and population and land use (Wondim, 2016).

Located downstream of the Ribb and Meki rivers, Dugeda Bora Woreda was studied as one of the most flood-affected areas in Southeast Ethiopia. Flood causative factors were developed in GIS and remote sensing environments, weighted and overlaid according to the principle of pairwise comparison, and flood risk and flood risk were generated using MCE technique. Flood recurrence analysis was performed using the annual daily maximum water level of rivers, and the expected flood level was calculated at different recovery periods including 100 year return period. DEM and baseline floods were also combined in a GIS environment to generate flood maps (Bishaw, 2012).

Fogera Woreda, was studied as one of the most severely flood affected areas particularly in the Ribb-Gumara Catchment using Geographic Information System And Remote Sensing

techniques, Northwest Ethiopia. Flood frequency analysis was done using Ribb and Gumara Rivers annual maximum daily gauge levels using Gumbel's method and the likely flood levels in different return periods were computed. The DEM and the 100 year return period base-flood were combined in the GIS environment in order to develop flood inundation maps. Additionally, flood causative factors were developed in the GIS and Remote Sensing environment; weighted and overlaid in the principle of pair-wise comparison using Multi Criteria Evaluation technique in order to arrive at flood hazard and risk mapping (Alemu, 2007).

Flood inundation mapping was studied at Fetam River passing Banja, Sekela, Burie, Guagusa Shikudad, and Womberma Districts in the Awi and West Gojam zones of the Amhara region using the HEC-RAS model, GIS for spatial data handling and HEC-GeoRAS for interfacing among HEC-RAS and GIS. The study results showed that the critical floods were damaging the areas around Fetam River, which is hazardous to social and economic growth due to loss of lives and destruction of properties. Built-up areas and agricultural fields are located along the river banks and are highly susceptible to flooding. The flooded areas on Fetam River have been represented depending on 5% incidence peak flows for different return periods (Desalegn & Mulu, 2021).

2.9 Mitigation Measures

Cities are complex and interdependent systems, extremely vulnerable to threats from both natural hazards and terrorism. Hazard mitigation is action taken to reduce or eliminate long-term risk to people and property from hazards and their effects (González et al., 2003).

Structural river training plans are traditionally known methods of flood mitigation and this method has been used in corporation with general flood management approach in most of flood plain areas. Flood risk reduction can access by reducing the magnitude of flood or vulnerability of effected area. Flood damages determination is not only important factor for risk management but also it is a significant parameter in evaluation of mitigation plan according to the type and size of measures (Heidari, 2009).

For sustainable development and environmental protection, non-structural measures have become popular solutions for flood hazard mitigation in the world. Most non-structural measures require risk analyses, which are carried out by physical or numerical models, as the rational basis for flood-alleviation planning. In many applications, different approaches were adopted for flood risk assessments via hydrological, ecological models (Chen, *et al.*, 2014).

3 METHODOLOGY

3.1 Location of the Study Area

Western Wabe Shebelle River basin is located in Oromia region, Southeastern Ethiopia. Its coordinate is located between latitude 6°40'00" - 7°30'00"N and longitude 38°40'00" - 39°40'00"E. The river reach within study area is approximately 121.48km in length running from North to Southeast. The total catchment area of the river basin delineated as watershed is about 5,040.58km^2.

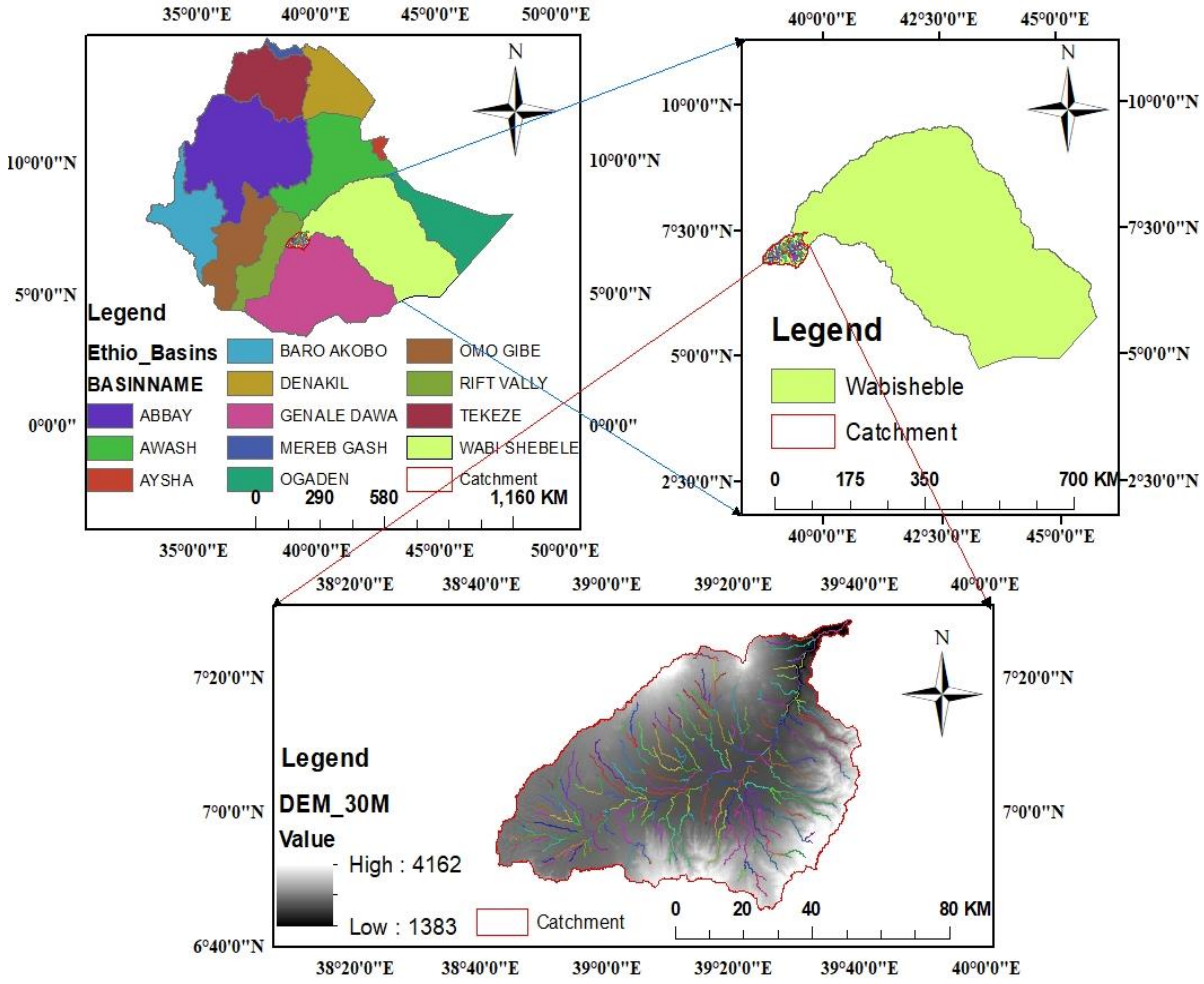

Figure 3.1 Study Area for Western Wabe Shebelle River basin watershed

3.2 Topography

The topography of Western Wabe Shebelle River is characterized by a wide range of elevations. The elevation ranges from 1383 to 4146 meters above sea level, and it flows from south to north. Knowing information about altitude and slopes, it is critical since it is used to calculate soil erodibility and measure rainfall erosivity. It is also an important aspect in defining land cover and characterizing suitable types of land use.

3.3 Climate

The climate of Western Wabe Shebelle River basin exhibits a wide range of temporal and spatial variability, which is predominantly determined by differences in altitude especially, Bale Mountains are reported to have had a glacier area possibly of up to 180km^2 during the last glacial period, from approximately 110,000 to 12,000 years (Osmaston, *et al.*, 2005).

But, no enough data were found on any scenarios of climate change impacts specifically for the basin catchment due to the shortage of information and absence of research studies done for the areas in the past years.

3.4 Data Preparation and Analysis

Many input data are required to analyze and achieve the objective of this study to have an accurate results. For this study case the required secondary data was collected from GIS (Geographic Information System) department, Ministry of water, Irrigation and Energy, Ethiopia (MoWE), Ethiopian National Metrology Agency (NMAE) and USGS satellite sources. The data collected for study area of Western Wabe Shebelle River basin are Digital Elevation Model (DEM), soil, land us/cover, rainfall and stream flow data as tabulated below.

Table 3.1 Sources for acquired data

Data	Source
Digital Elevation Model (30m by 30m)	ASTER Global Digital Elevation Model V003
Stream Flow and Soil	Ministry of Water, Irrigation and Energy, Ethiopia (MoWE)
Rainfall	National Metrology Agency (NMA) of Ethiopia
Land Use/Cover	USGS Landsat 8 OLI/TIRS C1 Level-1

The daily recorded and available rainfall data was only for 20 years (2000 to 2019) which is not recommended for analysis because it is less than 30 years and the recorded stream flow data was for 39 years (1981 to 2019) which is effectively optimum and recommended for data analysis that were collected and taken at Agarfa gaging station. The data were taken from Ethiopian National Metrology Agency (NMA) of Ethiopia and Ministry of water, Irrigation and Energy, Ethiopia (MoWE) as shown in the following table with the different rainfall gaging station and stream flow gaging station with their coordinate location, respectively.

Table 3.2 Rainfall gauging station in the study area

No.	Station Name	Longitude (in Degree)	Latitude (in Degree)

1	Adaba	39°24"0'	7°1"0'
2	Dinsho	39°38"37'	7°10"4.8'
3	Kofele	38°48"0'	7°4"1.2'
4	Siltana	39°23"24'	7°23"34.8'
5	Sire	38°58"2'	7°13"1.2'
6	Ego	39°3"0'	7°7"0.01'

Table 3.3 Stream flow gauging station

No.	Station Name	Site	Longitude (in Degree)	Latitude (in Degree)
1	Agarfa	At Agarfa	39°37"19.2'	7°26"56.4'

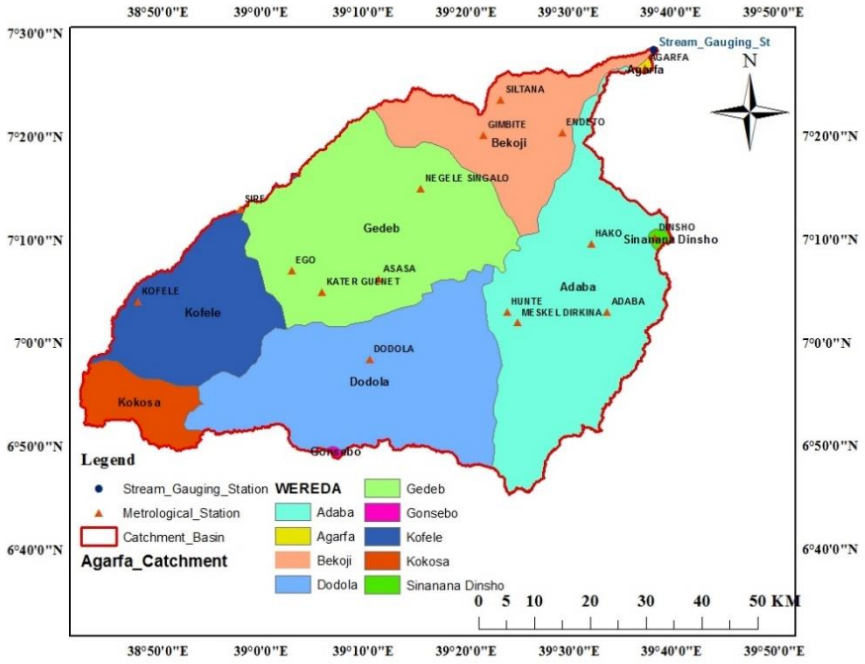

Figure 3.2 Rainfall and stream gauging station map in the basin catchment

3.4.1 **Filling Missing Data**

The precision of the outcome must be determined by the quality of available data. As a result, before using the data for analysis, it is necessary to check for missing data, inconsistencies, and accuracy. For this study case, the time for daily missing data was filled using multiple imputation methods by XLSTAT software, which is the best for filling missing data such as temperature, rainfall, and stream flow, as well as trend and homogeneity checks. Since XLSTAT 2019 is the most comprehensive tool for data analysis and statistical treatment with MS Excel, it is used in preparing, describing, visualizing, analyzing, and modeling data, correlation tests, parametric and non-parametric tests, outlier testing, homogeneity testing and trend testing.

The XLSTAT can allows the user to eliminate observations with missing values, apply a multiple imputation method or utilize a nearest neighbor strategy and algorithm for filling missing values for quantitative data. For this study case, the use of a multiple imputation method approach were used to fill the missing data for rainfall and stream flow. In filling the missing data, inconsistency problem should be checked, while data might be missing due to some instrument malfunction and recordings be failing for continuity. Thus, double mass curve was used for checking for data consistency.

The plot line should be straight and the R-squared value should lie between 0.6 - 1. As can be seen from the figure below, the linear trend line for R-squared was found to be 0.99 that could be rounded to 1. Hence, the data was consistent and can be used for analysis.

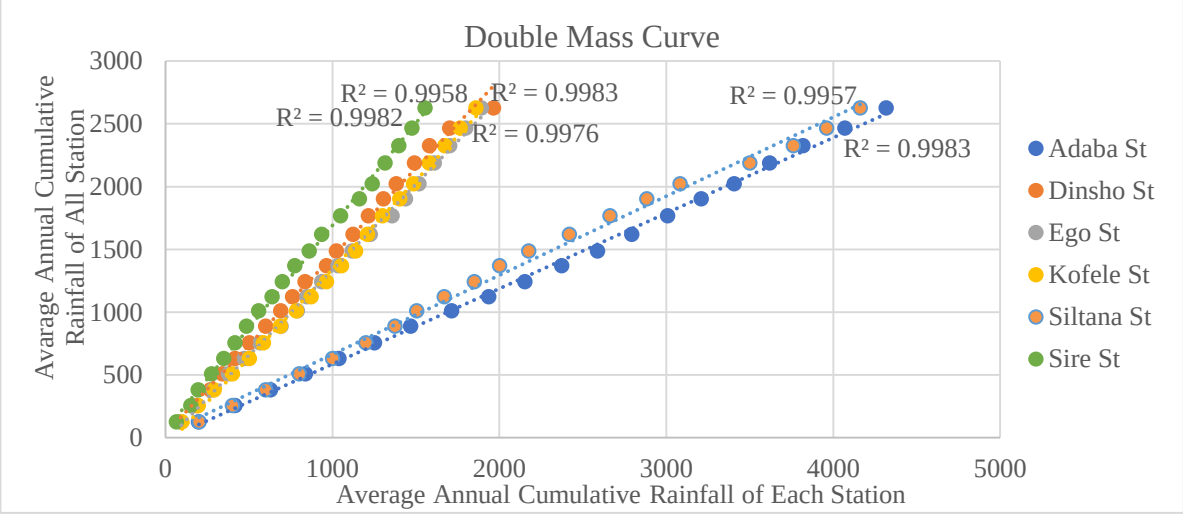

Figure 3.3 Double mass curve for checking the rainfall data consistency

3.4.2 **Test for Outliers**

The Water Resources Council method recommends that adjustments should be made for outliers. The outliers are data points that depart significantly from the trend of the remaining data. The retention or deletion of these outliers can significantly affect the magnitude of statistical parameters computed from the data, especially for small samples. Procedures for treating outliers require judgment involving both mathematical and hydrologic considerations (Ven Te Chow, *et al.*, 1988).

According to the Water Resources Council (1981), if the station skew is greater than +0.4, tests for high outliers are considered first; if the station skew is less than -0.4, tests for low outliers are considered first. Where the station skew is between ±0.4, tests for both high and low outliers should be applied before eliminating any outliers from the data set.

The following frequency equations can be used to detect high and low outliers respectively:

$$Y_H = \bar{y} + K_n S_y \quad \text{Eqn. (3.1)}$$

$$Y_L = \bar{y} - K_n S_y \quad \text{Eqn. (3.2)}$$

Where, Y_H = high outlier threshold in log units, Y_L = low outlier threshold in log units, $\bar{y}$ = mean value for log units in a recorded stream flow of a given sample size, S_y = standard deviation and K_n = sample size-based factor and used in one-sided tests that detect outliers at the 10% level of significance in normally distributed data.

Since, the case study sample size is 39 the K_n value 2.671 would be the suite factor (K_n values from Table 12.5.3 (Ven Te Chow, *et al.*, 1988)).

For this study case, the computed skew coefficient (Cs) is found to be 0.08572 which is between ±0.4, leading to tests for both high and low outliers using the equation (3.1) and (3.2).

$$Y_H = \bar{y} + K_n S_y = 2.75783 + 0.22864*2.671 = 3.3685$$

$$Y_L = \bar{y} - K_n S_y = 2.75783 - 0.22864*2.671 = 2.1471$$

Taking the anti-log of both Y_H and Y_L to compute the discharge (Q) that might be omitted or not from the sample, $Q_H = 10^{3.3685} = 2{,}336.29\,m^3/s$ and $Q_L = 10^{2.1471} = 140.32\,m^3/s$, respectively. Since all the sample size discharges in Table 3.5 are less than $2{,}336.29\,m^3/s$ for Q_H and greater than $140.32\,m^3/s$ for Q_L of the threshold value, hence there are no high and low outliers in this sample test. Therefore, all sample discharges were applicable for data analysis.

3.4.3 **Best Fit Probability Distribution Functions**

Flood frequency analysis was a critical parameter for water resource management and choosing the right probability distribution and parameter estimate method is crucial for on the ground flood frequency analysis. The yearly maximum steam flow at the location can be described using probability distribution functions such as Gumbel's, Generalized Extreme Value, Three-Parameter Log-Normal, Generalized Logistic and Pearson Type-III distributions. Goodness-of-fit tests and accuracy assessments are used to evaluate the performance of these distributions (Vrushali Wagh, *et al.*, 2020; Pal, *et al.*, 2020).

Probability distribution is a statistical concept in which the results of statistical experiments and their probabilities of occurrence are linked to probability distributions (Soon Kim Tiang, *et al*., 2020). The application of probability distribution model to annual flood flow assumes screening and application of non-parametric tests of randomness, independence, homogeneity and stationarity. It is only when empirical evidence was found to reject the non-parametric tests, before the available data is considered fitting for flood frequency analysis.

Among the several distribution methods that have been developed to estimate the parameters of probability distribution functions that can be estimated by maximum likelihood estimators (MLE), method of moments (MoM), by methods of L-Moments; the Methods of Moments (MoM) was good for limited range of parameters and more suitable due to three reasons than others: it is often simple to derive, it is consistent estimators for continuous type of probability distributions and it provide initial values in search for maximum likelihood estimates (Vivekanandan, 2015; Farooq, 2018) for data with lower skewness values and small sample sizes, whereas the method of L-moments was more suitable for data with higher skewness values and is appropriate for all sample sizes (Ologhadien, 2021).

Owing to its simplicity and being relatively easy to apply by equating the sample moments with the moments of the sample distribution functions, the MoM was used for this study case. Despite the fact that several probability distributions models have been considered in various situations, the study considers probability distributions models of Gumbel (EV1), Two-Parameter Lognormal (LN2), Log-Pearson Type III (LP3) and Generalized Extreme Value (GEV) and under the models, the GEV was chosen fitting best out of five probability distributions functions (PDFs) in this study.

Table 3.4 Probability models, sample parameters and moments

Probability Model	Probability Density Function	Range	Parameter	Quantile Function (QT)
EV1	$f(Q) = \frac{1}{\propto} e^{\left[-\frac{Q-\beta}{\alpha} - e^{\left(-\frac{Q-\beta}{\alpha}\right)}\right]}$ $F(Q) = e^{[-e^{\left(-\frac{Q-\beta}{\alpha}\right)}]}$	$-\infty \leq Q \leq \infty$ $0 \leq \beta \leq \infty$	$\mu = \beta + 0.5772\alpha$ $\sigma_Q^2 = 1.645\alpha^2$ $\alpha = \frac{\sqrt{6}S_y}{\pi}$ $\beta = \bar{Q} - 0.5772\alpha$	$Q_T = \beta + \alpha \ln[-\ln(1-\frac{1}{T})]$
LN2	$f(Q) = \frac{1}{Q\sigma_Q\sqrt{2\pi}} e^{-\left(\frac{(\log Q - \mu_Q)^2}{2\sigma_Q^2}\right)}$ $Q = \log Q$	$-\infty \leq Q \leq \infty$ $0 \leq x \leq \infty$	$Z = w - \frac{2.515517 + 0.802853w + 0.010328w^2}{1 + 1.432788w + 0.189269w^2 + 0.001308w^3} + P$ $P = 1\text{-}F = 1\text{-}(1\text{-}\frac{1}{T})$ $w = \sqrt{(-2\log(P))}$	$Q_T = e^{(\mu_Q + z\sigma_Q)}$
LP3	$f(Q) = \frac{(y-u)^\alpha}{\beta^2 Q\Gamma(\alpha+1)} e^{[\frac{-(y-u)}{\beta}]}$ $y = \ln Q$	$-\infty \leq Q \leq \infty$ $0 \leq Q \leq \infty$	Indirect MoM: $\mu_z = \gamma + \alpha\beta$ $\sigma_Q^2 = \alpha^2\beta$ $\beta = (^2/_{C_s})^2$	$Z_T = \ln Q_T$ $= \mu_z + K_T\sigma_Q$
GEV	$f(Q) = \frac{1}{\alpha}[1 - K\left(\frac{Q-\beta}{\alpha}\right)]^{\frac{1}{K}-1} e^{-[1-K\left(\frac{Q-\beta}{\alpha}\right)]^{\frac{1}{K}}}$	$\beta + \frac{\alpha}{K} > Q < \infty$ $-\infty < Q < \beta + \frac{\alpha}{K}$ $k \neq 0$	$K = \frac{\sqrt{6}}{\pi}\{0.5772 + [\ln(\ln\frac{T}{T-1})]\}$ $Y_T = -[\ln(\ln\frac{T}{T-1})]$ $\beta = \frac{\sigma_Q(Y_T - 0.5772)}{1.2825} + \bar{Q}$ $\alpha = \frac{\sqrt{6}S_y}{\pi}$	$Q_T = \beta + \frac{\alpha}{K}\{1 - [-\ln(1-\frac{1}{T})^K$
Normal	$f(x) = \frac{1}{\sigma\sqrt{2\pi}} e^{(-\frac{(x-\mu)^2}{2\sigma^2})}$	$-\infty \leq Q \leq \infty$	$K = w - \frac{2.515517 + 0.802853w + 0.010328w^2}{1 + 1.432788w + 0.189269w^2 + 0.001308w^3}$ $w = \sqrt{\ln(\frac{1}{p^2})}$ $P = \frac{1}{T}$	$X_T = \mu + K_T\sigma$
Where β, α, k and Q are the location, scale, shape parameters of the distributions and maximum discharge of stream flow, respectively.				

3.4.4 **Goodness of Fit Tests**

Goodness of fit tests can be reliably used in climate statistics like flood frequency tests to assist in finding the best distribution to use to fit the given data for analysis. These tests cannot be used to pick the best distribution, rather to reject possible distributions. These tests calculate test-statistics, which are used to deduce and analyze how well the data fits the given distribution. These tests describe the differences between the observed data values, and the expected values from the distribution being tested.

3.4.5 **EASY-FIT Software**

EASY-FIT is a program that identifies parameters in one-dimensional temporal systems using explicit model functions, steady-state systems, laplace transformations, differential algebraic equations, and ordinary differential equations systems (Schittkowski, 2002). It is a data analysis and simulation application that lets us fit and simulate statistical distributions with sample data, choose the best model, and utilize the results to make smoother decisions. This software can function as a stand-alone windows application and as an add-on for Excel spread sheet (Mehrannia & Pakgohar, 2014).

Many factors influence the choice of a distribution, including the method of comparing distributions, the method of parameter estimate, and the availability of data. The study employs three goodness-of-fit tests to assess different probability distributions.

1. Kolmogorov-Smirnov (K-S) Test

The Kolmogorov-Smirnov test statistic is based on both empirical and theoretical maximum vertical distance cumulative distribution functions (CDFs). A hypothesis is rejected if the test statistic is greater than the critical value at a given significance level, similar to the AD test statistic (Farooq, 2018; Millington, *et al.*, 2011).

For the significance level of $\alpha = 0.05$, the critical value calculated is depending on Easy-Fit software program for this study case. The samples are assumed to be from a cumulative distribution function (CDF) of F(x). The test statistic (D) is computed as:

$$D = \text{Max}|F_n(x) - F(x)| \quad \text{Eqn. (3.3)}$$

Where, F(x) = is the theoretical cumulative distribution function, and

$F_n(x)$ = is the empirical distribution function defined as:

$$F_n(x) = \begin{cases} 0, & x < x_{(i)} \\ \frac{1}{n}, & x_{(i)} < x_{(i+1)} \\ 1, & x > x_{(n)} \end{cases} \quad \text{Eqn. (3.4)}$$

For known distribution parameters, the distribution of the Kolmogorov-Smirnov statistic is independent of the considered distribution and the Easy-Fit software that generated the critical values of 0.07408, which best describes the GEV of a test statistic that can be used to determine the significance level.

2. Anderson-Darling (AD) Test

The Anderson-Darling test compares an observed cumulative distribution to an expected cumulative distribution function. The AD test gives more weight to the tail of the distribution than the K-S test, it is more powerful and has more weight. When used to extremely asymmetric distributions, such as those found in hydrological applications, the AD test has shown to be effective. If the statistic obtained is greater than a critical value at a particular significance level (α), the test rejects the hypothesis about the distribution level (Farooq, 2018; Millington, *et al.*, 2011).

The significance level most commonly used is α = 0.05, producing a critical value of 0.36758 fitting better ranking for GEV which gave maximum discharge for this study analysis. This number is then compared with the test distributions statistic to determine if it can be rejected or not.

The AD test statistic (AD^2) is:

$$AD^2 = -n - \frac{1}{n}\sum_{i=1}^{n}(2i-1)[Ln(F_{(x_i)}) + Ln(1 - F_{(x_{n-i+1})})] \quad \text{Eqn. (3.5)}$$

Where, AD^2 = Anderson-Darling test statistic

n = is the number of observations

$F_{(x_i)}$= is the Cumulative Density Function (CDF) for the data

3. Chi-Squared (x^2) Test

The Chi-Squared test is used to determine if a sample comes from a given distribution. It should be noted that this is not considered a high-power statistical test and is not very useful (Millington et al., 2011).

The test is based on binned data, and the number of bins (k) is determined by:

$$K = 1+\log_2 N \quad \text{Eqn. (3.6)}$$

Where N = sample size

The test statistic (x^2-test) is:

$$x^2 = \sum_{i=1}^{k}\frac{(O_i - E_i)^2}{E_i} \quad \text{Eqn. (3.7)}$$

$$E_i = F(x_2) - F(x_1) \quad \text{Eqn. (3.8)}$$

Where, O_i = is the observed frequency

E_i = is the expected frequency

x_1 and x_2 are the limits of i^{th} bin class

Hence, as the significance level, α = 0.05 produced a critical value of 0.83205 which best fits the GEV for this study analysis. Again, if the test statistic is greater than the critical value, the hypothesis is rejected.

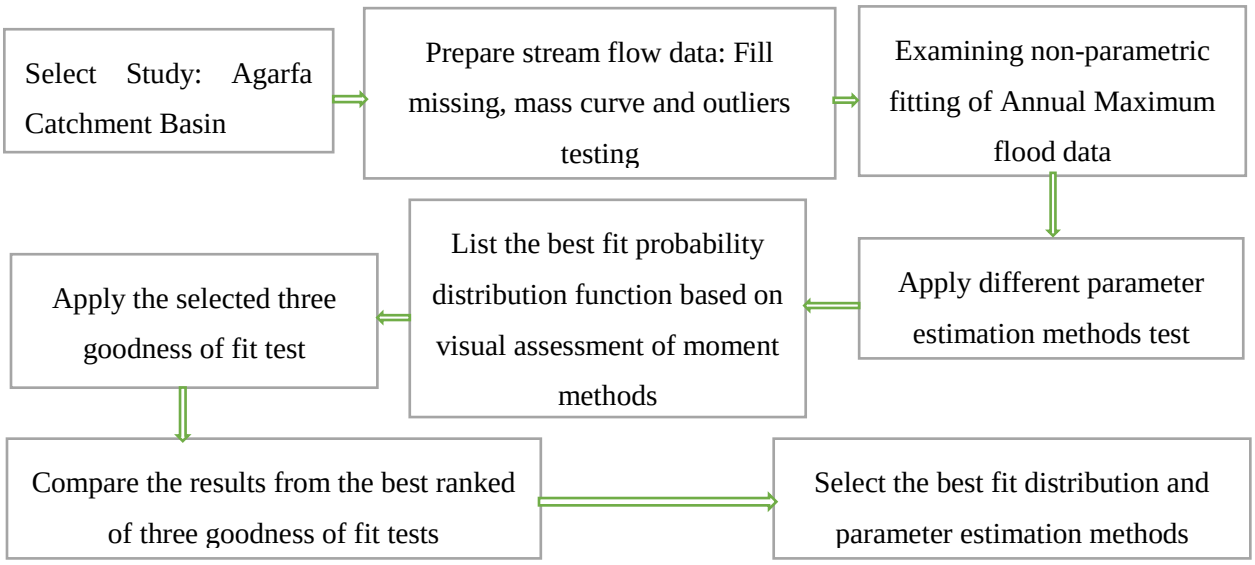

Figure 3.4 Flow chart procedure to select the best probability distributions

3.4.5.1 Statics Summary

Table 3.5 Descriptive statistics

Statistic	Value	Percentile	Value
Sample size	39	Min	125.91
Range	847.84	5%	169.6
Mean	555.49	10%	189.69
Variance	63679.0	25%(Q1)	373.04
Std. Deviation	252.35	50%(Median)	544.94
Coef. of Var.	0.45428	75%(Q3)	743.17
Std. Error	40.408	90%	938.58
Skewness	0.08572	95%	963.33
Kurtosis	-0.96868	Max	973.75

Table 3.6 Fitting distribution results

No.	Distribution	Parameters
1	GEV	k = -0.24254, $\alpha = 252.49$, $\mu = 549.68$
2	Normal	$\sigma = 252.35$, $\mu = 555.49$
3	Log-Pearson Type 3(LP3)	$\beta = -0.21874$, $\alpha = 6.3061$, $\gamma = 7.5725$
4	Pearson Type 3(PR3)	$\beta = 544.372$, $\alpha = 0.01022$, $u = -2.8764$
5	EV1	$\alpha = 1$, $\mu = 549.68$

Table 3.7 Goodness of fits summery

No.	Distribution	Kolmogorov-Smirnov		Anderson Darling		Chi-Squared	
		Statistic	Rank	Statistic	Rank	Statistic	Rank
1	GEV	0.07408	1	0.36758	1	0.83205	2
2	EV1	0.13804	4	1.6482	5	0.78925	1
3	LP3	0.10223	3	0.43317	2	3.9323	4
4	LN	0.15351	5	1.0053	5	7.1111	5
5	Normal	0.08671	2	0.44762	3	1.7777	3

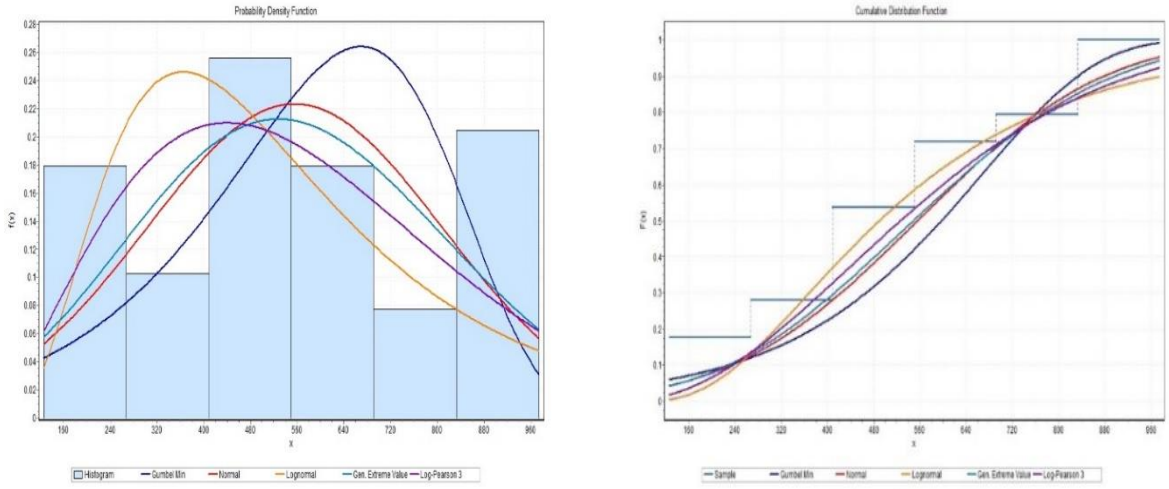

Figure 3.5 Histogram of PDF and CDF measured at selected Agarfa stream gauging station

As can be seen from Table 3.8 Goodness of fits summery, the GOF rank indicate that Kolmogorov-Smirnov and Anderson Darling test both give the General Extreme Value (GEV) best fitting statics and Chi- squared test gives EV1. The Extreme Value Distribution family of models, on the other hand, is used to represent data uncertainty, and the GEV distribution model is shown to be the best match distribution model testing.

The GEV model satisfied the selection criteria Kolmogorov- Smirnov Goodness of fit test and normality quantile-quantile (Q-Q plot) test, the variate class value which divides the sample into equal-sized probability distribution function were adopted under this study. The return levels are estimated for 10, 100, 200 and 1000 years which are consistently increasing with maximum discharge for long run in the future under GEV among the frequency distribution function selected for testing.

Table 3.8 Estimated maximum flood discharge for assumed design period for selection

Frequency Distribution Function	Estimated maximum flood discharge for a return period of T years			
	10	100	200	1000
LP 3	665.79	865.34	922.28	1053.53
GEV	1215.46	2595.62	3179.53	4978.06
EV1	484.97	462.20	460.94	459.93
LN2	587.17	893.95	986.54	1206.68
Normal	878.94	1142.66	1205.60	1335.38

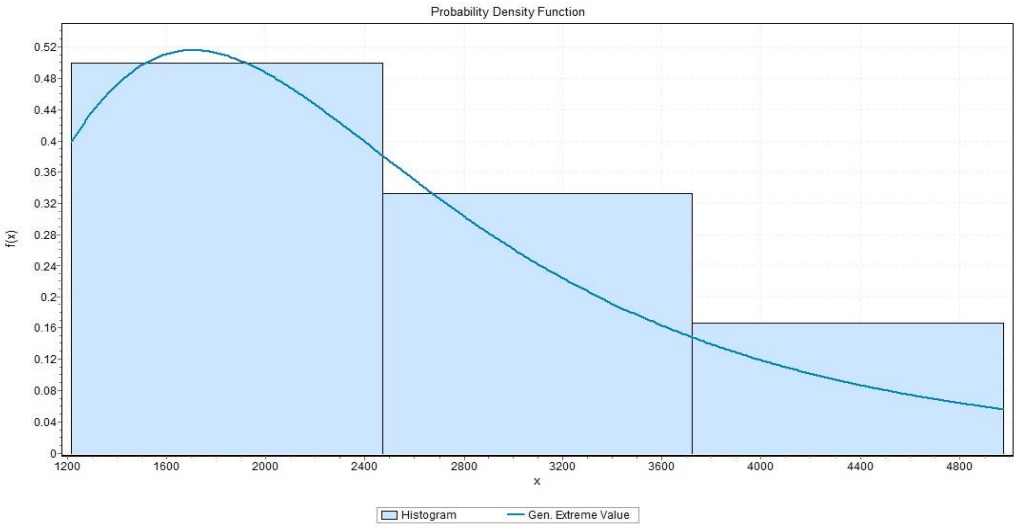

Figure 3.6 Best fitted PDF plot for estimated maximum flood discharge in return period

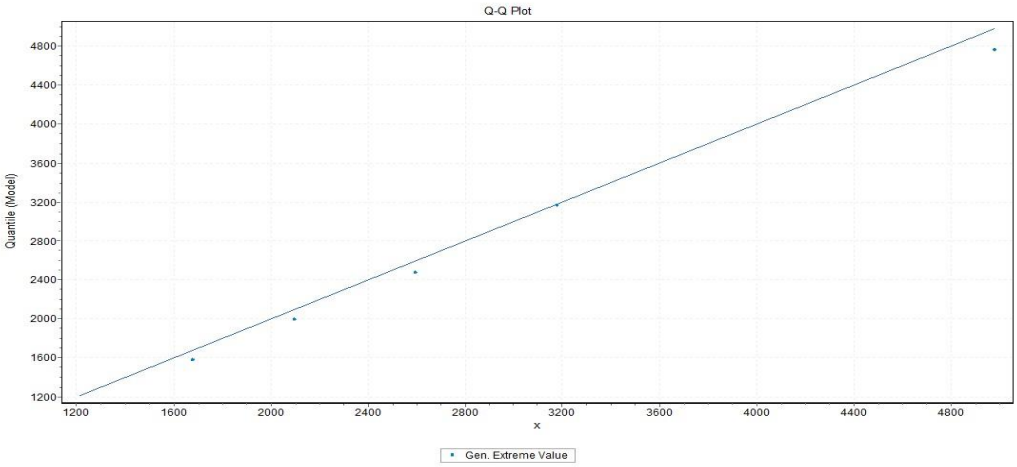

Figure 3.7 Normal Q-Q plot for estimated maximum flood discharge for given return period

3.5 Flood Hazard Development Factor

In order to develop the flood hazard map of the study area, the following interrelated components of five factors that could govern the environment was used as input data factors

for the incidence of flood disasters assessment that might occur in the basin of study area as discussed below in detail.

Particularly, flood causative factors in the study area were identified from questionnaire and literatures. Thus, the major causative factors are elevation, slope, land cover, rainfall, soil class types and drainage density were listed in order of their importance to flood hazard. Therefore, the following factor developed for flood hazard mapping.

3.5.1 **Elevation Factor**

Different elevations change the climatic features and this issue results in changes in vegetation and soil conditions. Elevation always plays an important role in flood susceptibility maps and dividing its categories using sequential classification method (Haghizadeh, *et al*., 2017). Elevation shares a great role with slope of topography of the study area based on its susceptibility to flooding as the lower the elevation value the higher the flood hazard and conversely the higher the elevation value the lower the flood hazard could always occur. The elevation map of study area was prepared from the reclassification of DEM.

As water flows from higher to lower elevation, lowland areas are more prone to flooding occurrences. The topographic elevation of Western Wabe Shebelle River basin catchment is varied from 1380m to 4146m. The upstream elevation is very high and lowest at the downstream surface. Thus, at upstream due to high elevation and steep slope there is high of runoff during high rainfall and cause high flooding at the downstream as result the slope of the land was flat, the river course allowed an overflow resulting in flood inundation.

Topography is defined by a Digital Elevation Model (DEM), which describes the elevation of any point in a given area at a specific spatial resolution as a digital file. A DEM was crucially needed for raster-based hydrological analysis in a GIS environment.

The study area DEM raster layer, which was reclassified into five group of flooding level using ArcGIS software, Spatial Analysis Tool, the classification was processed using the method of Equal Interval scale of DEM (30m resolution), using Reclassify Analysis. The lower the elevation area the higher the flooding level and vice versa. For this study case, based on the sequence of altitude difference to the vulnerability rating value to the flooding level of the elevation factor was ranked on Equal Interval scale per altitude range of the study area it covers as Very Low Flooding (3,243m - 4,146m), Low Flooding (2,819m - 3,242m), Moderate Flooding (2,510m - 2,818m), High Flooding (2,120m - 2,509m) and Very High Flooding (1,380m - 2,119m).

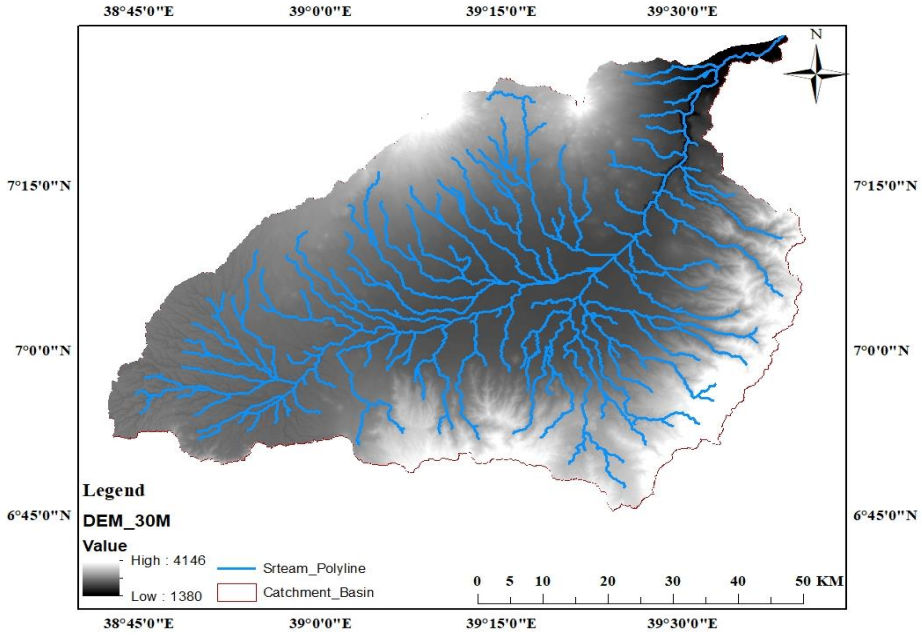

Figure 3.8 DEM of the study area

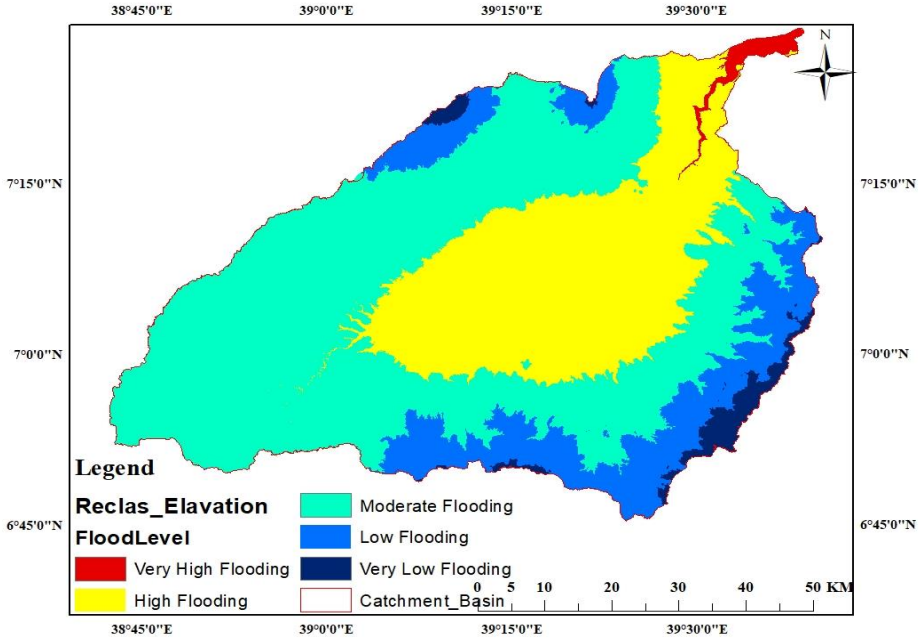

Figure 3.9 Reclassified elevation map and rating flooding level in the basin

3.5.2 **Slope Factor**

The slope is the proportion of a feature's steepness (degree of inclination) to its horizontal plane that has a great influence on flood hazard (Haghizadeh, *et al*., 2017). The flatter the slope, the higher is the probability of the area to be inundated with flood. Naturally, slops and elevations share important roles in affecting lowland areas as low slopes and elevations are

placed at high weights as potentially flooded areas and water is forced to flow from high elevations to low elevations, will cause the channel bursting excessively and reduce the rate of infiltration into the soil.

The slope raster layer, which was reclassified into five group of flooding level using the classification method of Equal Interval through processing the DEM (30m resolution), using ArcGIS software, Spatial Analysis Tool, Surface Slope Analysis. The flatter the area the higher the inundation level incidence after heavy rainfall. For this study case, based on the susceptibility rating value to flooding level due to the slope range in percentage was ranked as Very Low Flooding (93.4 - 506%), Low Flooding (45.8 - 93.3%), Moderate Flooding (23.9 - 45.7%), High Flooding (9.94 - 23.8%) and Very High Flooding (0 - 9.93%).

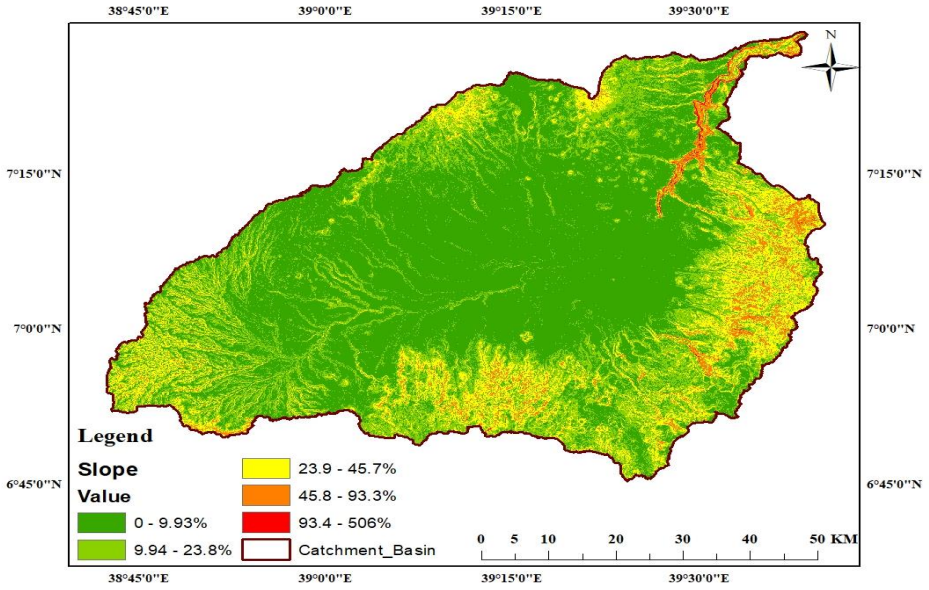

Figure 3.10 Slope map of basin catchment

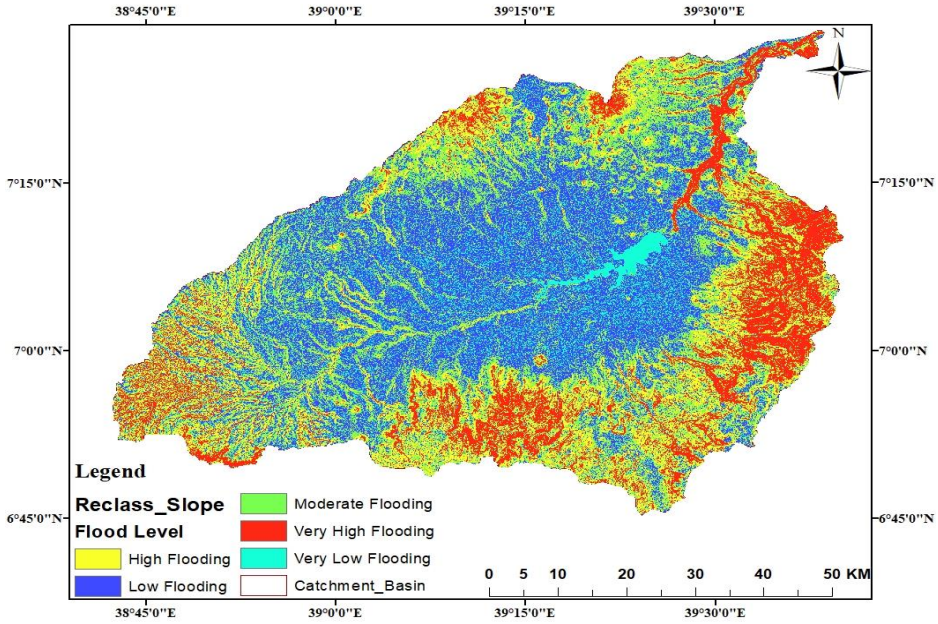

Figure 3.11 Reclassified slope map and rating of flooding level in the basin

3.5.3 **Land Cover Factor**

Land cover change is a dynamic, widespread, and fast-moving process triggered by natural phenomena and aggravated by human actions, resulting in changes that affect humans. For example, forestland is being converted to farmland, and settlement and urban development are reducing the amount of land available for food and timber production (Turi, *et al.*, 2019). Humans have significantly altered natural landscapes in deforested or drained places, potentially causing floods by either increasing or lowering antecedent soil moisture and prompting erosion (Rogger, *et al*., 2016).

Any kind of land cover in the catchment area have its productivity value which in turn affects the water quality whether it is positive or negative due to that in the built-up areas with pavements and buildings where little rainfall infiltrates into the soil causing high run-off and stream flow burst with high peaks of discharge surpassing the river basin causing flood inundation. Hence, land cover affects the level of infiltration, which is related to surface water and groundwater whereas forests and dense vegetation supporting infiltration, while in turn the urban land and grassland settlements enforces surface runoff flooding.

For this study case, the land cover was classified using supervised image classification method in Windows Image Analysis of ArcGIS. Thus, based on infiltration capacity level depending on the bare lands, agricultural, urban, water bodies and vegetative area clustering; the land cover factor classification was taken due to its susceptibility rating value to flooding level

based on land cover type that has greater influence and was ranked into five classes as Very Low Flooding (Forested lands), Low Flooding (Barren lands), Moderate Flooding (Water bodies), High Flooding (Agricultural lands) and Very High Flooding (Urban lands).

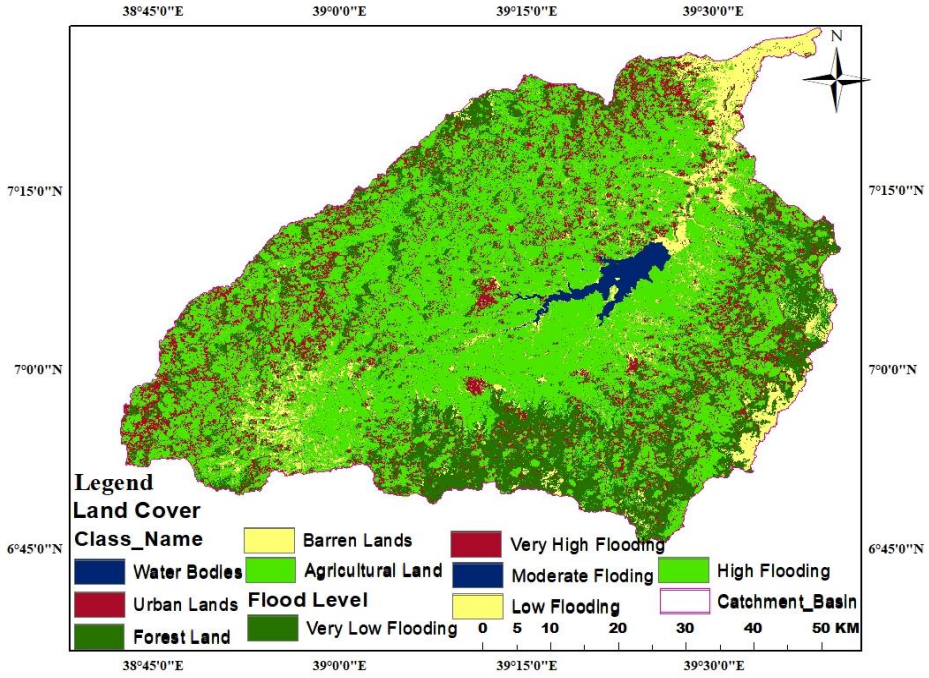

Figure 3.12 Clustered land cover and rating of flood level in the basin

3.5.4 **Rainfall Factor**

In order to determine flood hazard and risk assessment for a selected study area, the element of areal rainfall intensity data is essentially required. But, most of the time the only available and provided are data point for rainfall from elevation within and around the reading station measured by Meteorological Stations of NMA of Ethiopia has its own limitation due to the reading taken at station has shown fluctuation and therefore, the missing data for rainfall estimation was interpolated using the Inverse Distance Weighting (IDW) method, which is one of the most prevalent scattered point interpolation techniques.

According to the basic assumption of the IDW, the interpolating area could be influenced most strongly by neighboring points and less by distant points. The interpolating surface is a weighted average of the scatter points, and the weight assigned to each scatter point diminishes as the distance from the interpolation point to the scatter point increases (Kilinç, 2018; Tao Chen, *et al*., 2017)).

For this study case, the values of unknown points were calculated with a weighted average value of the six (6) point stations available at the known points. The spatial distribution of

rainfall intensity was considered based on the location of station in the study area. The annual average rainfall intensity raster layer; which was reclassified into five group of flooding level using the classification method of Equal Interval with annual average rainfall per hectare of catchment area, using ArcGIS software, Spatial Analysis Tool, Inverse Distance Weighting (IDW) interpolation analysis was implemented.

The higher the recorded average annual rainfall intensity then the higher the flooding level in the area. For this study case, based on the susceptibility rating to flooding level the rainfall intensity was ranked into five classes per hectare of catchment area as Very Low Flooding ($7.6x10^{-6} - 1.4x10^{-5}$ha), Low Flooding ($3.1x10^{-6} - 7.5x10^{-6}$ha), Moderate Flooding ($1.41x10^{-5} - 1.5x10^{-5}$ha), High Flooding ($0 - 2.3x10^{-6}$ha) and Very High Flooding ($2.4x10^{-6} - 3.1x10^{-6}$ha).

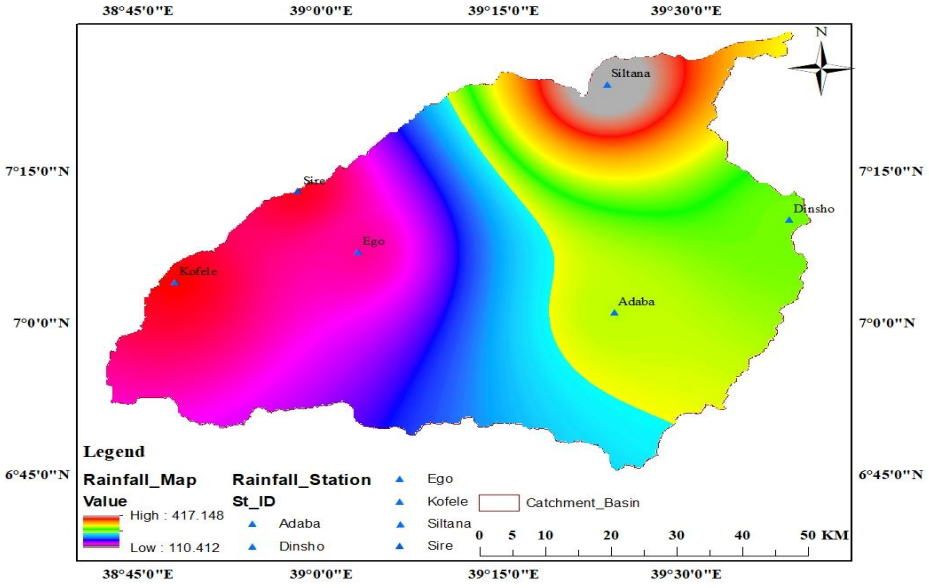

Figure 3.13 Rainfall map of the basin

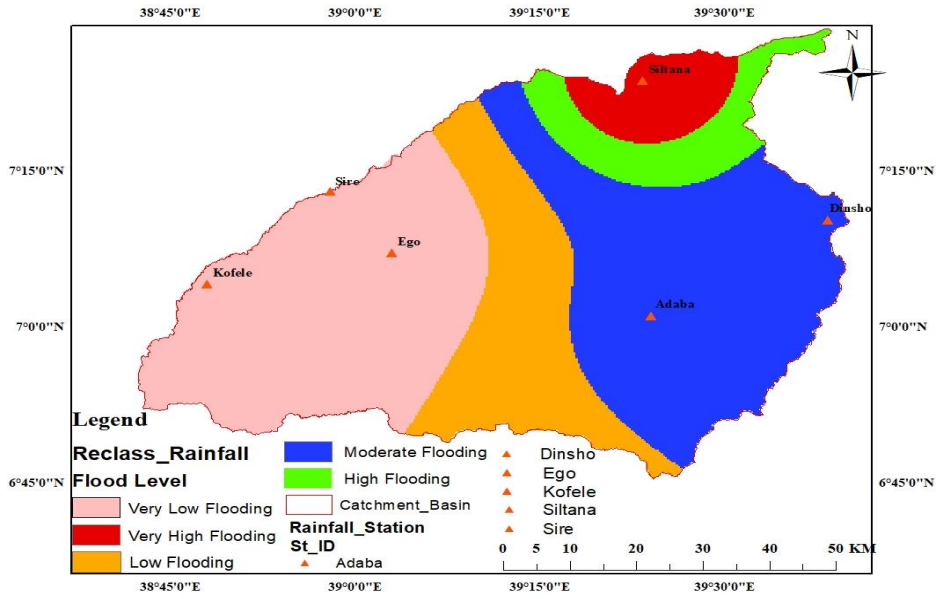

Figure 3.14 Reclassified rainfall map and rating flooding level in the basin

3.5.5 **Soil Factor**

Different soil types have different capacities to infiltrate water. The soil factors influencing the rate of infiltration are the total amount of soil porosity, the particle size distribution and the grain size distribution, soil structures (size distribution and structure of aggregates) and organic matter content of the soil. In general, sandy soils have higher saturated hydraulic conductivities than finer textured soils because of the larger pore space between the soil particles and the infiltration rate of clayey soils is much lower than that of sandy soils (Wang, *et al*., 2018).

Porous soils with stable soil aggregates have higher saturated hydraulic conductivity values than soils that are compact and dense. Soil texture classic type have a direct role in flooding effect due to grain size distribution, structures and degree of compaction of soil like coarse (>70% sand), moderately coarse, medium, moderately fine and fine (<40% clay) size (Alaoui et al., 2018). Hence, the basin soil texture was converted to raster format and reclassified based on their water infiltration capacity into flood rating result for soil factor map.

For this study case, based on soil infiltration capacity the susceptibility rating to flooding level was ranked into four classes depending on permeability of soil texture class factor as Low Flooding (Sandy loam soil: 36% - 45%km^2), Moderate Flooding (Loam soil: 15% - 24%km^2), High Flooding (Silty clay soil: 25% - 35%km^2) and Very High Flooding (Clay soil: 0% - 14%km^2).

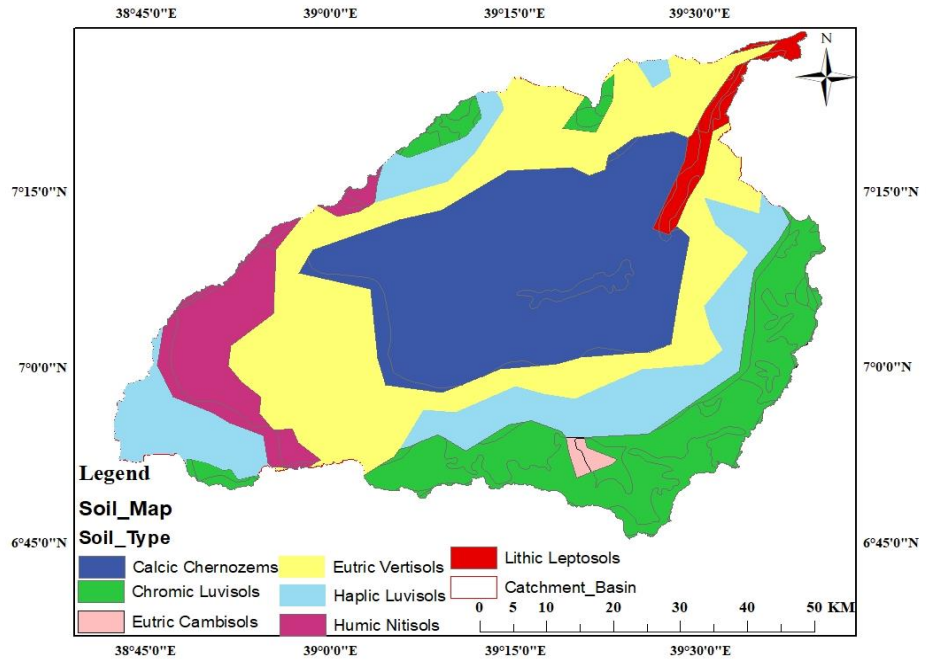

Figure 3.15 Soil map of the basin catchment

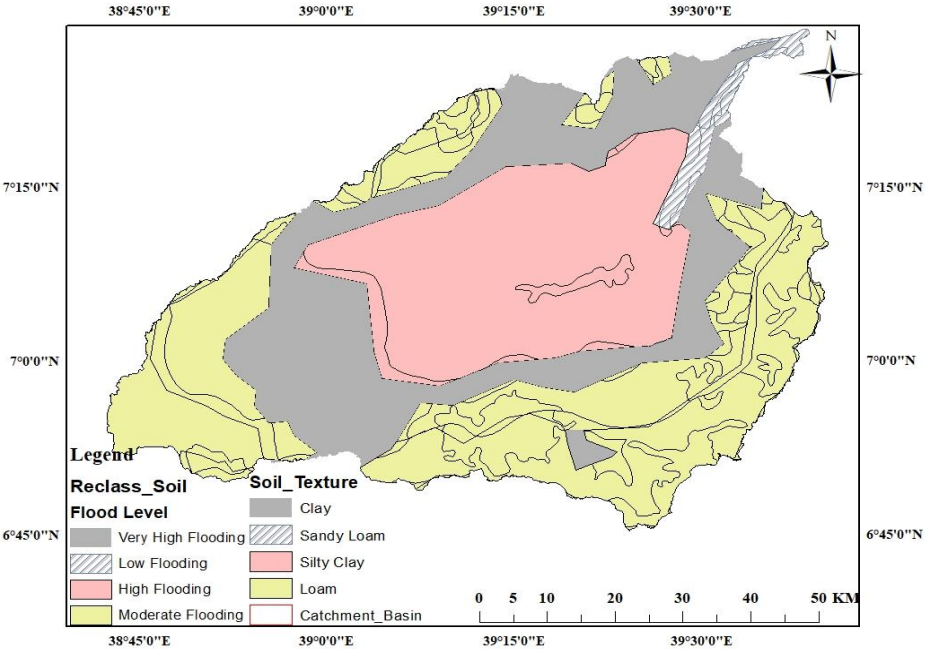

Figure 3.16 Soil texture map and rating of flooding level in the basin

3.5.6 **Drainage Density Factor**

Digital Elevation Model was used to extract the drainage network, to calculate the drainage density of the streams. The drainage network map of the basin was created using ArcGIS 10.8 software. From poly line features that fall within a radius around each cell, the spatial analyst's

line density module was utilized to quantify the magnitude of drainage density per unit area. Fundamentally, drainage density is a concept in hydrologic analysis that defined as the ratio of drainage length per basin area in the catchment, and is influenced by the permeability of surface materials, vegetation, slope and time (Dragičević, *et al.*, 2019).

It is very important in assessing flood hazard and risk within the study area and was generated from the digitized vector layer using ArcGIS spatial Analyst extension of Line Density Module. The total length of drainage is 1685.534m and the basin covers an area of 5040.58km^2. For this study case, based on the susceptibility rating value to flooding level the drainage density of the catchment was ranked into five classes as Very Low Flooding (0.079 - 0.086km/km^2), Low Flooding (0 - 0.0277km/km^2), Moderate Flooding (0.0278 - 0.0652km/km^2), High Flooding (0.0653 - 0.0767km/km^2) and Very High Flooding (0.0768 - 0.0789km/km^2).

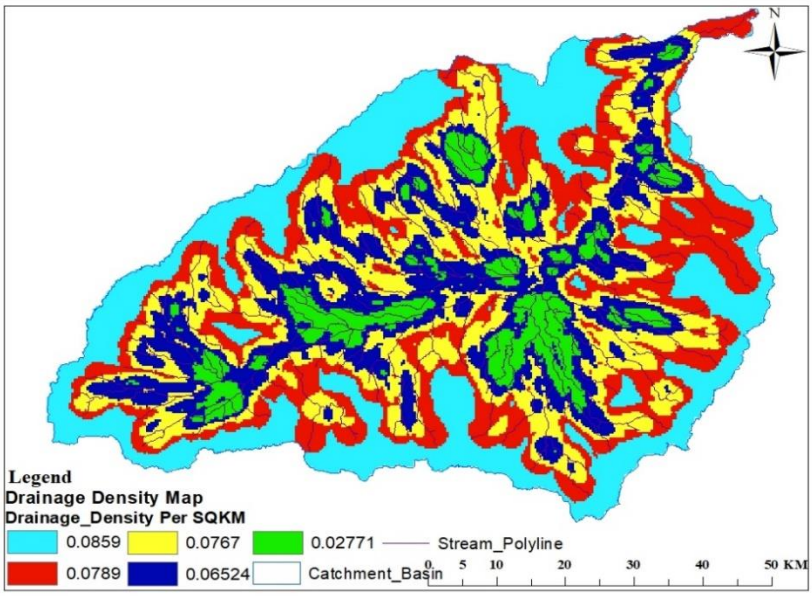

Figure 3.17 Drainage density in the catchment area

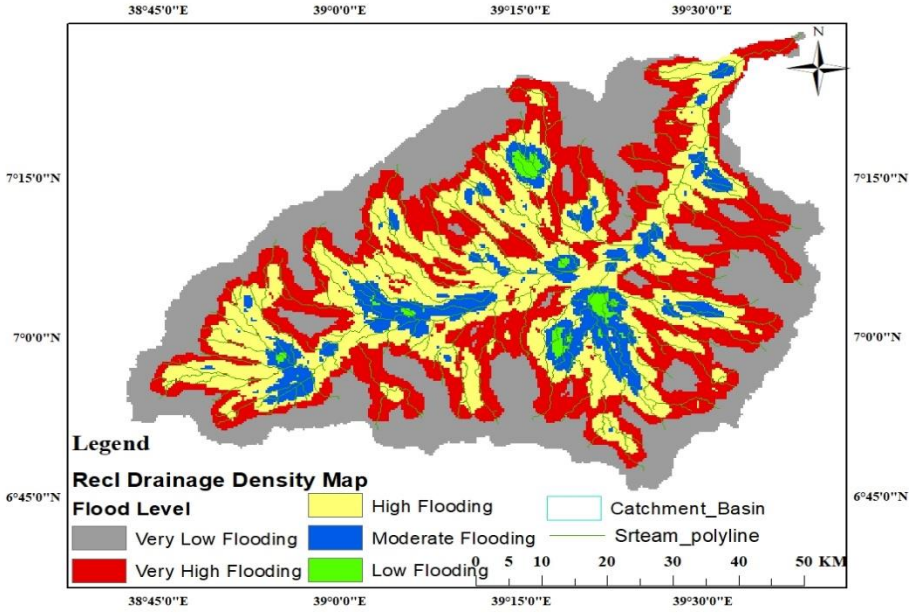

Figure 3.18 Reclassified drainage density and rating flooding level in the basin

3.6 Flood Hazard Assessment

Flood hazard characterizes the nature of flooding, the volume of water, the depth of water, the velocity of flows and the spatial and temporal dynamics. The analysis of past events helps to estimate the probability of a flood with given characteristics and the average time elapsed between the occurrence of a flood event and the next event of the same size (i.e. the return period is measured by frequency) (Foudi, *et al.*, 2015).

The flood hazard assessment needs to be presented using a simple classification as simple as possible indicating very high, high, moderate, low and very low hazard depending on its governing factors. Disaster assessment mapping uses different methods to integrate local knowledge, hydrological, meteorological and geomorphological data to depict flood-hazard areas in the basin. The last flood hazard feature necessitates the addition of local or field knowledge in the model. Assigning a ranks to a flood danger indicators, i.e. it necessitates local knowledge and can vary depending on factors such as soil texture, elevation, slope, rainfall, land cover and drainage density in the basin under study.

The net probability of occurrence of flooding in each flood hazard zone is estimated from the total sum of the weight of each contributing factor considered. To obtain this total sum weight, all of the contributing factor maps were overlaid. The total weight for estimating the probability of flooding in a particular flood hazard zone is equal to the sum of every contributing factor. The weighted overlay procedure in GIS allows the decision maker to

choose a list that meets a preset of criteria. The Raster Calculator in the ArcGIS Spatial Analyst tool was used for all of these procedures, including the compilation of contributing factor maps, the overlaying of all maps, and the estimation of hazardous regions.

Flash floods are one of the worst natural dangers on the planet, causing considerable damage and disruption to society. Several studies have looked at the effects of flash floods around the world in terms of significant financial losses, infrastructure destruction, relocation, and mortality. Extreme rainfall and large river discharge are predicted to rise as a result of climate change, increasing the possibility of frequent flash floods with greater intensity.

The main drivers of increased losses produced by natural disasters include the combined consequences of population development, inadequate land-use planning and management, and environmental degradation, as well as the impacts of climate change. Flash floods have been highlighted as a natural hazard having the greatest potential to cause catastrophic devastation to human society. The high risk associated with flash floods is due to its fundamental characteristic of quick start and occurrence in a short period of time, which severely limits the affected populations and concerned authorities' warning and response time.

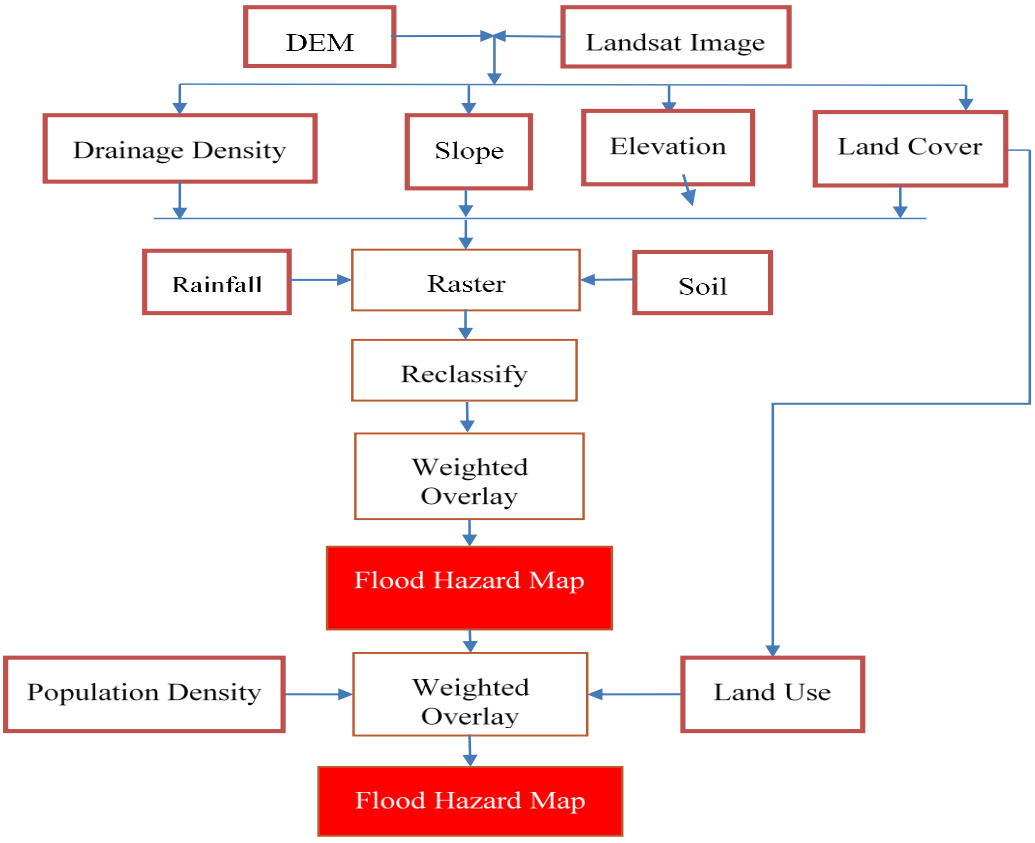

Figure 3.19 Flowchart for Flood Hazard and Risk Map

3.7 Flood Hazard Analysis

Hazard analyses give an estimation of the extent and intensity of flood scenarios and associate an exceedance probability to it. The standard technique is to run a flood frequency analysis on a set of discharge data and convert discharges associated with specific return periods, such as the 100 year event, into inundation extent and depths. This seemingly simple approach, however, has a number of drawbacks and uncertainties that must be taken into account (Apel et al., 2009).

Multi-Criteria Evaluation (MCE) is a procedure which needs several criteria to be evaluated to meet a specific objective technique that applied to assess flood hazard in the basin selected for studying using GIS. The standardized raster layers weighted using Eigen vector that is important to show the importance of each factor to compare and contrast to others in the contribution of flood hazard analysis.

As a result, in this study, the IDRISI Selva software was used for pair wise comparisons developed by Saaty's (1977) scale in the context of a decision-making process known as the Analytical Hierarchy Process (AHP), to estimate criteria in Eigen vector weighting (Saaty, 1977; Shahabi, *et al.*, 2014). Flood hazard analysis was computed by Weighted Overlay sum of elevation, slope, rainfall, soil, land cover and drainage density by multiplying with respective criteria weight factors computed in IDRISI and Excel sheet to develop flood hazard map in GIS.

Flood Hazard = 0.14[Elevation] + 0.15[Slope] + 0.16[Land Cover] + 0.17[Rainfall] + 0.18[Soil] + 0.20[Drainage density] ……..... Eqn. (3.9)

Table 3.9 Saaty's Scale for pair-wise comparison and consistency ratio for hazard factors

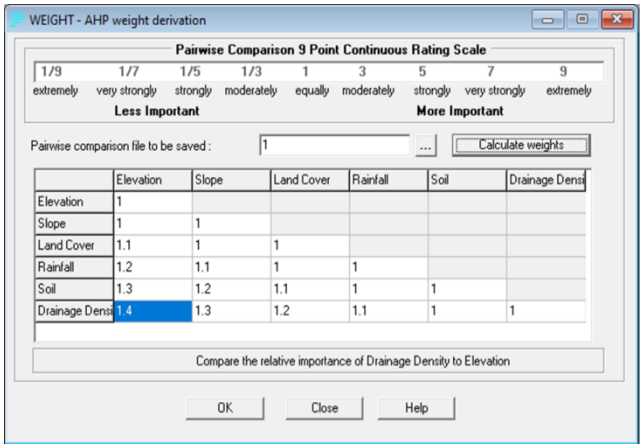

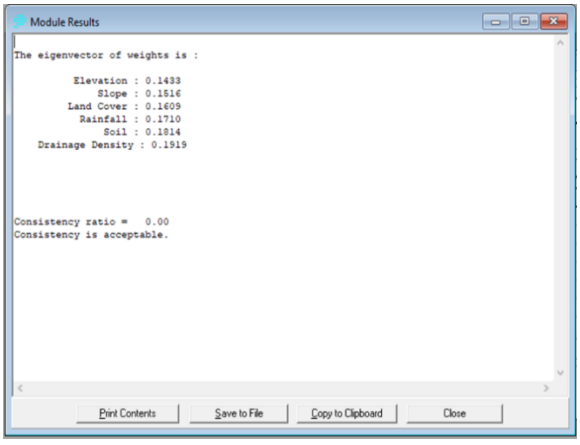

Table 3.10 Pair-wise comparison matrix assessing the importance of hazard factors in Excel

Pair-Wise Comparison	Elevation	Slope	Land Cover	Rainfall	Soil	Drainage Density
Elevation	1	1	0.909	0.833	0.769	0.714
Slope	1	1	1	0.909	0.833	0.769
Land Cover	1.1	1	1	1	0.909	0.833
Rainfall	1.2	1.1	1	1	1	0.909
Soil	1.3	1.2	1.1	1	1	1
Drainage Density	1.4	1.3	1.2	1.1	1	1
Sum	7	6.6	6.21	5.84	5.51	5.23

	Normalize Matrix						Eigen-Vector Criteria Weight	
Sum	7	6.6	6.21	5.84	5.51	5.23		
	Elevation	Slope	Rainfall	Land Cover	Soil	Drainage Density		
Elevation	0.143	0.152	0.146	0.143	0.140	0.137	Average	0.14
Slope	0.143	0.152	0.161	0.156	0.151	0.147	Average	0.15
Land Cover	0.157	0.152	0.161	0.171	0.165	0.159	Average	0.16
Rainfall	0.171	0.167	0.161	0.171	0.181	0.174	Average	0.17
Soil	0.186	0.182	0.177	0.171	0.181	0.191	Average	0.18
Drainage Density	0.200	0.197	0.193	0.188	0.181	0.191	Average	0.20
Sum	1	1	1	1	1	1	Ans:	1

Table 3.11 Weighted flood hazard ranking for Agarfa catchment

Weighted Flood Hazard Ranking for Agarfa Catchment-Basin				
Factors	Weight	Sub-Classic Rank	Ranking	Flooding Level
Elevation (Altitude Range)	0.14	3,243m - 4,146m	5	Very Low Flooding
		2,819m - 3,242m	4	Low Flooding
		2,510m - 2,818m	3	Moderate Flooding
		2,120m - 2,509m	2	High Flooding
		1,380m - 2,119m	1	Very High Flooding
Slope (% tage)	0.15	93.4 - 506%	5	Very Low Flooding
		45.8 - 93.3%	4	Low Flooding
		23.9 - 45.7%	3	Moderate Flooding
		9.94 - 23.8%	2	High Flooding
		0 – 9.93%	1	Very High Flooding
Land Cover (Infiltration Capacity Level)	0.16	Forested Lands	5	Very Low Flooding
		Barren Lands	4	Low Flooding
		Agricultural Lands	3	Moderate Flooding
		Water Bodies	2	High Flooding
		Urban Lands	1	Very High Flooding
Rainfall (Area-Hectare)	0.17	$7.6x10^{-6} - 1.4x10^{-5}$	5	Very Low Flooding
		$3.1x10^{-6} - 7.5x10^{-6}$	4	Low Flooding
		$1.41x10^{-5} - 1.5x10^{-5}$	3	Moderate Flooding
		$0 - 2.3x10^{-6}$	2	High Flooding
		$2.4x10^{-6} - 3.1x10^{-6}$	1	Very High Flooding
Soil (Texture Class)	0.18	Sandy loam	4	Low Flooding
		Loam	3	Moderate Flooding
		Silty Clay	2	High Flooding
		Clay	1	Very High Flooding
Drainage Density (km/km^2)	0.20	0.079 - 0.086	5	Very Low Flooding
		0 - 0.0277	4	Low Flooding
		0.0278 - 0.0652	3	Moderate Flooding
		0.0653 - 0.0767	2	High Flooding
		0.0768 - 0.0789	1	Very High Flooding

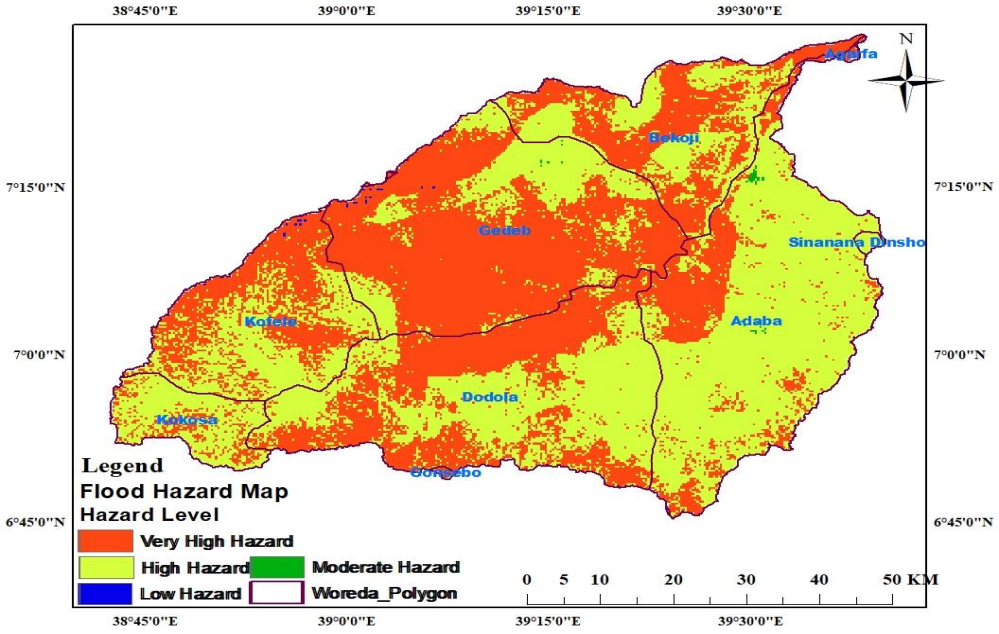

Figure 3.20 Flood hazard map of the study area

3.8 Flood Risk Development Factor

The development of flood risk map of the study area, was prepared taking the three interrelated components factors of land use, population density and the flood hazard layer developed were weighted overlay as input data factors for the prediction of flood risk disaster assessment that might occur in the basin of study area as discussed below in detail.

Hence, the importance and essence of this study was considering the elements of population density, land use and the flood hazard layer developed within the basin are used to drive the assessment of the flood risk in the Western Wabe Shebelle River basin watershed using Weighted Overlay process and the procedure follows as of flood hazard map preparation.

3.8.1 Land Use Factor

Land use describes activities, often associated with people that take place on the land and represent the current use of properties (i.e. multi-family residential homes, shopping centers, row crops, tree nurseries, state parks, reservoirs, cultivated lands, public roads and grazing) and undefined (i.e. exposed sand, rock out-crop, riverine forest, forestland, water bodies and wetlands) (Wondim, 2016).

Any kind of land uses in the catchment area have aggravated flood risk due to the activities of people that take place on the land cover; properties as multi-family residential homes, state parks, reservoirs, cultivated lands, public roads and grazing, and undefined (i.e. exposed sand,

rock outcrop, riverine forest, forestland, water bodies) affecting infiltration into the soil causing high run-off and stream flow burst with high peaks of discharge surpassing the river basin causing flood inundation. Hence, land use affects the level of infiltration, which is related to surface water and groundwater whereas forests and dense vegetation supporting infiltration, while in turn the urban land and grassland settlements enforces surface runoff flooding.

For this study case, based on infiltration capacity level depending on land use clustering; the land use factor classification was taken due to its susceptibility rating value to flooding level influence and was ranked into five classes per hectares it cover as Very Low Flooding (Forest lands, riverine forests: 1% – 13%ha), Low Flooding (Exposed sands: 37% - 47%ha), Moderate Flooding (Cultivated lands, public roads, state parks: 48% - 59%ha), High Flooding (Rock outcrops: 25% - 36%ha) and Very High Flooding (Built-up areas: 14% - 24%ha).

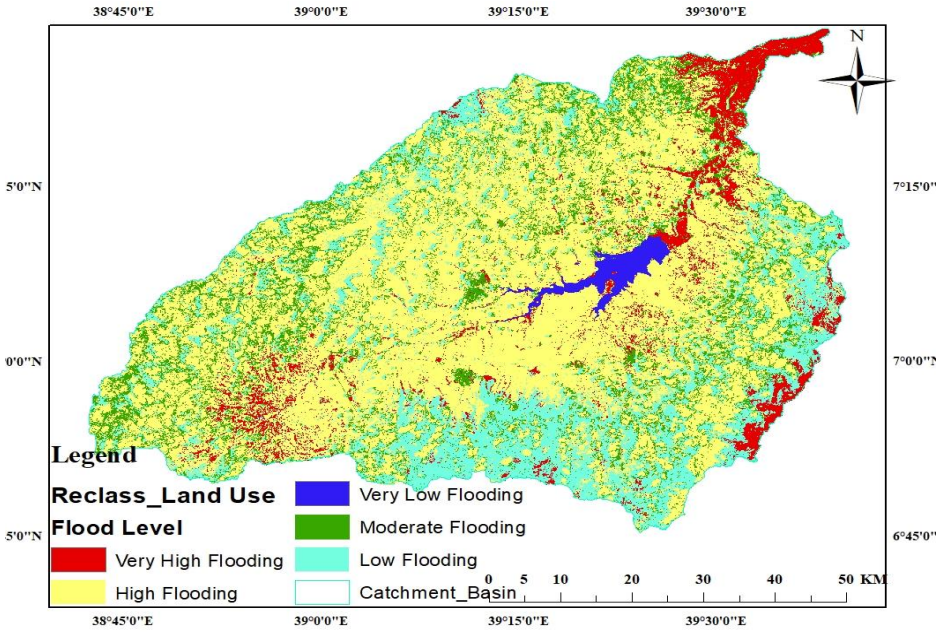

Figure 3.21 Reclassified Land use and rating of flood level in the basin

3.8.2 **Population Density Factor**

Populations are not evenly distributed over the earth's landmass due to some physical, socio-economic and demographic factors like climate, topography, soil, energy and mineral resources, accessibility in terms of distance from the coast, natural harbors, navigable rivers or canals, cultural traits, economic activities, technologies employed (including farming type), and social organization, changes caused by natural increase and migration.

The political boundaries, political stability, disturbances, migration and trade controls, government policies, and transportation facilities are all factors to consider that determines the population density as a number of people per square of land area, which allows for a comprehensive comparison of settlement intensity across geographic. The gross population density technique is used to calculate the number of persons per square kilometer in the watershed.

The statistics of the population data under the study area was taken from the Ethiopian administrative population projection. Ethiopian is currently one the fastest growing with a rate of 3.02% per year and has a population density of 32.046 per square kilometer, which ranks 123 in the world.

For this study case, the population density map was reclassified based on the assumption that the higher the population density range in the catchment area per square kilometer, the more vulnerable it was to the flood hazard and vice versa. Hence, the vulnerability rating value to flooding level was ranked into five classes depending on the population density range factor as Very Low Flooding (21.86 - 58.74Popn/km^2), Low Flooding (58.75 - 95.61Popn/km^2), Moderate Flooding (95.62 - 132.5Popn/km^2), High Flooding (132.6 - 169.4Popn/km^2) and Very High Flooding (169.5 - 206.2Popn/km^2).

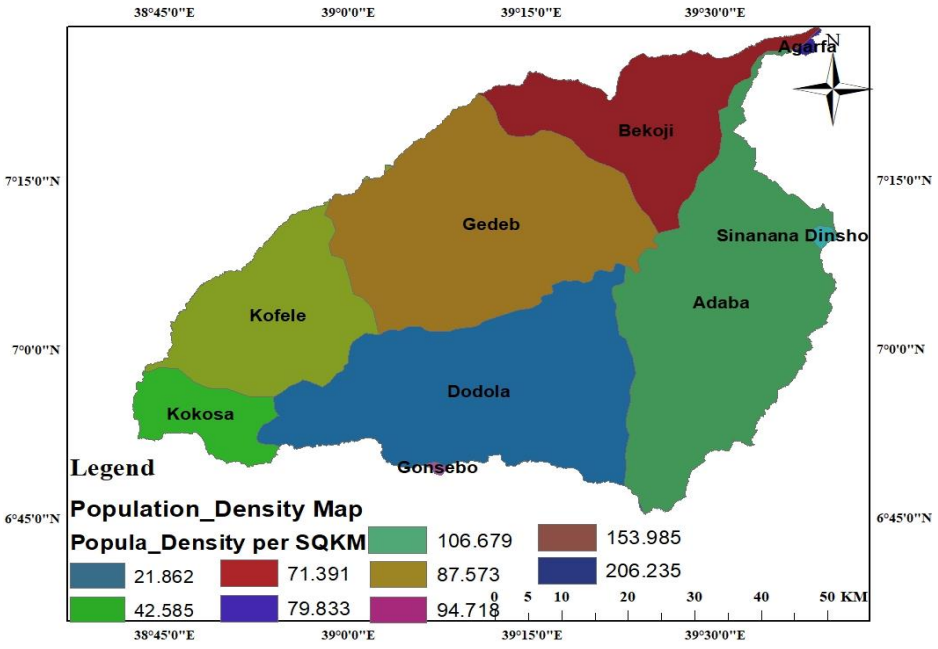

Figure 3.22 Population density map per square kilometer

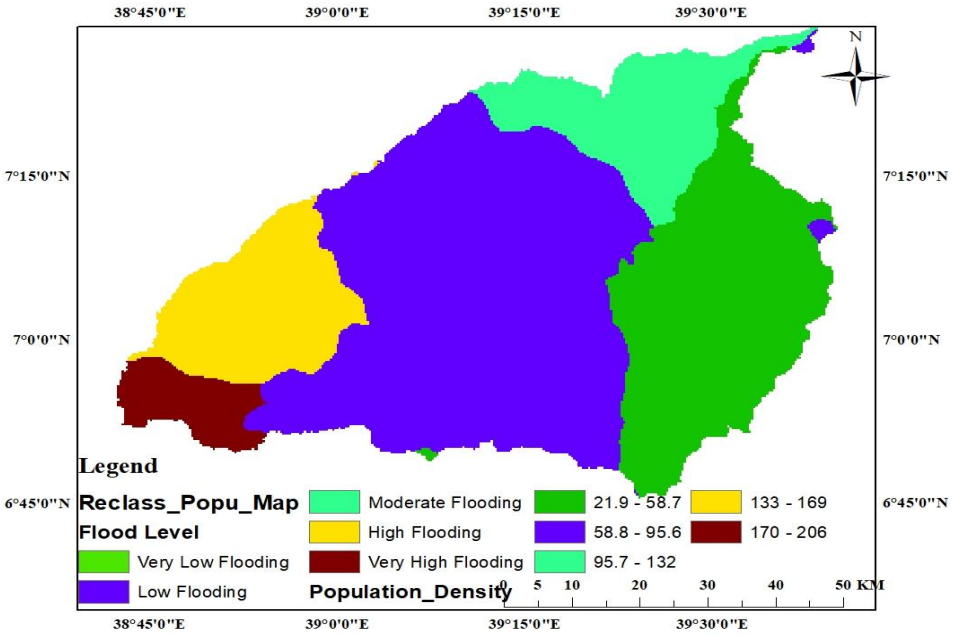

Figure 3.23 Reclassified population map and rating of flood level in the basin

3.8.3 **Flood Hazard Factor**

The flood hazard layer developed in the previous section through weighted overlay process from the raster format of elevation, slope, rainfall, soil class types and drainage density factors multiplied with their respective criteria weight functions has produced flood hazard factor that could be as input data reused for flood risk analysis as discussed in section 3.7.

3.9 Flood Risk Assessment

In analyzing flood risk, flood exposure and flood vulnerability should be integrated with flood hazard to give a comprehensive resource of reference for flood risk managers. Flood hazard is defined as the risk of harm, damage from an occurrence that happens at a single location. The potential for human risk and property damage during flood occurrences is characterized as exposure to flood hazard.

Flood risk assessment equation:

Flood Risk = Hazard*Exposure*Vulnerability ……..…….....…. Eqn. (3.10)

3.10 Flood Risk Analysis

Risk-oriented approaches and risk analyses are gaining popularity in the fields of flood design and flood risk management because they allow one to analyze the cost-effectiveness of mitigation measures and hence optimize investments. It is the product of physical and statistical aspects of actual flooding (flood return period, flood size and depth) and

vulnerability, defined as flood risk, i.e. exposure of people and property to flooding as well as the sensitivity of objects at risk of flood damage (Apel, *et al.*, 2009).

Hence, the flood risk analysis for this study was computed by Weighted Overlay sum of flood hazard, land use and population density by multiplying with respective criteria weight factors computed in IDRISI Selva and Excel sheet to develop flood risk map in GIS.

Flood Risk = 0.333[Flood hazard] + 0.333[Land use] + 0.333[Population density].. Eqn. (3.11)

Table 3.12 Saaty's Scale for pair-wise comparison and consistency ratio for risk factors

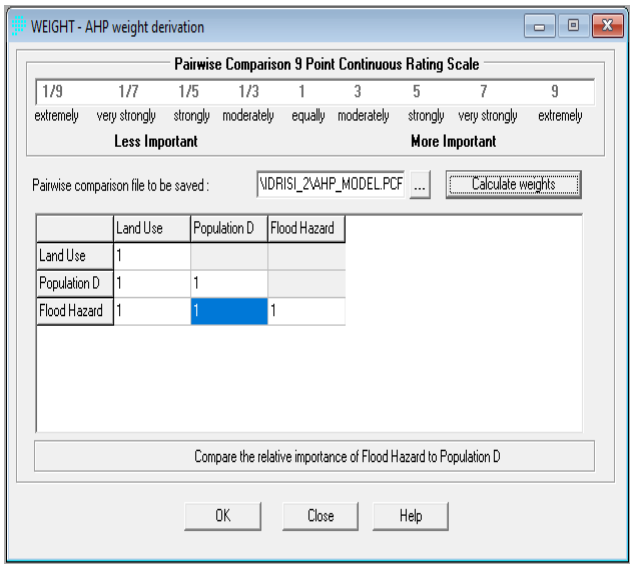

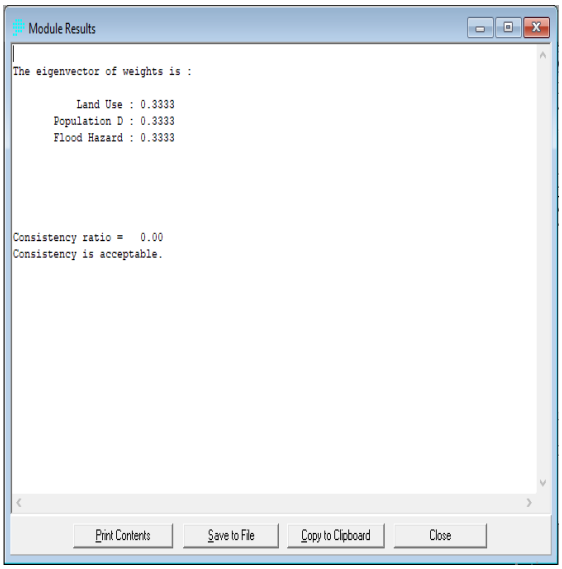

Table 3.13 Pair-wise comparison matrix assessing the importance of risk factors in Excel

Pair-Wise Comparison		Flood Hazard	Land Use	Population Density	
Flood Hazard		1	1	1	
Land Use		1	1	1	
Population Density		1	1	1	
Sum		3	3	3	
	Normalize Matrix			Eigen-Vector Criteria Weight	
Sum	3	3	3		
	Flood Hazard	Land Use	Population Density		
Flood Hazard	0.333	0.333	0.333	Average	0.33
Land Use	0.333	0.333	0.333	Average	0.33
Population Density	0.333	0.333	0.333	Average	0.33
Sum	1	1	1	Ans:	1.00

Table 3.14 Weighted flood risk ranking for Agarfa catchment

Weighted Flood Risk Ranking for Agarfa Catchment-Basin				
Factors	Weight	Sub-Classic Rank	Ranking	Flooding Level
Flood Hazard (% tage)	0.333	0.1% - 47.74%	4	Low Flooding
		0 - 0.05%	3	Moderate Flooding
		0.06% - 0.09%	2	High Flooding
		47.75% - 52.1%	1	Very High Flooding
Land Use (Clustered by infiltration level)	0.333	Forestlands, riverine forests	5	Very Low Flooding
		Exposed sands	4	Low Flooding
		Cultivated lands, public roads, state parks	3	Moderate Flooding
		Rock outcrops	2	High Flooding
		Built-up areas	1	Very High Flooding
Population Density $(\frac{\text{Total Population}}{km^2})$	0.333	21.86 - 58.74	5	Very Low Flooding
		58.75 - 95.61	4	Low Flooding
		95.62 - 132.5	3	Moderate Flooding
		132.6 - 169.4	2	High Flooding
		169.5 - 206.2	1	Very High Flooding

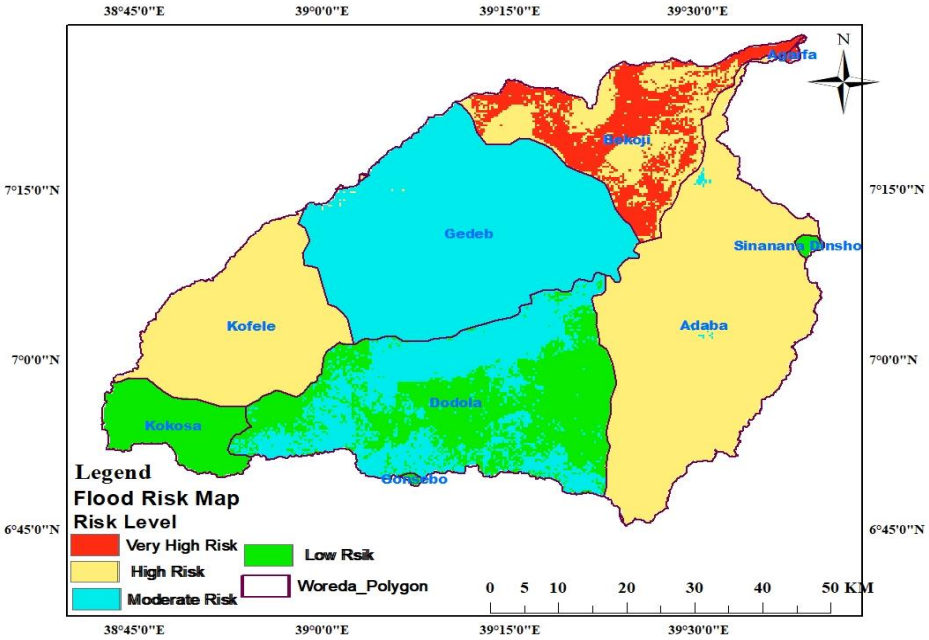

Figure 3.24 Flood risk map of study area

3.11 Flood Inundation Mapping

An inundation occurs when a large body of water submerges land and the channel's capacity is exceeded and water flows bursts over of it. Several factors, including the size and character of the river, the vegetation in and around the river, downstream water levels and others, decide

whether or not floods occur in a certain place (Desalegn and Mulu, 2021b; Namara, *et al.*, 2021).

3.11.1 **HEC-GeoRAS and ArcGIS**

Hydrologic Engineering Center-Geospatial River Analysis System (HEC-GeoRAS) uses functions that associated with ArcGIS Spatial Analyst, 3D Analyst Tool for converting the DEM raster to TIN terrain, for setting up spatial data input for Hydrologic Engineering Center's River Analysis System (HEC-RAS) models from digital terrain models and other GIS datasets (Merwade, 2016).

Using GIS for hydraulic modeling and setting up analysis environment for HEC-GeoRAS normally involves three steps: data pre-processing; model execution and results of post-processing or visualization.

3.11.2 **Creating RAS Layers**

Because of its compatibility with GIS software, Hydrologic Engineering Center-Geospatial River Analysis System (HEC-GeoRAS) software is extensively used to create river geometries such as stream centerlines, left and right banks, channel flow routes, and cross-sectional lines and normal depth was assigned at the downstream boundary condition in the HEC-RAS model using slope friction (Mokhtar, *et al.*, 2018).

The geometry file for HEC-RAS contains information on cross-sections, hydraulic structures, river banks and other physical attributes of river channels. The pre-processing using HEC-GeoRAS involves creating these attributes in GIS, and then exporting them to the HEC-RAS geometry file. In HEC-GeoRAS, each attribute is stored in a separate feature class called as RAS Layer. Accordingly, before creating river attributes in GIS, first creating an empty GIS layers using the RAS Geometry menu on the HEC-GeoRAS toolbar is the crucial step to start working with RAS Layers.

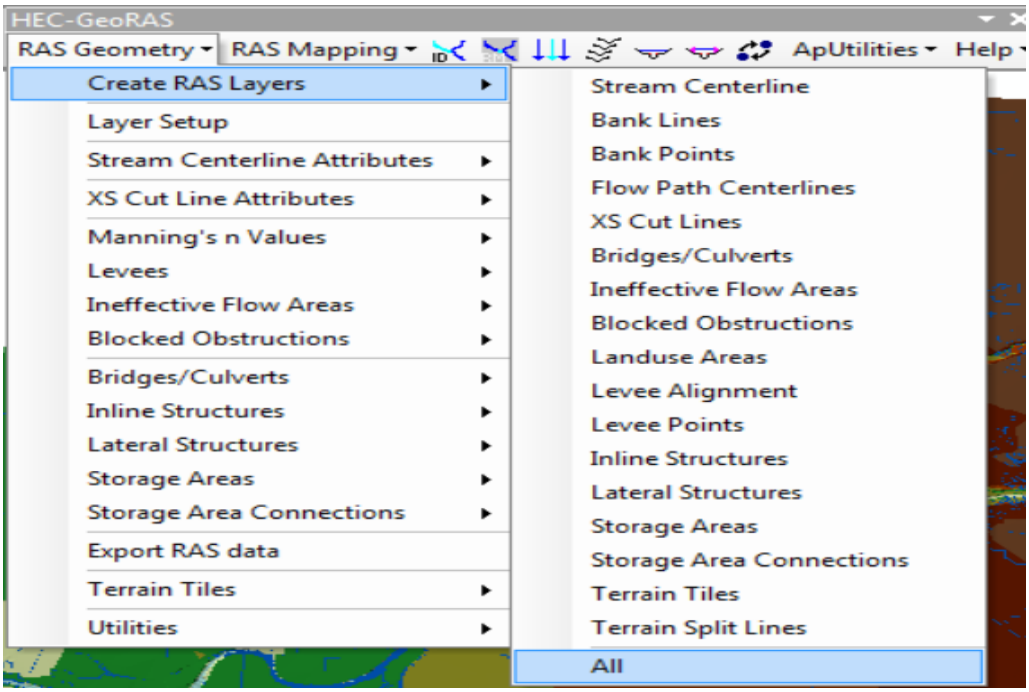

Figure 3.25 RAS Layer creating toolbar

After creating RAS layers, the following most important four RAS Geometry layers are used to create (digitize) the HEC-GeoRAS geometry file for study of Agarfa basin catchment.

1. Creating River Centerline

The river reach network for HEC-GeoRAS is established using the river centerline. The next step is to name the reaches after they have been digitized. In HEC-GeoRAS, each river must have its own name, and each reach within a river must have its own name.

The process in this case begins at the upstream end of the Agarfa basin catchment and ends at the downstream end. After digitizing all of the reaches, the user was issued a river name. The necessary names were assigned by using the Assign River code/Reach code menu option.

2. Creating River Banks

Bank lines separate the main canal and the overbank floodplain parts. Based on information regarding bank locations, different qualities for cross-sections are assigned. To account for extra roughness caused by vegetation, overbank sections have higher Manning's n values than the main channel. The procedure of producing bank lines is identical to that of creating a channel centerline, with the exception that there are no specific criteria for line alignment and connectivity. They can be digitized in either the flow's direction or in the opposite direction, and they can be continuous or broken.

3. Creating Flow Paths Centerlines

There are three sorts of lines in the flow path layer: centerline; left over-bank; and right over-bank. As a result, flow path lines are utilized to determine the downstream reach length between main channel cross-sections and overbank locations. The river centerline, which we generated previously, can be utilized as the flow path centerline if it lies roughly in the center of the main channel (Merwade, 2016).

4. Creating Cross-sections

To construct a ground profile along channel flow, cut lines in cross-section are utilized to obtain elevation data from the landscape. HEC-GeoRAS features include embankment stations (locations that separate the main river channel from the floodplain), downstream reach length (distance between cross-sections), and Manning. It is determined by combining the cutting line with other RAS (River Analysis System) layers (such as centerline and the flow path line) intersect to calculate. Due to that a sufficient number of cross-sections must be created in order to produce a good depiction of the channel bed and floodplain, which is crucial.

The following principles must be observed while digitizing cross-section cut lines: cut lines must be perpendicular to the flow direction; cut lines must span the entire flood extent to be modeled and digitization must always be done from left bank to right bank looking the downstream flow.

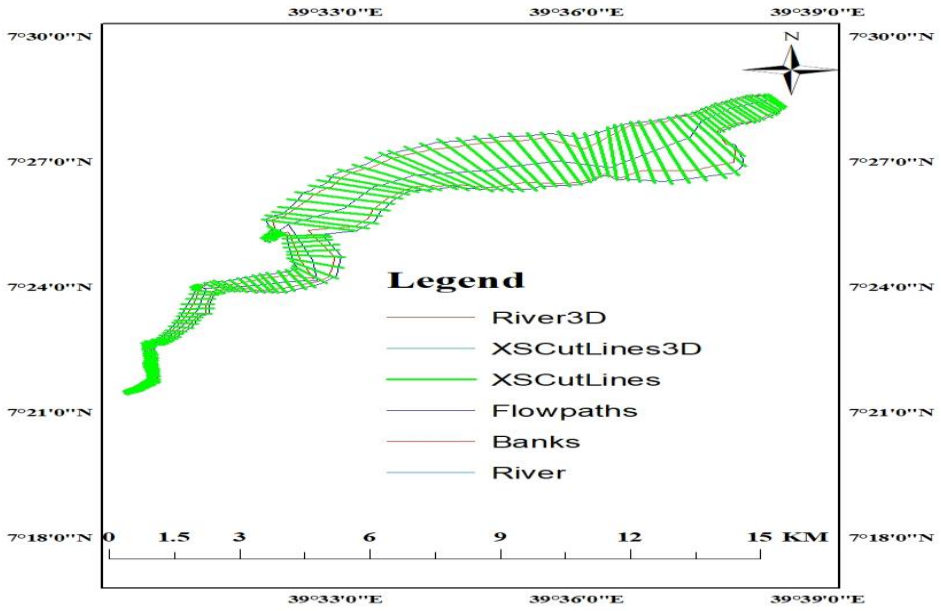

Figure 3.26 Upper Wabe Shebelle River geometry created in HEC-GeoRAS

3.11.3 **Hydraulic Modeling**

Based on the modeling approach, the Hydrologic Engineering Center's River Analysis System (HEC-RAS) was used for hydraulic modeling using a river cross-section dataset, Manning's n values, and flow data including flow rates, flow change locations, and boundary conditions (Zin, *et al.*, 2015). The 2D hydraulic flood propagation models are very important for flood hazard assessment. For model parameterizations such as terrain slope, cross sections, and flow pattern, flood models require a precise representation of the floodplain in the form of hydro-enforced terrain data, which is generally prepared with a DEM.

Stream representation in a DEM is necessary for a 2D flood model and can be achieved using DEM hydro-enforcement. Furthermore, the resolution and accuracy of the DEM used in flood simulations are critical. The depth and area of flood inundation, as well as exposure to land cover/use, are significant aspects of flood hazard assessment (Worlddem, 2019) .

HEC-RAS software allows the user to perform hydraulic calculations of a one-dimensional (1D) and two-dimensional (2D) flowing unstable river. It is an integrated system of software, designed for interactive use in a multi-tasking, multi-user network environment. The system includes four components of hydraulic analysis for: calculating the profile of the surface of water with a steady flow; one and two-dimensional modeling of unsteady flow; mobile boundary calculations for sediment transport; and modeling water temperature and transport.

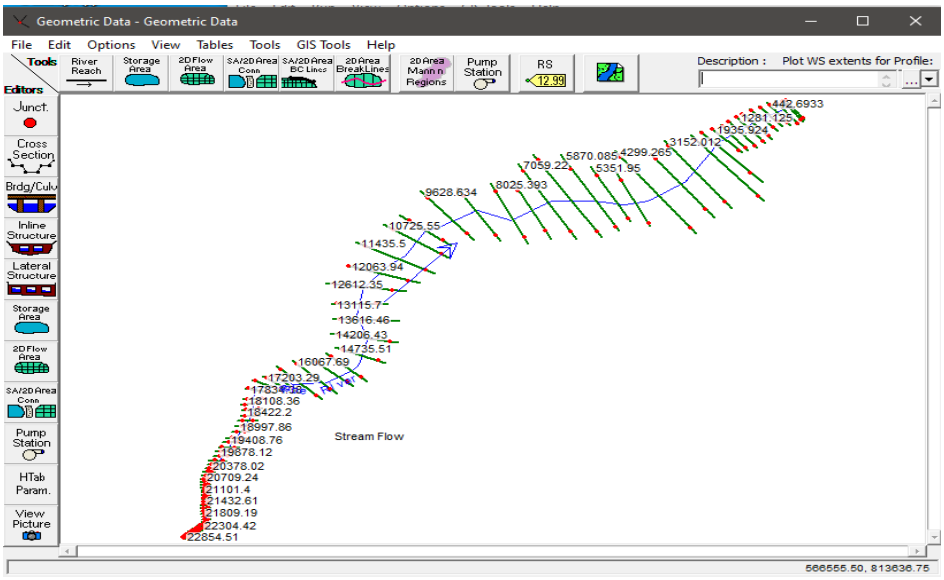

Figure 3.27 Exported geometric data from HEC-GoeRAS for 1D analysis in HEC-RAS

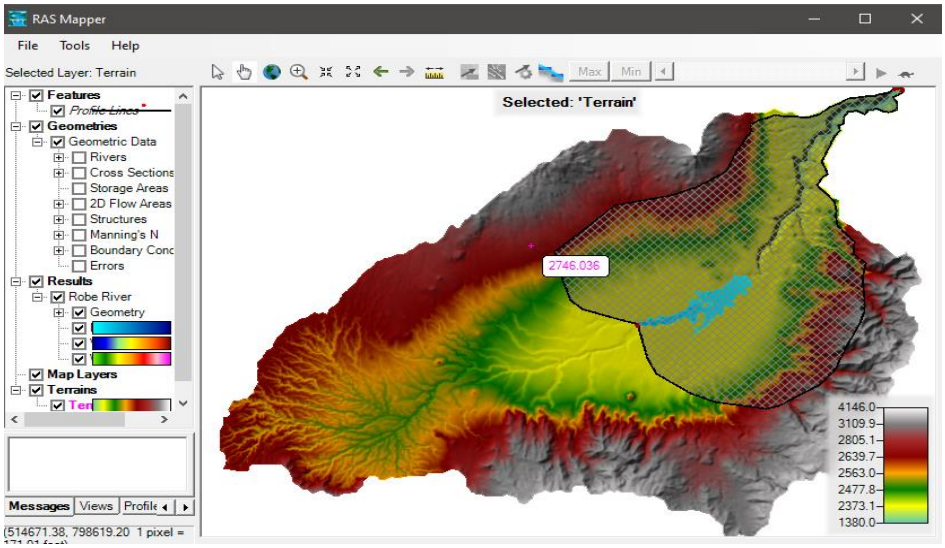

Figure 3.28 2D flow area computational mesh

After calculating the model results in HEC-RAS, they can be subsequently processed in GeoRAS, and floodplain depths and ranges can be mapped along with other relevant spatial results such as model velocity distribution, ice depths, sediment transport, and terrain mapping for very large data sets and uses a strategy of divide and conquer.

Large terrains can be decomposed into smaller tiles, with studies performed on each tile and results synthesized to create maps of HEC-RAS, modeling results for a wider area. In the event of flooding, the spatial framework for hydraulic analysis, together with public assets like highways, freeways, shelter locations, and evacuation routes, aids in the protection of lives and property.

3.12 Mitigation Measures

Cities are complex and interdependent systems, extremely vulnerable to threats from both natural hazards and terrorism. Hazard mitigation is action taken to reduce or eliminate long-term risk to people and property from hazards and their effects (González et al., 2003).

Structural river training plans are traditionally known methods of flood mitigation and this method has been used in corporation with general flood management approach in most of flood plain areas. Flood risk reduction can access by reducing the magnitude of flood or vulnerability of effected area. Flood damages determination is not only important factor for risk management but also it is a significant parameter in evaluation of mitigation plan according to the type and size of measures (Heidari, 2009).

For sustainable development and environmental protection, non-structural measures have become popular solutions for flood hazard mitigation in the world. Most non-structural measures require risk analyses, which are carried out by physical or numerical models, as the rational basis for flood-alleviation planning. In many applications, different approaches were adopted for flood risk assessments via hydrological, hydraulic or ecological models (Chen, *et al.*, 2014).

4 RESULTS AND DISCUSSIONS

4.1 Flood Frequency Analysis

For this study case, the flood frequency evaluation was performed using the method of moments (MoM) and Generalized Extreme Value (GEV) model satisfied the selection criteria of Kolmogorov- Smirnov of goodness of fit test and normality quantile-quantile plot test that the variate class value which divides the sample into equal-sized probability distribution function were adopted. The return period levels were estimated for 10, 100, 200 and 1000 years which are consistently increasing with maximum discharge for long run in the future under GEV model was among the frequency distribution function selected for testing.

4.2 Best Fitted Probability Distribution Functions

This study highlights the statistical scope of a mathematical modeling using the EASY-FIT software applications, to reach at the optimum results for the appropriate method of flood frequency analysis. The Generalized Extreme Value (GEV) was selected fitting the analysis among the five probability distribution functions of Gumbel's (EV1), Two-Parameter Lognormal (LN2) and Log-Pearson Type III (LP3). Generalized Extreme Value (GEV) was tested to select and pick up the best fit probability distributions functions (PDFs) that yield or evaluate annual maximum flood discharge. Hence, fitting best analysis the GEV gave maximum peak discharge of 1,215.46m^3/s, 2,595.62m^3/s, 3,179.53m^3/s and 4,978.06m^3/s for a return period of 10, 100, 200 and 1000 years respectively.

The Methods of Moments (MoM) were used due to its simplicity to analyze, develop, estimate the parameters of probability distribution functions and the selected GEV satisfied the selection criteria of Kolmogorov-Smirnov, a goodness of fit test was used to compute the maximum flood discharge for the predicted return period.

4.3 Estimated Design Discharge

The maximum peak discharge data recorded at the stream flow gauging station plays a key role in model calibration and validation. Flood magnitudes in (m^3/s) was computed based on the best fitted GEV distribution for 10, 100, 200 and 1000 year return periods at the Agarfa gauging station was used for flood inundation mapping.

Table 4.1 Flood return periods at Agarfa stream flow gauging station

No	Return Period (T years)	Magnitude(m^3/s)
1	10	1215.46
2	100	2595.62
3	200	3179.53
4	1000	4978.06

4.4 Flood Hazard and Risk Map

For this study case, the assessment for flood hazard was prepared for evaluation using the factors of elevation, slope, land cover, rainfall, soil texture and drainage density using the simple classification technique indicating as very high, high, medium, low and very low hazard depending on governing their factors. Multi-Criteria Evaluation (MCE) technique was also applied to assess the flood hazards in the basin using GIS and the standardized raster layers were weighted using Eigen vector in IDRISI Selva software for pair wise comparisons developed by Saaty's scale in decision-making process using the Analytical Hierarchy Process (AHP) that was used for comparing and contrasting to the criteria weight solved in Excel sheet for approving the consistency ratio of 0% less than 10% and proving its acceptability for analysis.

Flood hazard map was prepared by Weighted Overlay process as sum of elevation, slope, land cover, rainfall, soil texture and drainage density by multiplying with their respective criteria weight factors for developing flood hazard map in GIS. The flood hazard map was classified into four classes based on the its susceptibility rating value to the flood hazard level and was ranked per hazard level range of the study area in percentage extent it covers as Low Hazard (0 - 0.05%), Moderate Hazard (0.06% - 0.09%), High Hazard (0.1% - 47.74%) and Very High Hazard (47.75% - 52.1%).

As can be seen from the map of flood hazard in fig 4.1 very high hazard level was developed covering wide areas in Woredas such as Agarfa, Bekoji, Gedeb, Gonsebo, Kofele, but partially extending into Kokosa and Adaba; high hazard level also developed largely in Sinana-Dinsho, Adaba while in scanty extending into Bekoji, Gedeb, Gonsebo, Kofele, exceptionally half and half in Dodola Woreda for very high and high hazard level. Unfortunately, moderate hazard level and low hazard level was detected in Adaba, Gedeb and Kofele, respectively.

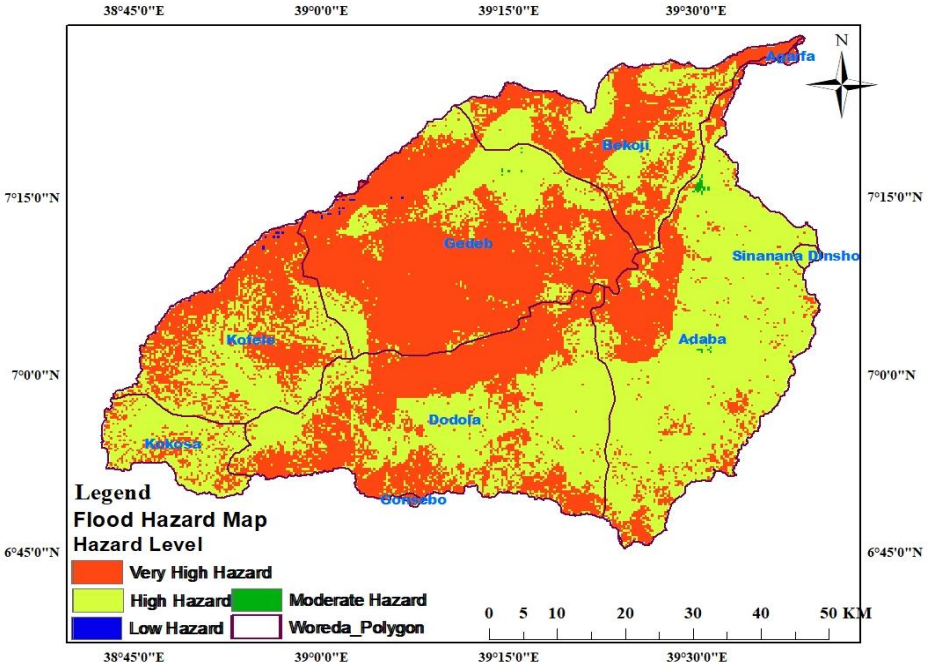

Figure 4.1 The projected flood hazard map

Additionally, the development of flood risk map for this study area was prepared taking the most core three interrelated components factors of land use, population density and the flood hazard. The Eigen vector in for pair wise comparisons developed by Saaty's scale in IDRISI in decision-making process, using the Analytical Hierarchy Process (AHP) computed for flood risk approves the consistency ratio of 0% less than 10% and was acceptable for analysis.

It was developed through Weighted Overlay as sum of population density, land use and flood hazard layer factors for the prediction of flood risk disaster assessment for Western Wabe Shebelle River basin catchment using Weighted Overlay process. The flood risk map was classified into four classes based on the vulnerability rating value to the flooding level and was ranked per risk level range of the study area in percentage extent it covers as Low Risk (6.54% - 16.68%), Moderate Risk (16.69% - 34.99%), High Risk (35% - 41.78%) and Very High Risk (0% - 6.53%).

As can be seen from the map of flood hazard in fig 4.2 very high risk level was developed covering wide areas in Woredas such as Agarfa and Bekoji; high risk level was also developed largely in Adaba, Kofele while scantly it extended into Bekoji Woreda; moderate risk level fully developed in Gedeb but partially in Dodola, Gonsebo and Adaba, and low risk level was largely detected in Kokosa, Sinana-Dinsho and partially in Gonsebo and Dodala.

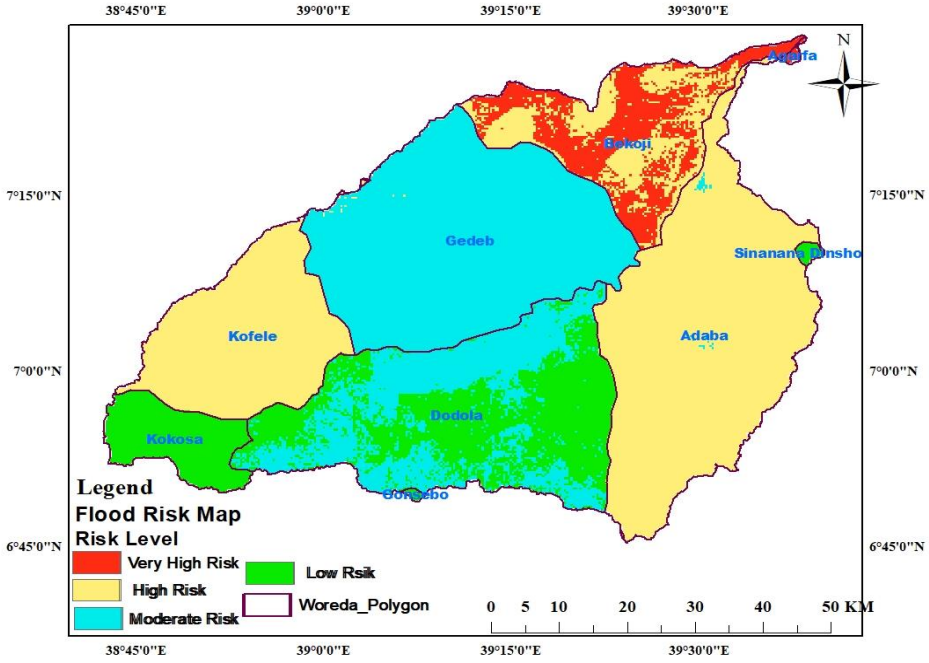

Figure 4.2 The projected flood risk map

4.5 Flood Inundation Mapping

Flood inundation mapping is used to outline zones which are more susceptible to flood along the river when the release of a stream surpasses the bank line stage along the river and the integrated software of HEC RAS and HEC-GeoRAS with ArcGIS was used for creating flood inundation depth and extent (Shrestha and Lohpaisankrit, 2016; Yin, *et al.*, 2013).

For this study case, HEC-RAS and ArcGIS with its extension HEC-GeoRAS was used for developing the flood inundation maps through converting DEM raster of study area to TIN using 3D Analyst Tool in GIS. HECRAS is a powerful software package and easy to use for determining water surface profiles in a wide variety of streamsflow.

After RAS pre-processing in HEC-GeoRAS as GIS2RAS.RASImport.sdf file is exported and fed into HEC-RAS for preparing and then exporting again as HECRAS.RASExport.sdf file, that was used for post-processing in RAS Mapping tool in HEC-GeoRAS to generate flood inundation mapping as water surface generation and floodplain delineation using raster into polygon shape files that define the extents of flooding for a given area. The resulting flood inundation maps are useful for municipal planning purposes, emergency action plans, flood insurance rates and ecological studies for catchment of study area.

The inundated areas along the Western Wabe Shebelle River basin were 105.2ha, 143.6ha, 153.9ha and 178.4ha for 10(PF 1), 100(PF 2), 200(PF 3) and 1000(PF 4) years return period,

respectively. The flooded area in the 1000 years return period was the highest compared to any other return period due to the increased streamflow. As can be seen from the model results, nearly all of the river's lower reaches were flooded with high inundation depths, which diminished as the river flowed from upstream to downstream. The flood depth was large up to 4.59m and hence, the consequence of flooding effects on life and property was extremely very high.

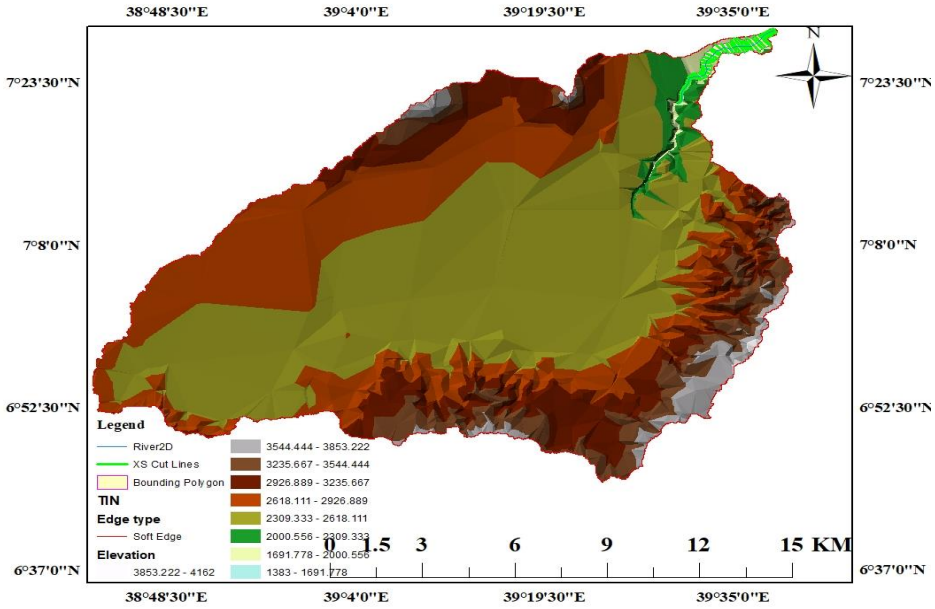

Figure 4.3 TIN raster created from DEM of study area

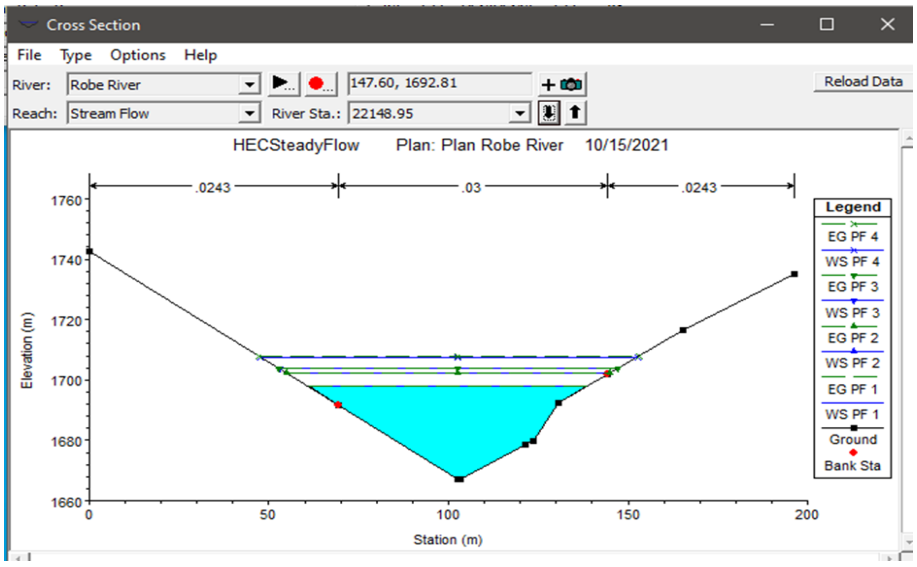

Figure 4.4 Stream flow cross-section profile

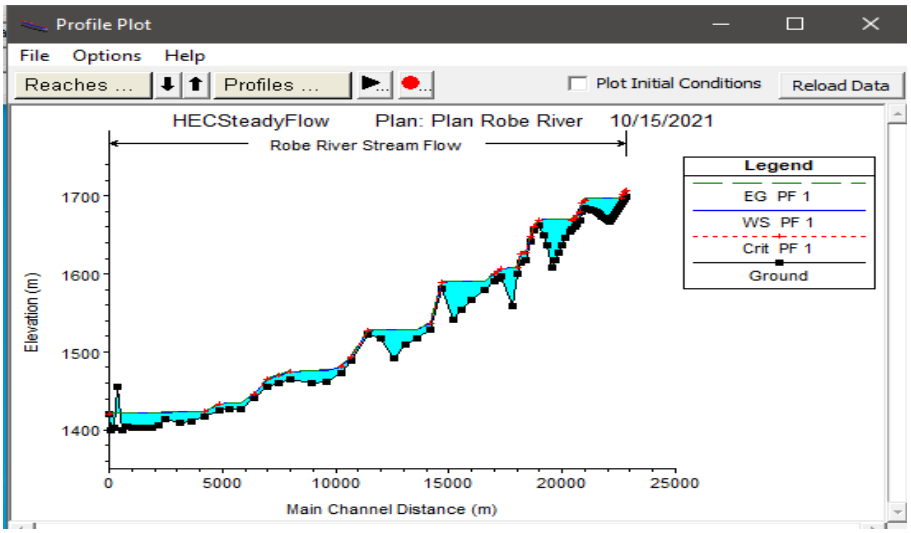

Figure 4. 5 Profile plot of main channel for river flow

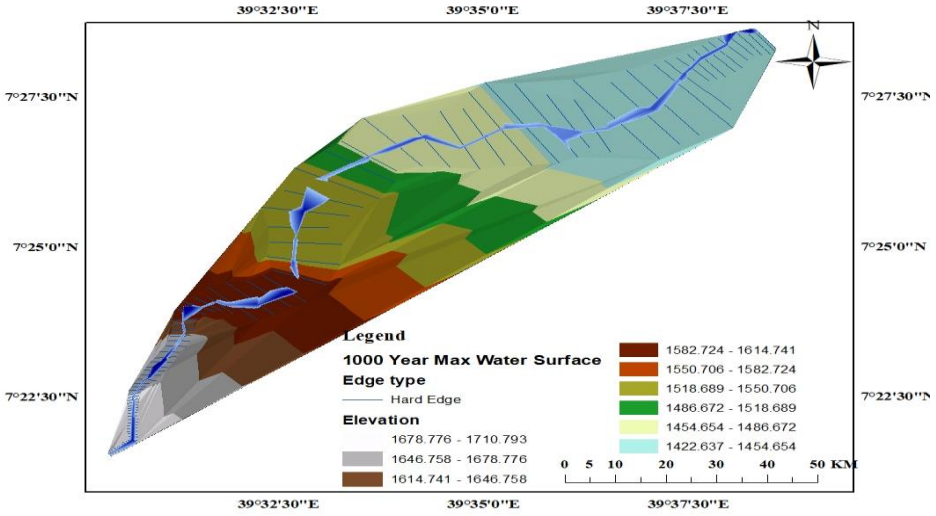

Figure 4.6 1000 year generated maximum water surface inundation mapping

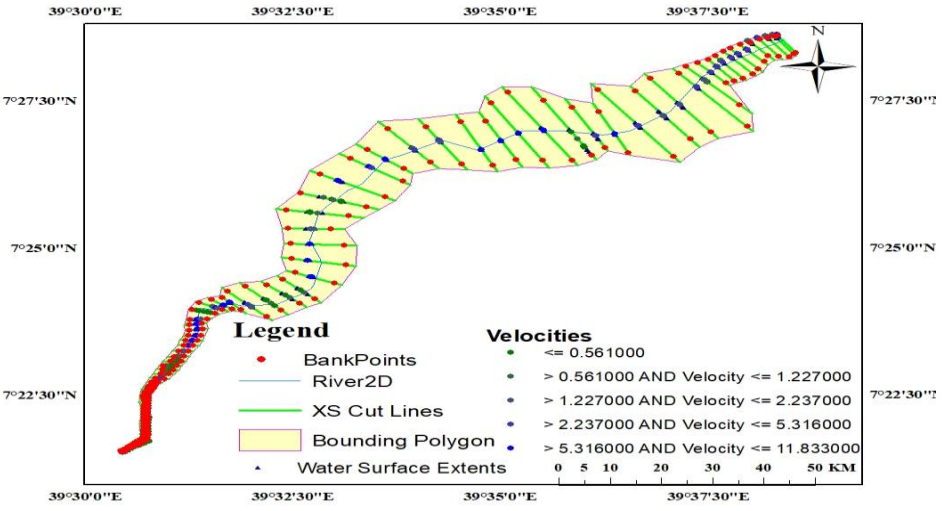

Figure 4.7 Floodplain mapping using XS cut lines bounding polygon limits

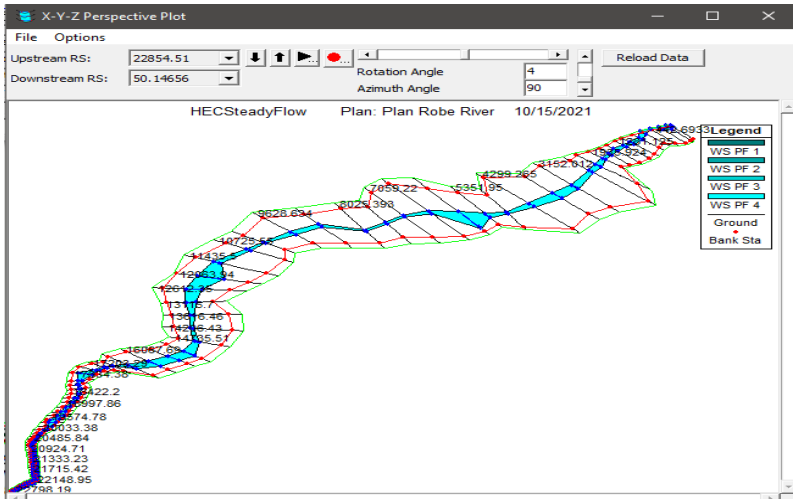

Figure 4.8 3D perspective plot view of river flow channel in HEC-RAS

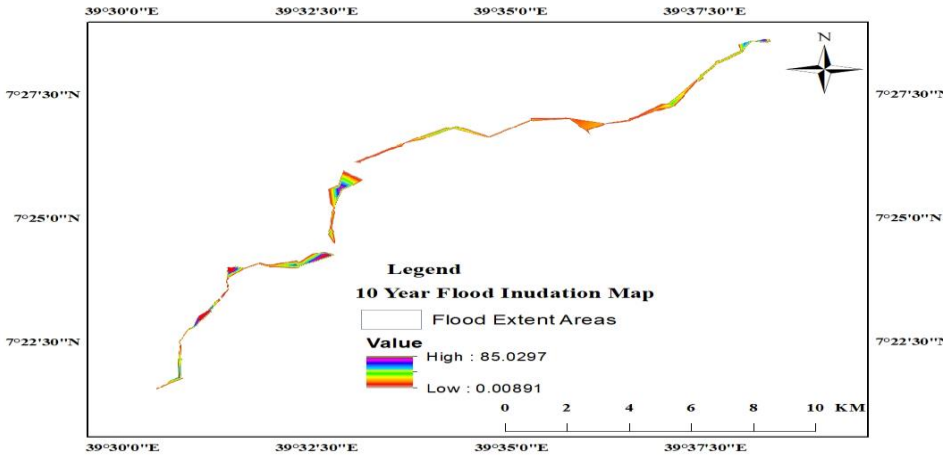

Figure 4.9 10 years return period flood inundation mapping

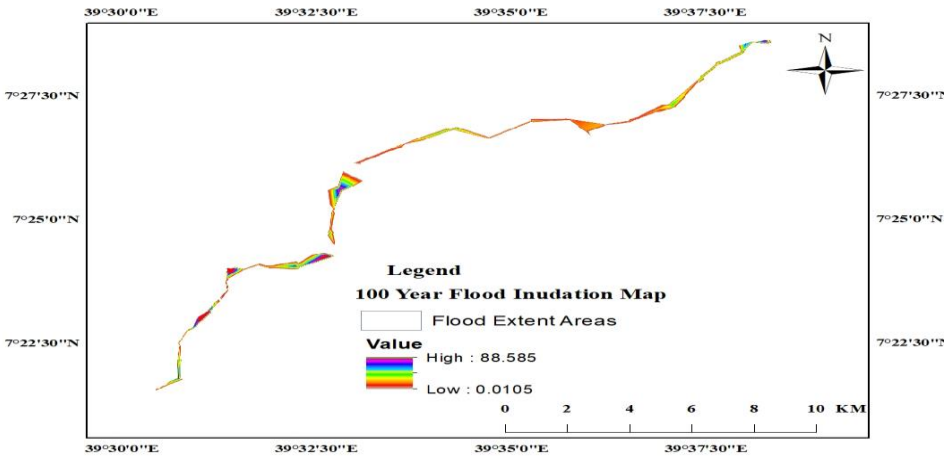

Figure 4.10 100 years return period flood inundation mapping

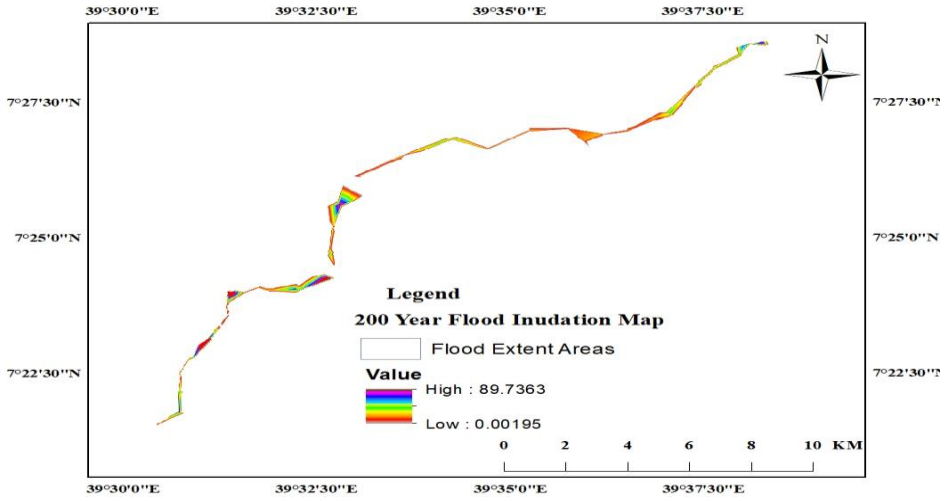

Figure 4.11 200 years return period flood inundation mapping

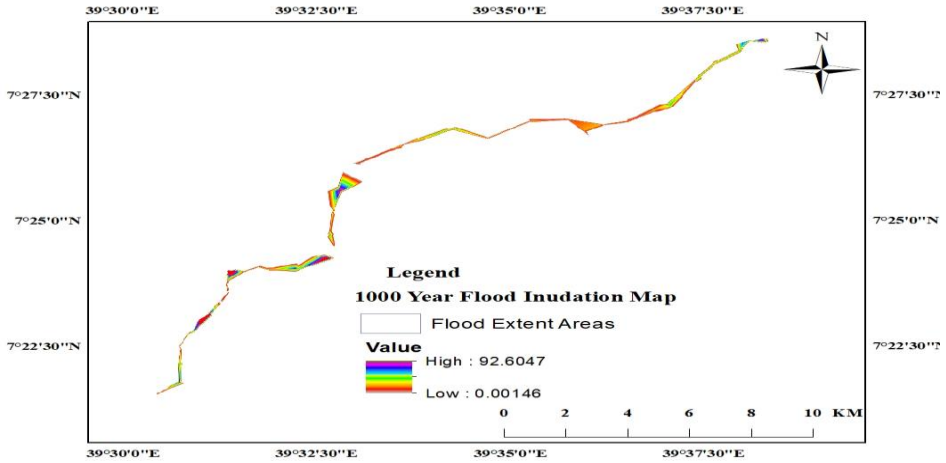

Figure 4.12 1000 years return period flood inundation mapping

4.6 Mitigation Measures

Recently risk of flood disaster has been increasing due to rapid urbanization and developmental activities the area which in turn has influenced and expected to increase more in the future by climate change impact. An intensive flood control and mitigation measure system is required for such flood problem due to that the flood disasters cause serious damage such as loss of lives, infrastructures, properties and livelihoods in the catchment.

Hence, the assessment for flood hazard and damage is a prerequisite for flood risk management in the river basin to apply the mitigation plans which are mostly evaluated in quantified terms as it is an important measures in decision making process. Therefore, the analysis for flood hazards and quantitative assessment of potential flood damage is very essential for mitigating and managing the flood risks in basin catchment.

In order to reduce flood risk in the future, the implementation of flood mitigation measures and adaptation planning, it is necessary to understand future changes in precipitation and flood hazard conditions considering climate change scenarios, which is necessary to assess the flood hazard and an expected risks in the future.

5 CONCLUSION AND RECOMMENDATION

5.1 Conclusion

The study was concentrated and focused mainly on selecting best fitting probability distribution, developing flood hazard map, flood risk map, flood inundation mapping and assessment of Western Wabe Shebelle River basin, Southeastern Ethiopia. The overflow of the Robe River causes floodplain which was a problem in Agarfa basin catchment; especially, during summer seasons due to the over bursting of the river.

The best fitted probability distribution was Generalized Extreme Value (GEV) out of the five probability distribution functions used for computing maximum discharge in analysis and gave maximum peak discharge of 1,215.46m^3/s, 2,595.62m^3/s, 3,179.53m^3/s and 4,978.06m^3/s for a return period of 10, 100, 200 and 1000 years respectively. The Methods of Moments (MoM) were used due to its simplicity to analyze, develop, estimate the parameters of probability distribution functions and the selected GEV satisfied the selection criteria of Kolmogorov-Smirnov of goodness of fit test determined maximum flood discharge for the predicted return period.

The flood hazard assessment was done for factors of elevation, slope, land cover, rainfall, soil texture and drainage density using the simple classification technique indicating as very high, high, medium, low and very low hazard depending on their governing factors. Multi-Criteria Evaluation (MCE) technique was applied, to assess flood hazard in the basin using GIS and the standardized raster layers were weighted using Eigen vector in IDRISI Selva software for pair wise comparisons developed by Saaty's scale in decision-making process, using the Analytical Hierarchy Process (AHP) the consistency ratio of 0% less than 10%; proving it optimum, efficient and acceptable for analysis.

Flood hazard analysis was prepared by Weighted Overlay process as sum of elevation, slope, land cover, rainfall, soil texture and drainage density by multiplying with their respective criteria weight factors for developing flood hazard map in GIS. The flood hazard map was classified into four classes based on the its susceptibility rating value to the flood hazard level and was ranked per hazard level range of the study area in percentage extent it covers as Low Hazard (0 - 0.05%), Moderate Hazard (0.06% - 0.09%), High Hazard (0.1% - 47.74%) and Very High Hazard (47.75% - 52.1%).

Thus, the study results concludes that the basin area of catchment in Woredas such as Agarfa, Bekoji, Gedeb, Gonsebo, Kofele partially extending into the Kokosa and Adaba were more

vulnerable to very high flood hazard level while high flood hazard level were seen in Sinana-Dinsho, Adaba but scantly extending into Bekoji, Gedeb, Gonsebo, Kofele, exceptionally half and half in Dodola Woreda for very high and high hazard level due to the recurrent river flooding in the area. The downstream flow areas were in need of more concern due to the developing of hazard levels that extended to the central and some marginalized areas of the catchment were more and more prone to the very high and high hazard levels.

The development of flood risk map was done taking the most core three interrelated components factors of land use, population density and the flood hazard layer. The Eigen vector for pair wise comparisons developed by Saaty's scale in IDRISI for decision-making process; the Analytical Hierarchy Process (AHP) computed and compared to the plainly solved in Excel sheet for approving flood risk the consistency ratio of 0% less than 10%, proving it optimum, efficient and acceptable for analysis.

The flood risk was developed through weighted overlay as sum of population density, land use and flood hazard layer factors for the prediction of flood risk disaster assessment for Western Wabe Shebelle River basin catchment using Weighted Overlay process. The flood risk map was classified into four classes based on the vulnerability rating value to the flooding level and was ranked per risk level range of the study area in percentage extent it covers as Low Risk (6.54% - 16.68%), Moderate Risk (16.69% - 34.99%), High Risk (35% - 41.78%) and Very High Risk (0% - 6.53%).

Hence, the study results concludes that the basin area of catchment in Woredas such as Agarfa and Bekoji were more vulnerable to very high flood risk level while high flood risk level were seen largely in Adaba, Kofele while in scanty extending into the Bekoji Woreda, moderate risk level fully developed in Gedeb but partially seen in Dodola, Gonsebo and Adaba, and low risk level was largely detected in Kokosa, Sinana-Dinsho and partially in Gonsebo and Dodala. The downstream flow areas were in need of more concern because it is more vulnerable to very high risk level whilst the central and some marginalized areas were more prone areas to high risk, moderate risk and low risk levels.

The inundation mapping was developed in RAS Mapping tool of HEC-GeoRAS, the water surface generation and floodplain mapping is performed using the water surface elevations on the XS cut lines, within the limits of the bounding polygon for the different flow patterns and the intended return period scenarios. The inundated areas along the Upper Wabe Shebelle

River basin were 105.2ha, 143.6ha, 153.9ha, and 178.4ha for 10, 100, 200 and 1000 years return period, respectively.

The flooded area in the 1000 years return period was the highest compared to any other return period due to the increased streamflow. As can be seen from the model results, nearly all of the river's lower reaches were flooded with high inundation depths, which diminished as the river flowed from upstream to downstream. The flood depth was excessive that ranges from 0.0015m to 92.6m and hence, the consequence of flooding effects on life and property was extremely very high.

5.2 Recommendation

Recently risk of flood disaster has been increasing due to rapid urbanization and developmental activities the area which in turn has influenced and expected to increase more in the future by climate change impact. An intensive flood control and mitigation measure system is required for such flood problem due to that the flood disasters cause serious damage such as loss of lives, infrastructures, properties and livelihoods in the catchment.

Hence, the assessment for flood hazard and damage is a prerequisite for flood risk management in the river basin to apply the mitigation plans which are mostly evaluated in quantified terms as it is an important measures in decision making process. Therefore, the analysis for flood hazards and quantitative assessment of potential flood damage is very essential for mitigating and managing the flood risks in basin catchment.

In order to reduce flood risk in the future, the implementation of flood mitigation measures and adaptation planning, it is necessary to understand future changes in precipitation and flood hazard conditions considering climate change scenarios, which is necessary to assess the flood hazard and an expected risks in the future.

Generally stating, the concerned bodies like from NGO’s, government administrative and the local authorities and communities in the area should play a great role for the manipulation of the whole biodiversity and fight the challenging climate change sustaining ambient environment from hazards in the catchment. Therefore, in the reduction of losses an accurate prediction of flood inundation areas and dissemination of information on the inundation areas to emergency managers, city planners and the general public is critically necessary. Accurate predictions of flooded areas are also critical to formulating and quantifying flood insurance rates.

As necessary as possible for preventing the developing flood damages in the area, the alternative mitigation measures must be taken shall include: educating the communities to build-up their capacities and participating them in the environmental protection from man-made disasters (that is, unprotected felling of trees, throwing rubbish or rubbish into open land, and not paying attention to the drainage system because it has been discharged normally); involving concerned bodies like NGO's, government administrative and the local authorities and communities in the area they should play a great role for the manipulation of the whole biodiversity and fighting the challenging climate change continuously; practicing the plantation of the trees to prevent soil degradation and thereby increasing soaking of raindrop into soil; taking the application of structural determinations that focuses on reducing the impacts of flooding on communities by building levees, floodwalls and improving drainage systems and taking the non-structural measures like land-use control, sampling signal measures, relocations and early flood warnings systems are among the preventive action that could help in controlling flood damage at the site of study.

REFERENCES

Alaoui, A., Rogger, M., Peth, S., & Blöschl, G. (2018). Does soil compaction increase floods ? A review. *Journal of Hydrology*, *557*, 631–642. https://doi.org/10.1016/j.jhydrol.2017.12.052

Alemu, W. G. (2007). *Flood Hazard and Risk Assessment Using GIS and Remote Sensing in Fogera Woreda , Northwest Ethiopia*. https://doi.org/10.1007/978-94-007-0689-7

Apel, H., Aronica, G. T., Kreibich, H., & Thieken, A. H. (2009). Flood risk analyses—how detailed do we need to be? *Natural Hazards*, *49*(1), 79–98.

Bathrellos, G. D., Karymbalis, E., Skilodimou, H. D., Gaki-Papanastassiou, K., & Baltas, E. A. (2016). Urban flood hazard assessment in the basin of Athens Metropolitan city, Greece. *Environmental Earth Sciences*, *75*(4), 319.

Bhatt, G. D., Sinha, K., Deka, P. K., & Kumar, A. (2014). *Flood Hazard and Risk Assessment in Chamoli District , Uttarakhand Using Satellite Remote Sensing and GIS Techniques*. *3*(8), 15348–15356. https://doi.org/10.15680/IJIRSET.2014.0308039

Bishaw, K. (2012). *Application of GIS and remote sensing techniques for flood Hazard and risk assessment: The case of Dugeda bora Woreda of Oromiya regional state, Ethiopia*.

Chen, Albert S.; Hsu, Ming-Hsi; Teng, W.-H. et al. (2014). *ORE Open Research Exeter*. https://doi.org/10.1007/s11069-005-4659-7.Establishing

Desalegn, H., & Mulu, A. (2021). Mapping flood inundation areas using GIS and HEC-RAS model at Fetam River, Upper Abbay Basin, Ethiopia. *Scientific African*, *12*, e00834. https://doi.org/10.1016/j.sciaf.2021.e00834

Dottori, F., Salamon, P., Bianchi, A., Alfieri, L., & Hirpa, F. A. (2016). Advances in Water Resources Development and evaluation of a framework for global flood hazard mapping. *Advances in Water Resources*, *94*, 87–102. https://doi.org/10.1016/j.advwatres.2016.05.002

Dragičević, N., Karleuša, B., & Ožanić, N. (2019). Different approaches to estimation of drainage density and their effect on the Erosion Potential Method. *Water (Switzerland)*, *11*(3), 1–14. https://doi.org/10.3390/w11030593

Farooq, M. (2018). *Flood frequency analysis of river swat using Log Pearson type 3 , Generalized Extreme Value , Normal , and Gumbel Max distribution methods*.

Farooq, M., Shafique, M., & Khattak, M. S. (2019). Flood hazard assessment and mapping of River Swat using HEC-RAS 2D model and high-resolution 12-m TanDEM-X DEM (WorldDEM). *Natural Hazards*, *97*(2), 477–492. https://doi.org/10.1007/s11069-019-

03638-9

Forest, S. R., Esfandiari, M., Abdi, G., Jabari, S., & Mcgrath, H. (2020). *Flood Hazard Risk Mapping Using a Pseudo*. *1*, 1–23.

Forkuo, E. K. (2011). Flood hazard mapping using aster image data with GIS. *Internacional Journal Of Geomatics And Geociences*, *1*(4), 932–950.

Foudi, S., Osés-eraso, N., & Tamayo, I. (2015). Land Use Policy Integrated spatial flood risk assessment : The case of Zaragoza. *Land Use Policy*, *42*, 278–292. https://doi.org/10.1016/j.landusepol.2014.08.002

Getahun and Gebre. (2015). *Flood Hazard Assessment and Mapping of Flood Inundation Area of the Awash Civil & Environmental Engineering Flood Hazard Assessment and Mapping of Flood Inundation Area of the Awash River Basin in Ethiopia using GIS and HEC-GeoRAS / HEC-RAS Model*. *August*. https://doi.org/10.4172/2165-784X.1000179

González, D., Newman, G., Combs, T., Kolosna, C., & Berke, P. (2003). *Godschalk 2003 Urban hazard mitigation creating resilient cities Urban Hazard Mitigation : Creating Resilient Cities*.

Goodell, C.1; Warren, C. . (2006). *Flood Inundation Mapping using HEC-RAS*. 18–23.

Haghizadeh, A., Siahkamari, S., Haghiabi, A. H., & Rahmati, O. (2017). *Forecasting flood-prone areas using Shannon ' s*. https://doi.org/10.1007/s12040-017-0819-x

Heidari, A. (2009). *Structural master plan of flood mitigation measures*. *1*, 61–75.

Jhong, B.-C., Tachikawa, Y., Tanaka, T., Udmale, P., & Tung, C.-P. (2020). A generalized framework for assessing flood risk and suitable strategies under various vulnerability and adaptation scenarios: A case study for residents of Kyoto city in Japan. *Water*, *12*(9), 2508.

Jian, W., Li, S., Lai, C., Wang, Z., Cheng, X., Lo, E. Y.-M., & Pan, T.-C. (2021). Evaluating pluvial flood hazard for highly urbanised cities: a case study of the Pearl River Delta Region in China. *Natural Hazards*, *105*(2), 1691–1719.

Jing Lin Ng, Soon Kim Tiang, Yuk Feng Huang, N S Muhammad, J Abdullah and P Y Julien, R. A. A.-M. and R. R. (2020). *Investigation of the best fit probability distribution for annual maximum rainfall in Kelantan River Basin Investigation of the best fit probability distribution for annual maximum rainfall in Kelantan River Basin*. https://doi.org/10.1088/1755-1315/476/1/012118

Journal, I. (n.d.). *IRJET- PROBABILITY DISTRIBUTION OF FLOOD FREQUENCY ANALYSIS*.

Kilinç, H. Ç. (2018). *Estimation of Rainfall Distribution Map of Turkey By IDW and Kriging Interpolation Method American Journal of Engineering Research (AJER). 6*, 238–241.

Luu, C., Tran, H. X., Pham, B. T., Al-Ansari, N., Tran, T. Q., Duong, N. Q., Dao, N. H., Nguyen, L. P., Nguyen, H. D., & Thu Ta, H. (2020). Framework of spatial flood risk assessment for a case study in Quang Binh province, Vietnam. *Sustainability*, *12*(7), 3058.

Mamo, S., Berhanu, B., & Melesse, A. M. (2019). Historical flood events and hydrological extremes in Ethiopia. In *Extreme Hydrology and Climate Variability* (pp. 379–384). Elsevier.

McCann, J. C. (1995). *People of the plow: An agricultural history of Ethiopia, 1800–1990*. Univ of Wisconsin Press.

Meekma, R., & Byard, G. (2013). *HEC-GeoRAS Walkthrough Workshop*.

Mehrannia, H., & Pakgohar, A. (2014). Using EASY FIT Software for Goodness-Of-Fit Test and Data Generation. *International Journal of Mathematical Archive*, *5*(1), 118–124.

Menon, V. P. G., & Ajin, R. S. (2014). RS & GIS Based Spatial Mapping of Flash Floods in Karamana and Vamanapuram River Basin, Thiruvananthapuram District, Kerala. *Kerala, India*.

Merwade, V. (2016). *Tutorial on using HEC-GeoRAS with ArcGIS 10 . x and HEC- RAS Modeling*. 1–38.

Merwade, V., Olivera, F., Arabi, M., & Edleman, S. (2003). *Uncertainty in Flood Inundation Mapping : Current Issues and Future Directions*.

Millington, N., Das, S., And, & Simonovic, S. P. (2011). *The Comparison of GEV, Log-Pearson Type 3 and Gumbel Distributions in the Upper Thames River Watershed under Global Climate Models*. *September*.

Mokhtar, E. S., Pradhan, B., Ghazali, A. H., Zulhaidi, H., & Shafri, M. (2018). *Assessing flood inundation mapping through estimated discharge using GIS and HEC-RAS model*.

Musolino, G., Ahmadian, R., & Falconer, R. A. (2020). Comparison of flood hazard assessment criteria for pedestrians with a refined mechanics-based method. *Journal of Hydrology X*, *9*, 100067.

Namara, W. G., Damisse, T. A., & Tufa, F. G. (2021). Application of HEC-RAS and HEC-GeoRAS model for Flood Inundation Mapping, the case of Awash Bello Flood Plain, Upper Awash River Basin, Oromiya Regional State, Ethiopia. *Modeling Earth Systems and Environment, 2015*. https://doi.org/10.1007/s40808-021-01166-9

Ologhadien, I. (2021). *Flood Flow Probability Distribution Model Selection on Niger / Benue River Basins in Nigeria*. *20*(5), 76–94. https://doi.org/10.9734/JERR/2021/v20i517315

Osmaston, H. A., Mitchell, W. A., & Osmaston, J. A. N. (2005). Quaternary glaciation of the Bale Mountains, Ethiopia. *Journal of Quaternary Science: Published for the Quaternary Research Association*, *20*(6), 593–606.

Pal, K., Panda, K. C., Sharma, G., & Mandloi, S. (2020). Flood Frequency Analysis for Burhi Gandak River Basin. *International Journal of Environment and Climate Change*, *10*(6), 82–89. https://doi.org/10.9734/ijecc/2020/v10i630207

Petaccia, G. (2020). *Performances of the New HEC-RAS Version 5 for 2-D Hydrodynamic-Based Rainfall-Runo ff Simulations at Basin Scale : Comparison with a State-of-the Art Model*. 1–19.

Rieu-clarke, A. S. (2008). *A Survey of International Law Relating to Flood Management : Existing Practices and Future Prospects A Survey of International Law Relating to Flood Management : Existing Practices and Future Prospects*. *48*(3).

Rogger, M., Agnoletti, M., Alaoui, A., Bathurst, J. C., Bodner, G., Borga, M., Chaplot, V., Gallart, F., Glatzel, G., Hall, J., Holden, J., Holko, L., Horn, R., Kiss, A., Quinton, J. N., Leitinger, G., Lennartz, B., Parajka, J., Peth, S., … Viglione, A. (2016). *Water Resources Research*. *June 2013*, 5209–5219. https://doi.org/10.1002/2017WR020723.Received

Romali, N. S., Yusop, Z., & Ismail, A. Z. (2018). *Application of HEC-RAS and Arc GIS for floodplain mapping in Segamat town , APPLICATION OF HEC-RAS AND ARC GIS FOR FLOODPLAIN MAPPING IN SEGAMAT TOWN , MALAYSIA*. *January*. https://doi.org/10.21660/2018.43.3656

Safaripour, M., Monavari, M., Zare, M., Abedi, Z., & Gharagozlou, A. (2012). Flood Risk Assessment Using GIS (Case Study: Golestan Province, Iran). *Polish Journal of Environmental Studies*, *21*(6).

Schittkowski, K. (2002). EASY-FIT: A software system for data fitting in dynamical systems. *Structural and Multidisciplinary Optimization*, *23*(2), 153–169. https://doi.org/10.1007/s00158-002-0174-6

Shahabi, H., Keihanfard, S., Ahmad, B. Bin, & Amiri, M. J. T. (2014). Evaluating Boolean, AHP and WLC methods for the selection of waste landfill sites using GIS and satellite images. *Environmental Earth Sciences*, *71*(9), 4221–4233.

Shrestha, S., & Lohpaisankrit, W. (2016). Flood hazard assessment under climate change scenarios in the Yang River Basin , Thailand. *International Journal of Sustainable Built*

Environment, October. https://doi.org/10.1016/j.ijsbe.2016.09.006

Tao Chen , Liliang Ren , Fei Yuan , Xiaoli Yang 2, Shanhu Jiang 2, T. T. 2, & Yi Liu, C. Z. and L. Z. 2. (2017). *Comparison of Spatial Interpolation Schemes for Rainfall Data and Application in*. 1–18. https://doi.org/10.3390/w9050342

Turi, T., Hayicho, H., & Kedir, H. (2019). *Evaluating Land Use / Land Cover Change and Its Socioeconomic Implications in Agarfa District of Bale Zone , Southeastern Ethiopia*. 369–388. https://doi.org/10.4236/jep.2019.103022

V, S. S. S., Roy, P. S., Chakravarthi, V., & G, S. R. (2017). *Flood risk assessment using multi-criteria analysis : a case study from Kopili River Basin , Assam , India*. *5705*(December). https://doi.org/10.1080/19475705.2017.1408705

Ven Te Chow, Maidment, D. R., & Mays, L. W. (1988). *Applied Hydrology*.

Vivekanandan, N. (2015). *Frequency Analysis of Annual Maximum Flood Discharge Using Method of Moments and Maximum Likelihood Method of Gamma and Extreme Value Family of Probability Distributions*. *1*(3), 141–146.

Vivekanandan, N. (2020). *Selection of Best Fit of Extreme Value Family of Distributions for Frequency Analysis of River Flow Data*. *7*(5), 13–18.

Wang, Y., Chen, F., Zhang, M., Chen, S., & Tan, X. (2018). *The effects of the reverse seasonal flooding on soil texture within the hydro-fluctuation belt in the Three Gorges reservoir , China*. 109–115. https://doi.org/10.1007/s11368-017-1725-1

Ward, P. J., Blauhut, V., Bloemendaal, N., Daniell, J. E., Ruiter, M. C. de, Duncan, M. J., Emberson, R., Jenkins, S. F., Kirschbaum, D., & Kunz, M. (2020). Natural hazard risk assessments at the global scale. *Natural Hazards and Earth System Sciences*, *20*(4), 1069–1096.

Weldegebriel, Z. B., & Amphune, B. E. (2017). Livelihood resilience in the face of recurring floods: an empirical evidence from Northwest Ethiopia. *Geoenvironmental Disasters*, *4*(1), 1–19.

Wondim, Y. K. (2016). *Flood Hazard and Risk Assessment Using GIS and Remote Sensing in Lower Awash Sub-basin , Ethiopia*. *6*(9), 69–86.

Worlddem, T. D. E. M. (2019). Flood hazard assessment and mapping of River Swat using HEC-RAS 2D Flood hazard assessment and mapping of River Swat using HEC - RAS 2D model and high - resolution 12 - m TanDEM - X DEM. *Natural Hazards, June 2020*. https://doi.org/10.1007/s11069-019-03638-9

Yin, J., Yu, D., Yin, Z., Wang, J., & Xu, S. (2013). Multiple scenario analyses of Huangpu

River flooding using a 1D/2D coupled flood inundation model. *Natural Hazards*, *66*(2), 577–589. https://doi.org/10.1007/s11069-012-0501-1

Zin, W. W., Kawasaki, A., & Win, S. (2015). *River flood inundation mapping in the Bago River Basin , Myanmar*. *9*(4), 97–102. https://doi.org/10.3178/hrl.9.97

PPENDIXES

A. The XSCutLines3D created in RAS Geometry of HEC-GeoRas

XSCutLines3D											
OID	Shape Length	XS2DID	HydroID	ProfileM	River Code	Reach Code	Left Bank	Right Bank	Left Length	Chanl Length	Right Length
0.0	293.2	13.0	86.0	32714.7	Main River	Upstream	0.4	0.7	167.3	173.6	180.9
1.0	347.8	14.0	87.0	32541.0	Main River	Upstream	0.4	0.7	156.9	156.8	157.3
2.0	370.6	15.0	88.0	32384.2	Main River	Upstream	0.4	0.7	142.9	159.4	175.9
3.0	379.8	16.0	89.0	32224.8	Main River	Upstream	0.3	0.7	184.1	191.7	199.1
4.0	426.1	17.0	90.0	32033.1	Main River	Upstream	0.3	0.7	176.0	179.1	182.1
5.0	454.6	18.0	91.0	31854.0	Main River	Upstream	0.3	0.7	172.3	194.3	215.0
6.0	498.7	19.0	92.0	31659.8	Main River	Upstream	0.3	0.7	279.9	300.7	319.7
7.0	614.4	20.0	93.0	31359.1	Main River	Upstream	0.4	0.7	285.5	313.4	338.7
8.0	705.2	21.0	94.0	31045.7	Main River	Upstream	0.4	0.7	292.1	287.8	293.6
9.0	702.0	22.0	95.0	30757.9	Main River	Upstream	0.4	0.8	331.1	350.6	341.3
10.0	822.7	23.0	96.0	30407.3	Main River	Upstream	0.3	0.7	402.2	393.7	379.4
11.0	825.8	24.0	97.0	30013.6	Main River	Upstream	0.3	0.8	468.6	476.0	471.6
12.0	883.6	25.0	98.0	29537.6	Main River	Upstream	0.4	0.8	399.0	411.7	411.5
13.0	860.6	26.0	99.0	29125.8	Main River	Upstream	0.4	0.8	366.0	424.3	413.6
14.0	952.4	27.0	100.0	28701.5	Main River	Upstream	0.5	0.8	291.0	338.0	375.5
15.0	843.0	28.0	101.0	28363.6	Main River	Upstream	0.4	0.7	272.1	330.9	369.7
16.0	809.3	29.0	102.0	28032.7	Main River	Upstream	0.3	0.7	250.7	280.7	299.0
17.0	870.9	30.0	103.0	27752.0	Main River	Upstream	0.3	0.7	280.8	307.6	321.2
18.0	964.3	31.0	104.0	27444.4	Main River	Upstream	0.4	0.8	515.7	483.3	474.0
19.0	1152.7	32.0	105.0	26961.1	Main River	Upstream	0.4	0.7	511.2	464.5	442.6
20.0	1114.1	33.0	106.0	26496.6	Main River	Upstream	0.4	0.7	579.7	621.2	574.5
21.0	1532.6	34.0	107.0	25875.4	Main River	Upstream	0.5	0.8	756.0	679.9	676.8
22.0	1452.2	35.0	108.0	25195.4	Main River	Upstream	0.5	0.7	587.6	702.9	698.4
23.0	1347.2	36.0	109.0	24492.6	Main River	Upstream	0.4	0.6	522.6	556.9	547.1
24.0	1354.6	37.0	110.0	23935.7	Main River	Upstream	0.3	0.6	644.5	663.4	657.9
25.0	1576.2	38.0	111.0	23272.3	Main River	Upstream	0.3	0.5	705.0	728.0	758.2
26.0	1634.1	39.0	112.0	22544.3	Main River	Upstream	0.3	0.6	844.3	873.5	911.5
27.0	2008.1	40.0	113.0	21670.8	Main River	Upstream	0.4	0.7	899.8	834.9	754.4
28.0	1900.0	41.0	114.0	20835.9	Main River	Upstream	0.3	0.6	1364.9	1348.	1494.
29.0	2274.6	42.0	115.0	19487.8	Main River	Upstream	0.3	0.6	893.4	817.5	713.7
30.0	1922.5	43.0	116.0	18670.2	Main River	Upstream	0.3	0.6	437.0	476.6	598.9
31.0	1597.5	44.0	117.0	18193.6	Main River	Upstream	0.2	0.6	264.4	1120.	778.4
36.0	1126.6	49.0	122.0	17073.5	Main River	Midstream	0.3	0.5	566.3	634.6	652.7
37.0	1231.7	50.0	123.0	16438.9	Main River	Midstream	0.4	0.5	424.2	440.1	493.1
38.0	1146.0	51.0	124.0	15998.8	Main River	Midstream	0.3	0.5	405.7	408.7	429.0
39.0	1202.7	52.0	125.0	15590.1	Main River	Midstream	0.2	0.5	410.6	412.0	421.8
40.0	1302.1	53.0	126.0	15178.1	Main River	Midstream	0.2	0.6	434.0	281.4	105.6
41.0	1347.6	54.0	127.0	14896.7	Main River	Midstream	0.2	0.7	707.5	578.2	470.9
42.0	1359.0	55.0	128.0	14318.5	Main River	Midstream	0.3	0.6	573.5	559.4	520.0
43.0	1380.8	56.0	129.0	13759.1	Main River	Midstream	0.2	0.6	420.0	492.7	567.9
44.0	1732.3	57.0	130.0	13266.4	Main River	Midstream	0.3	0.6	529.4	569.3	532.8
45.0	1686.8	58.0	131.0	12697.1	Main River	Midstream	0.3	0.7	418.4	667.4	1085.
46.0	2019.1	59.0	132.0	12029.7	Main River	Midstream	0.3	0.8	542.2	668.2	1058.
47.0	1943.8	60.0	133.0	11361.5	Main River	Midstream	0.3	0.8	585.5	574.2	622.5
48.0	2382.2	61.0	134.0	10787.3	Main River	Midstream	0.3	0.7	951.2	695.4	609.4
49.0	2885.1	62.0	135.0	10091.9	Main River	Midstream	0.3	0.8	916.8	703.9	565.5
50.0	2987.9	63.0	136.0	9388.0	Main River	Midstream	0.3	0.8	897.9	755.5	658.2
51.0	2536.7	64.0	137.0	8632.5	Main River	Midstream	0.3	0.8	633.8	469.5	358.1
52.0	2428.0	65.0	138.0	8163.1	Main River	Midstream	0.4	0.9	572.0	385.0	280.5
53.0	2127.6	66.0	139.0	7778.0	Main River	Midstream	0.3	0.9	580.8	404.8	321.8
54.0	2293.6	67.0	140.0	7373.2	Main River	Downstream	0.3	0.9	581.0	513.1	519.4
55.0	2439.1	68.0	141.0	6860.1	Main River	Downstream	0.2	0.9	691.1	581.7	482.1
56.0	2575.7	69.0	142.0	6278.4	Main River	Downstream	0.2	0.9	679.7	670.8	492.5
57.0	2732.7	70.0	143.0	5607.7	Main River	Downstream	0.2	0.9	686.7	618.5	517.6

58.0	2765.2	71.0	144.0	4989.1	Main River	Downstream	0.1	0.9	696.1	530.6	491.9
59.0	2763.2	72.0	145.0	4458.5	Main River	Downstream	0.2	0.9	724.5	687.6	687.3
60.0	2627.5	73.0	146.0	3770.9	Main River	Downstream	0.1	0.9	651.9	505.7	462.3
61.0	2474.9	74.0	147.0	3265.2	Main River	Downstream	0.2	0.9	661.0	435.7	389.1
62.0	2198.8	75.0	148.0	2829.5	Main River	Downstream	0.2	1.0	569.6	430.7	419.3
63.0	2476.8	76.0	149.0	2398.8	Main River	Downstream	0.2	0.9	580.3	547.5	524.9
64.0	2663.4	77.0	150.0	1851.2	Main River	Downstream	0.1	0.9	406.9	517.9	573.6
65.0	2956.2	78.0	151.0	1333.3	Main River	Downstream	0.1	0.8	368.3	507.9	572.1
66.0	2988.0	79.0	152.0	825.5	Main River	Downstream	0.1	0.8	289.6	408.1	487.4
67.0	2914.4	80.0	153.0	417.3	Main River	Downstream	0.1	0.8	260.3	373.1	471.4
68.0	2846.9	81.0	154.0	44.2	Main River	Downstream	0.1	0.8	115.3	44.2	234.6

B. Robe river reach profile output table plan in HEC-RAS

Profile Output Table - Standard Table 1

File Options Std. Tables Locations Help

HEC-RAS Plan: ROBE RIVER River: Robe River Reach: Stream Flow

Stream Flow	River Station	Profile	Q Total	Min Ch El	W.S. Elev	Crit W.S.	E.G. Elev	E.G. Slope	Vel Chnl	Flow Area	Top Width	Froude # Chl
			m^3/s	m	m	m	m	m/m	m/s	m^2	m	
Reach	22855	PF 1	1215	1698	1708	1708	1710	0	7	183	40	1
Reach	22855	PF 2	2596	1698	1711	1711	1714	0	8	331	50	1
Reach	22855	PF 3	3180	1698	1712	1712	1715	0	9	385	53	1
Reach	22855	PF 4	4978	1698	1715	1715	1719	0	10	537	60	1
Reach	22798	PF 1	1215	1696	1705	1705	1707	0	7	179	39	1
Reach	22798	PF 2	2596	1696	1708	1708	1711	0	8	337	54	1
Reach	22798	PF 3	3180	1696	1709	1709	1713	0	8	398	58	1
Reach	22798	PF 4	4978	1696	1712	1712	1716	0	9	570	70	1
Reach	22733	PF 1	1215	1693	1702	1702	1704	0	7	181	40	1
Reach	22733	PF 2	2596	1693	1705	1705	1708	0	8	332	54	1
Reach	22733	PF 3	3180	1693	1706	1706	1710	0	8	394	58	1
Reach	22733	PF 4	4978	1693	1709	1709	1713	0	9	570	70	1
Reach	22650	PF 1	1215	1689	1698	1698	1700	0	7	181	40	1
Reach	22650	PF 2	2596	1689	1701	1701	1704	0	8	330	54	1
Reach	22650	PF 3	3180	1689	1702	1702	1706	0	8	387	58	1
Reach	22650	PF 4	4978	1689	1705	1705	1709	0	9	583	71	1
Reach	22577	PF 1	1215	1686	1697		1698	0	4	288	50	1
Reach	22577	PF 2	2596	1686	1702		1703	0	5	551	69	1
Reach	22577	PF 3	3180	1686	1703		1704	0	5	652	75	1
Reach	22577	PF 4	4978	1686	1707		1708	0	5	978	92	0
Reach	22509	PF 1	1215	1683	1698		1698	0	2	489	65	0
Reach	22509	PF 2	2596	1683	1702		1703	0	3	822	85	0
Reach	22509	PF 3	3180	1683	1704		1704	0	3	946	91	0
Reach	22509	PF 4	4978	1683	1707		1708	0	4	1334	108	0
Reach	22441	PF 1	1215	1680	1698		1698	0	2	711	78	0
Reach	22441	PF 2	2596	1680	1702		1703	0	2	1106	98	0
Reach	22441	PF 3	3180	1680	1704		1704	0	3	1250	104	0
Reach	22441	PF 4	4978	1680	1708		1708	0	3	1690	121	0
Reach	22372	PF 1	1215	1676	1698		1698	0	1	986	92	0
Reach	22372	PF 2	2596	1676	1702		1702	0	2	1448	112	0
Reach	22372	PF 3	3180	1676	1704		1704	0	2	1613	118	0
Reach	22372	PF 4	4978	1676	1708		1708	0	2	2113	135	0
Reach	22304	PF 1	1215	1673	1698		1698	0	1	1302	107	0
Reach	22304	PF 2	2596	1673	1702		1702	0	1	1831	127	0
Reach	22304	PF 3	3180	1673	1704		1704	0	2	2019	133	0
Reach	22304	PF 4	4978	1673	1708		1708	0	2	2579	150	0

Reach	22223	PF 1	1215	1670	1698		1698	0	1	1897	135	0
Reach	22223	PF 2	2596	1670	1702		1702	0	1	2563	157	0
Reach	22223	PF 3	3180	1670	1704		1704	0	1	2797	164	0
Reach	22223	PF 4	4978	1670	1708		1708	0	2	3488	183	0
Reach	22149	PF 1	1215	1667	1698		1698	0	1	1243	77	0
Reach	22149	PF 2	2596	1667	1702		1702	0	2	1620	90	0
Reach	22149	PF 3	3180	1667	1704		1704	0	2	1751	94	0
Reach	22149	PF 4	4978	1667	1708		1708	0	2	2138	105	0
Reach	22064	PF 1	1215	1669	1698		1698	0	1	1329	88	0
Reach	22064	PF 2	2596	1669	1702		1702	0	2	1755	101	0
Reach	22064	PF 3	3180	1669	1704		1704	0	2	1902	105	0
Reach	22064	PF 4	4978	1669	1708		1708	0	2	2335	116	0
Reach	21983	PF 1	1215	1671	1698		1698	0	1	1285	87	0
Reach	21906	PF 4	4978	1672	1708		1708	0	2	2222	114	0
Reach	21809	PF 1	1215	1674	1698		1698	0	1	1185	85	0
Reach	21809	PF 2	2596	1674	1702		1702	0	2	1594	98	0
Reach	21809	PF 3	3180	1674	1704		1704	0	2	1736	102	0
Reach	21809	PF 4	4978	1674	1708		1708	0	2	2154	113	0
Reach	21715	PF 1	1215	1676	1698		1698	0	1	1124	84	0
Reach	21715	PF 2	2596	1676	1702		1702	0	2	1528	97	0
Reach	21715	PF 3	3180	1676	1704		1704	0	2	1669	101	0
Reach	21715	PF 4	4978	1676	1708		1708	0	2	2083	112	0
Reach	21624	PF 1	1215	1678	1698		1698	0	1	1054	83	0
Reach	21624	PF 2	2596	1678	1702		1702	0	2	1452	96	0
Reach	21624	PF 3	3180	1678	1704		1704	0	2	1591	100	0
Reach	21624	PF 4	4978	1678	1707		1708	0	3	2000	111	0
Reach	21530	PF 1	1215	1680	1698		1698	0	1	988	86	0
Reach	21530	PF 2	2596	1680	1702		1702	0	2	1406	102	0
Reach	21530	PF 3	3180	1680	1704		1704	0	2	1554	107	0
Reach	21530	PF 4	4978	1680	1707		1708	0	3	1995	121	0
Reach	21433	PF 1	1215	1681	1697		1698	0	3	441	55	0
Reach	21433	PF 2	2596	1681	1702		1702	0	4	705	70	0
Reach	21433	PF 3	3180	1681	1703		1704	0	4	800	74	0
Reach	21433	PF 4	4978	1681	1707		1708	0	5	1099	87	0
Reach	21333	PF 1	1215	1682	1697		1698	0	3	392	52	0
Reach	21333	PF 2	2596	1682	1701		1702	0	4	637	66	0
Reach	21333	PF 3	3180	1682	1703		1704	0	4	727	71	0
Reach	21333	PF 4	4978	1682	1706		1708	0	5	1011	83	0
Reach	21249	PF 1	1215	1683	1697		1698	0	3	351	49	0
Reach	21249	PF 2	2596	1683	1701		1702	0	4	581	63	0
Reach	21249	PF 3	3180	1683	1702		1704	0	5	666	68	0
Reach	21249	PF 4	4978	1683	1706		1708	0	5	939	81	0
Reach	21177	PF 1	1215	1683	1697		1698	0	4	315	47	0
Reach	21177	PF 2	2596	1683	1701		1702	0	5	530	61	1
Reach	21177	PF 3	3180	1683	1702		1703	0	5	610	65	1
Reach	21177	PF 4	4978	1683	1706		1707	0	6	873	78	1
Reach	21101	PF 1	1215	1684	1696		1697	0	4	277	44	1
Reach	21101	PF 2	2596	1684	1700		1702	0	5	479	58	1
Reach	21101	PF 3	3180	1684	1702		1703	0	6	555	63	1
Reach	21101	PF 4	4978	1684	1705		1707	0	6	813	76	1
Reach	21017	PF 1	1215	1685	1694	1694	1697	0	7	173	35	1
Reach	21017	PF 2	2596	1685	1698	1698	1701	0	8	318	47	1
Reach	21017	PF 3	3180	1685	1699	1699	1703	0	9	374	51	1
Reach	21017	PF 4	4978	1685	1704		1707	0	7	689	69	1
Reach	20925	PF 1	1215	1680	1691	1691	1695	0	8	155	25	1

Reach	20925	PF 2	2596	1680	1696	1696	1700	0	9	284	34	1
Reach	20925	PF 3	3180	1680	1697	1697	1702	0	9	335	36	1
Reach	20925	PF 4	4978	1680	1701	1701	1706	0	10	480	43	1
Reach	20836	PF 1	1215	1668	1680	1680	1682	0	7	164	29	1
Reach	20836	PF 2	2596	1668	1684	1684	1687	0	9	301	40	1
Reach	20836	PF 3	3180	1668	1685	1685	1689	0	9	354	43	1
Reach	20836	PF 4	4978	1668	1688	1688	1693	0	10	510	52	1
Reach	20709	PF 1	1215	1664	1676	1676	1678	0	7	164	29	1
Reach	265	PF 1	1215	1402	1422		1422	0	0	2626	131	0
Reach	265	PF 2	2596	1402	1426		1426	0	0	3122	140	0
Reach	265	PF 3	3180	1402	1427		1427	0	1	3293	143	0
Reach	265	PF 4	4978	1402	1430		1430	0	1	3737	151	0
Reach	118	PF 1	1215	1399	1422		1422	0	0	3492	171	0
Reach	118	PF 2	2596	1399	1426		1426	0	0	4130	177	0
Reach	118	PF 3	3180	1399	1427		1427	0	1	4347	179	0
Reach	118	PF 4	4978	1399	1430		1430	0	1	4898	185	0
Reach	50	PF 1	1215	1420	1420	1420	1422	0		197	51	0
Reach	50	PF 2	2596	1420	1423	1423	1425	0	2	360	70	1
Reach	50	PF 3	3180	1420	1424	1424	1427	0	3	428	76	1
Reach	50	PF 4	4978	1420	1426	1426	1430	0	4	634	93	1

C. Hydraulic property tables for steady flow in HEC-RAS

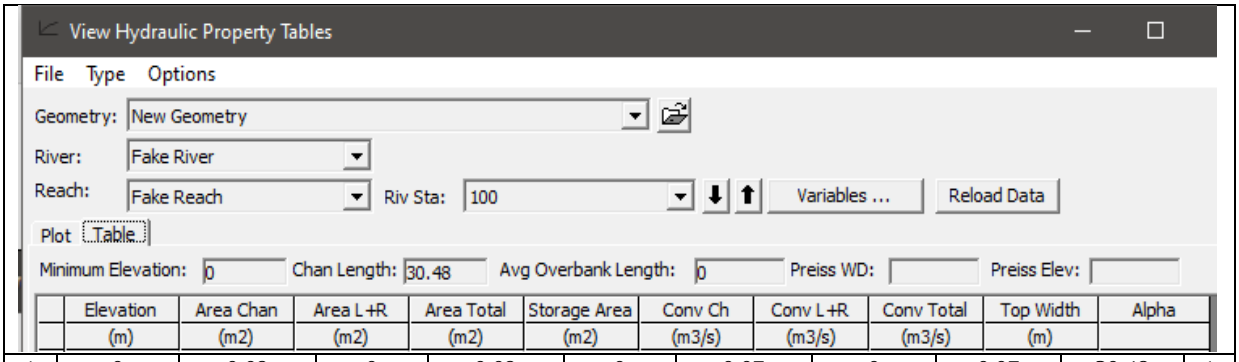

	Elevation (m)	Area Chan (m2)	Area L+R (m2)	Area Total (m2)	Storage Area (m2)	Conv Ch (m3/s)	Conv L+R (m3/s)	Conv Total (m3/s)	Top Width (m)	Alpha
1	0	0.09	0	0.09	0	0.07	0	0.07	30.48	1
2	0.05	1.39	0	1.39	0	5.93	0	5.93	30.48	1
3	0.14	4.18	0	4.18	0	36.8	0	36.8	30.48	1
4	0.23	6.97	0	6.97	0	86	0	86	30.48	1
5	0.32	9.76	0	9.76	0	150	0	150	30.48	1
6	0.41	12.54	0	12.54	0	227	0	227	30.48	1
7	0.5	15.33	0	15.33	0	316	0	316	30.48	1
8	0.59	18.12	0	18.12	0	416	0	416	30.48	1
9	0.68	20.9	0	20.9	0	526	0	526	30.48	1
10	0.77	23.69	0	23.69	0	646	0	646	30.48	1
11	0.86	26.48	0	26.48	0	774	0	774	30.48	1
12	0.96	29.26	0	29.26	0	911	0	911	30.48	1
13	1.05	32.05	0	32.05	0	1057	0	1057	30.48	1
14	1.14	34.84	0	34.84	0	1210	0	1210	30.48	1
15	1.23	37.63	0	37.63	0	1370	0	1370	30.48	1
16	1.32	40.41	0	40.41	0	1538	0	1538	30.48	1
17	1.41	43.2	0	43.2	0	1712	0	1712	30.48	1
18	1.5	45.99	0	45.99	0	1893	0	1893	30.48	1
19	1.59	48.77	0	48.77	0	2081	0	2081	30.48	1
20	1.68	51.56	0	51.56	0	2275	0	2275	30.48	1
21	1.77	54.35	0	54.35	0	2474	0	2474	30.48	1
22	1.87	57.14	0	57.14	0	2680	0	2680	30.48	1

23	1.96	59.92	0	59.92	0	2891	0	2891	30.48	1
24	2.05	62.71	0	62.71	0	3108	0	3108	30.48	1
25	2.14	65.5	0	65.5	0	3329	0	3329	30.48	1
26	2.23	68.28	0	68.28	0	3556	0	3556	30.48	1
27	2.32	71.07	0	71.07	0	3789	0	3789	30.48	1
28	2.41	73.86	0	73.86	0	4025	0	4025	30.48	1
29	2.5	76.65	0	76.65	0	4267	0	4267	30.48	1
30	2.59	79.43	0	79.43	0	4513	0	4513	30.48	1
31	2.68	82.22	0	82.22	0	4764	0	4764	30.48	1
32	2.78	85.01	0	85.01	0	5019	0	5019	30.48	1
33	2.87	87.79	0	87.79	0	5279	0	5279	30.48	1
34	2.96	90.58	0	90.58	0	5542	0	5542	30.48	1

D. Population density per square kilometer in the catchment area

No.	Wereda	Population			Area (km^2)	Density $Popn/km^2$	Elevation (m)
		Rural	Urban	Total			
1	Bekoji	16,876	148,912	165,788	1554.1	106.68	2764
2	Kofele	11,665	168,043	179,708	1167.0	153.99	2678
3	Gedeb	10,903	109,479	120,382	1270.9	94.72	2660
4	Agarfa	7,410	59,200	66,610	933.0	71.39	2236
5	Adaba	9,997	87,589	97,586	2291.6	42.58	2924
6	Sinanana Dinsho	23,535	113,819	137,354	1720.5	79.83	2665
7	Dodola	16,976	109,519	126,495	1444.5	87.57	2721
8	Kokosa	1,784	87,050	88,834	430.7	206.24	2636
9	Gonsebo	3,059	44,965	48,024	2196.7	21.86	2202

E. Maximun yearly stream flow discharge at Agarfa gauging station

Year	1981	1982	1983	1984	1985	1986	1987	1988
$Q(m^3/s)$	963.330	247.89	743.17	169.60	291.62	486.52	613.13	544.94
Year	1989	1990	1991	1992	1993	1994	1995	1996
$Q(m^3/s)$	480.94	464.18	479.23	962.92	373.04	925.25	881.25	519.09
Year	1997	1998	1999	2000	2001	2002	2003	2004
$Q(m^3/s)$	612.45	973.75	394.92	526.13	189.69	141.91	553.29	219.62
Year	2005	2006	2007	2008	2009	2010	2011	2012
$Q(m^3/s)$	430.84	814.10	853.99	938.58	863.33	247.89	743.17	169.60
Year	2013	2014	2015	2016	2017	2018	2019	
$Q(m^3/s)$	291.62	486.52	613.13	544.94	680.94	664.18	579.23	